

UNCLASSIFIED

AD NUMBER

AD848909

LIMITATION CHANGES

TO:

Approved for public release; distribution is unlimited.

FROM:

Distribution authorized to U.S. Gov't. agencies and their contractors; Critical Technology; JAN 1969. Other requests shall be referred to Air Force Weapons Laboratory, Kirtland AFB, NM87117. This document contains export-controlled technical data.

AUTHORITY

AFWL ltr, 30 Nov 1971

THIS PAGE IS UNCLASSIFIED

AFWL-TR-68-114

AFWL-TR-
68-114

AD848909



**THEORETICAL STUDY OF CHARGE EXCHANGE
CROSS SECTIONS**

A. Dalgarno T. G. Webb G. A. Victor

**GCA Corporation
Bedford, Massachusetts 01730
Contract F29601-67-C-0088**

TECHNICAL REPORT NO. AFWL-TR-68-114

January 1969

**AIR FORCE WEAPONS LABORATORY
Air Force Systems Command
Kirtland Air Force Base
New Mexico**

MAR 13 1969

This document is subject to special export controls and each transmittal to foreign governments or foreign nationals may be made only with prior approval of AFWL (WLRT) , Kirtland AFB, NM, 87117.

THEORETICAL STUDY OF CHARGE EXCHANGE CROSS SECTIONS

A. Dalgarno

T. G. Webb

G. A. Victor

GCA Corporation
GCA Technology Division
Bedford, Massachusetts 01730
Contract F29601-67-C-0088

TECHNICAL REPORT NO. AFWL-TR-68-114

This document is subject to special export controls and each transmittal to foreign governments or foreign nationals may be made only with prior approval of AFWL (WLRT), Kirtland AFB, NM, 87117. Distribution is limited because of the technology discussed in the report.

FOREWORD

This report was prepared by the GCA Corporation, GCA Technology Division, Bedford, Massachusetts, under Contract F29601-67-C-0088, MIPR 528-66. The research was performed under Program Element 61102H, Project 5710, Subtask 07.003 (RHA3061), and was funded by the Defense Atomic Support Agency (DASA).

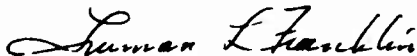
Inclusive dates of research were 16 June 1967 to 20 August 1968. The report was submitted 2 January 1969 by the Air Force Project Officer, Captain Joseph S. Greene, Jr. (WLRT). The contractor's report number is GCA-TR-68-3-A.

Information in this report is embargoed under the Department of State ITIARs. This report may be released to foreign governments by departments or agencies of the US Government subject to approval of AFWL (WLRT), Kirtland AFB, NM, 87117.

This technical report has been reviewed and is approved.



JOSEPH S. GREENE, JR., Captain, USAF
Project Officer



TRUMAN L. FRANKLIN, Colonel, USAF
Chief, Theoretical Branch



CLAUDE K. STAMBAUGH, Colonel, USAF
Chief, Research Division

ABSTRACT

(Distribution Limitation Statement No. 2)

Charge exchange cross sections for fast heavy ions representative of several groups in the periodic table with atmospheric and other atoms have been calculated by using a quantal two-state one-electron method. The principal ions considered have been singly charged K, I, and Cr while target atoms and/or molecules have been N, O, Ar, Ne, H and He. Singly charged lithium, sodium, rubidium, and cesium have also been considered as projectiles in the target gases.

Stripping cross sections for fast heavy ions incident on atmospheric and other atoms have been calculated by using an independent scattering model based on the Born approximation.

The relationship between the quantal predictions and available experimental results is illustrated and certain improvements to the simple theory are discussed. A comparison is also made between the electron loss theory and available experimental results.

Capture into excited states is discussed, and estimates are made of the appropriate cross sections.

The rate of energy loss by heavy ions in air is discussed.

CONTENTS

<u>Section</u>		<u>Page</u>
I	INTRODUCTION	1
II	QUANTAL THEORY OF CHARGE EXCHANGE	2
	Theory of Fast Collisions	2
	Exchange and Distortion Refinements	5
	Capture into Excited States	7
III	QUANTUM THEORY OF ELECTRON LOSS IN HEAVY BODY COLLISIONS	14
	Introduction	14
	Theory	15
IV	RESULTS	20
	Charge Exchange	20
	Electron Stripping Cross Sections	70
V	ENERGY LOSS OF FAST HEAVY IONS IN GASES	90
	Appendix I	97
	Appendix II	103
	References	117
	Distribution	120

ILLUSTRATIONS

<u>Figure</u>		<u>Page</u>
1	Charge Exchange Cross Sections for Capture into the n=2 and n=3 States of Lithium from Atomic Oxygen.	9
2	Charge Exchange Cross Sections for Capture into the n=2 and n=3 States of Lithium from Neon.	10
3	Charge Exchange Cross Section for Capture into the n=3 State of Sodium from Atomic Oxygen.	12
4	Charge Exchange Cross Section for Capture into the n=3 State of Sodium from Neon.	13
5	The Integrands, in Atomic Units, of Equation (35) for Helium using the Scattering Factors of Reference 24. The Solid Curve is the Inelastic Integrand, the Dashed Curve the Elastic Integrand.	19
6	Charge Exchange Cross Section for Capture into the Ground State for Singly Charged Potassium in Atomic Hydrogen.	28
7	Charge Exchange Cross Section for Capture into the Ground State for Singly Charged Potassium in Helium.	29
8	Charge Exchange Cross Section for Capture into the Ground State for Singly Charged Potassium in Neon.	30
9	Charge Exchange Cross Section for Capture into the Ground State for Singly Charged Potassium in Argon. The Experimental Results are from Reference 31.	31
10	Charge Exchange Cross Section for Capture into the Ground State for Singly Charged Potassium in Atomic Nitrogen. The Experimental Results are from Reference 31.	32
11	Charge Exchange Cross Section for Capture into the Ground State for Singly Charged Potassium in Atomic Oxygen. The Experimental Results are from Reference 31.	33
12	Charge Exchange Cross Section for Capture into the Ground State for Singly Charged Iodine in Atomic Hydrogen.	34
13	Charge Exchange Cross Section for Capture into the Ground State for Singly Charged Iodine in Helium.	35
14	Charge Exchange Cross Section for Capture into the Ground State for Singly Charged Iodine in Neon.	36

ILLUSTRATIONS (continued)

<u>Figure</u>		<u>Page</u>
15	Charge Exchange Cross Section for Capture into the Ground State for Singly Charged Iodine in Argon. The Experimental Results are from Reference 31.	37
16	Charge Exchange Cross Section for Capture into the Ground State for Singly Charged Iodine in Atomic Nitrogen. The Experimental Results are from Reference 31.	38
17	Charge Exchange Cross Section for Capture into the Ground State for Singly Charged Iodine in Atomic Oxygen. The Experimental Results are from Reference 31.	39
18	Charge Exchange Cross Section for Capture into the Ground State for Singly Charged Chromium in Atomic Hydrogen.	40
19	Charge Exchange Cross Section for Capture into the Ground State for Singly Charged Chromium in Helium.	41
20	Charge Exchange Cross Section for Capture into the Ground State for Singly Charged Chromium in Neon.	42
21	Charge Exchange Cross Section for Capture into the Ground State for Singly Charged Chromium in Argon.	43
22	Charge Exchange Cross Section for Capture into the Ground State for Singly Charged Chromium in Atomic Nitrogen.	44
23	Charge Exchange Cross Section for Capture into the Ground State for Singly Charged Chromium in Atomic Oxygen.	45
24	Charge Exchange Cross Section for Capture into the Ground State for Singly Charged Lithium in Atomic Hydrogen.	46
25	Charge Exchange Cross Section for Capture into the Ground State for Singly Charged Lithium in Helium.	47
26	Charge Exchange Cross Section for Capture into the Ground State for Singly Charged Lithium in Neon.	48
27	Charge Exchange Cross Section for Capture into the Ground State for Singly Charged Lithium in Argon.	49
28	Charge Exchange Cross Section for Capture into the Ground State for Singly Charged Lithium in Atomic Nitrogen.	50

ILLUSTRATIONS (continued)

<u>Figure</u>		<u>Page</u>
29	Charge Exchange Cross Section for Capture into the Ground State for Singly Charged Lithium in Atomic Oxygen.	51
30	Charge Exchange Cross Section for Capture into the Ground State for Singly Charged Sodium in Atomic Hydrogen.	52
31	Charge Exchange Cross Section for Capture into the Ground State for Singly Charged Sodium in Helium.	53
32	Charge Exchange Cross Section for Capture into the Ground State for Singly Charged Sodium in Neon.	54
33	Charge Exchange Cross Section for Capture into the Ground State for Singly Charged Sodium in Argon.	55
34	Charge Exchange Cross Section for Capture into the Ground State for Singly Charged Sodium in Atomic Oxygen.	56
35	Charge Exchange Cross Section for Capture into the Ground State for Singly Charged Sodium in Atomic Nitrogen.	57
36	Charge Exchange Cross Section for Capture into the Ground State for Singly Charged Rubidium in Atomic Hydrogen.	58
37	Charge Exchange Cross Section for Capture into the Ground State for Singly Charged Rubidium in Helium.	59
38	Charge Exchange Cross Section for Capture into the Ground State for Singly Charged Rubidium in Neon.	60
39	Charge Exchange Cross Section for Capture into the Ground State for Singly Charged Rubidium in Argon.	61
40	Charge Exchange Cross Section for Capture into the Ground State for Singly Charged Rubidium in Atomic Oxygen.	62
41	Charge Exchange Cross Section for Capture into the Ground State for Singly Charged Rubidium in Atomic Nitrogen.	63
42	Charge Exchange Cross Section for Capture into the Ground State for Singly Charged Cesium in Atomic Hydrogen.	64
43	Charge Exchange Cross Section for Capture into the Ground State for Singly Charged Cesium in Helium.	65

ILLUSTRATIONS (continued)

<u>Figure</u>		<u>Page</u>
44	Charge Exchange Cross Section for Capture into the Ground State for Singly Charged Cesium in Neon.	66
45	Charge Exchange Cross Section for Capture into the Ground State for Singly Charged Cesium in Argon.	67
46	Charge Exchange Cross Section for Capture into the Ground State for Singly Charged Cesium in Atomic Oxygen.	68
47	Charge Exchange Cross Section for Capture into the Ground State of Lithium using 1s and 2s Representations of the Lithium Wavefunction. The 1s Representation is used for the Argon Target Gas.	69
48	Electron Stripping Cross Section for Hydrogen Atoms Incident on Atomic Hydrogen. The Experimental Results are: ○, Ref. 32; □, Ref. 33; △, Ref. 34.	71
49	Electron Stripping Cross Section for Hydrogen Atoms Incident on Atomic Nitrogen. The Experimental Results are: ○, Ref. 32; □, Ref. 33; △, Ref. 34.	72
50	Electron Stripping Cross Section for Hydrogen Atoms Incident on Argon. The Experimental Results are: ○, Ref. 32; □, Ref. 33; △, Ref. 34.	73
51	Collisional Detachment Cross Section for Negative Hydrogen Ions Incident on Helium. The Experimental Results are from Ref. 32.	75
52	Electron Stripping Cross Section for Sodium Ions on Helium Showing the Total Cross Section and the Contributions of the Different Shells.	76
53	Electron Stripping Cross Sections for More Highly Stripped Chromium Ions Incident on Argon Including Inner Shell Contributions.	78
54	Valance Shell Contribution to the Electron Stripping Cross Section for More Highly Stripped Chromium Ions Incident on Argon.	79
55	Electron Stripping Cross Sections for Various Projectile Systems in Helium Gas.	80

ILLUSTRATIONS (continued)

<u>Figure</u>		<u>Page</u>
56	Electron Stripping Cross Sections for Various Projectile Systems in Helium Gas.	81
57	Electron Stripping Cross Sections for Various Projectile Systems in Atomic Nitrogen Gas.	82
58	Electron Stripping Cross Sections for Various Projectile Systems in Atomic Nitrogen Gas.	83
59	Electron Stripping Cross Sections for Various Projectile Systems in Atomic Oxygen Gas.	84
60	Electron Stripping Cross Sections for Various Projectile Systems in Atomic Oxygen Gas.	85
61	Electron Stripping Cross Sections for Various Projectile Systems in Neon.	86
62	Electron Stripping Cross Sections for Various Projectile Systems in Neon.	87
63	Electron Stripping Cross Sections for Various Projectile Systems in Argon.	88
64	Electron Stripping Cross Sections for Various Projectile Systems in Argon.	89
65	Cross Section for Energy Loss in Electron Stripping Processes for Various Ions in Argon Gas.	94
66	Cross Section for Energy Loss in Electron Stripping Processes for Various Ions in Argon Gas.	95
67	The Electron Stripping Program.	105

TABLES

<u>Table</u>		<u>Page</u>
I	Ionization Potentials and 1s Model Parameters	4
II	Cross Sections σ_{10} (Units of 10^{-17} cm^2) Calculated for K^+ Projectiles (1s Model)	21
III	Cross Sections σ_{10} (Units of 10^{-17} cm^2) Calculated for I^+ Projectiles (1s Model)	22
IV	Cross Sections σ_{10} (Units of 10^{-17} cm^2) Calculated for Cr^+ Projectile (1s Model)	23
V	Cross Sections σ_{10} (Units of 10^{-17} cm^2) Calculated for Li^+ Projectile (1s Model)	24
VI	Cross Sections σ_{10} (Units of 10^{-17} cm^2) Calculated for Na^+ Projectile (1s Model)	25
VII	Cross Sections σ_{10} (Units of 10^{-17} cm^2) Calculated for Rb^+ Projectile (1s Model)	26
VIII	Cross Sections σ_{10} (Units of 10^{-17} cm^2) Calculated for Cs^+ Projectile (1s Model)	27

BLANK PAGE

SECTION I

INTRODUCTION

In this work, a model explored in reference 1 has been applied to the calculation of further charge exchange cross sections for collisions between heavy ions and atmospheric ions and molecules. Modifications to the simple theory are suggested and discussed. The method used is the 1s model two-state quantal description applied to the ground states. Estimates are also made of the capture cross sections into excited states of the projectile atoms.

Calculations of the cross section for electron loss have been performed by using a modification of a theory developed by Nikolaev and Dmitriev (Ref. 2). In this model the projectile electrons are assumed to be each scattered independently by the target atom, according to the Born approximation. In reference 2, a final integration over a simple analytic form factor, which is replaced herein by numerical quadrature over any tabulated form factor, is required.

The theory of charge exchange and refinements thereto are discussed in Section II. Section III contains a discussion of the electron loss theory. In Section IV, available experimental results are compared with the calculated results while the Appendixes describe the computer programs developed.

SECTION II

QUANTAL THEORY OF CHARGE EXCHANGE

1. Theory of Fast Collisions

A brief review is presented of the theory given in reference 3 as applied to a two-state one-electron system. Atomic units are employed throughout. Consider point A to move past point B at a constant velocity \vec{v} , i.e., a rectilinear trajectory characterized by an impact parameter ρ . Let a single electron have position vectors \underline{x}_a , \underline{x}_b and \underline{x} with respect to A, B and the midpoint of AB, respectively. Let the electron see potentials $V_a(r_a)$ and $V_b(r_b)$ centered on the appropriate points, and let there exist bound state wavefunctions

$$\left[T + V_a(r_a) - i \frac{\partial}{\partial t} \right] \varphi_i(\underline{x}_a) \exp(-i E_i t) = 0 \quad (1)$$

considering A to be at rest and

$$\left[T + V_b(r_b) - i \frac{\partial}{\partial t} \right] \varphi_j(\underline{x}_b) \exp(-i E_j t) = 0 \quad (2)$$

considering B to be at rest where T is the kinetic energy operator. If the midpoint of AB is taken to be at rest, wavefunctions simply derived from φ_i and φ_j are solutions of the time dependent Schrodinger equation; thus:

$$\left[T + V_a(r_a) - i \frac{\partial}{\partial t} \right] \varphi_i(\underline{x}_a, \underline{x}) \exp\left[-i \left(E_i + \frac{1}{8} v^2 \right) t\right] = 0 \quad (3)$$

and

$$\left[T + V_b(r_b) - i \frac{\partial}{\partial t} \right] \varphi_j(\underline{x}_b, \underline{x}) \exp\left[-i \left(E_j + \frac{1}{8} v^2 \right) t\right] = 0 \quad (4)$$

where

$$\varphi_i(\underline{x}_a, \underline{x}) = \varphi_i(\underline{x}_a) \exp\left(-\frac{1}{2} i \underline{v} \cdot \underline{x}\right) \quad (5)$$

and

$$\varphi_j(\underline{x}_b, \underline{x}) = \varphi_j(\underline{x}_b) \exp\left(\frac{1}{2} i \underline{v} \cdot \underline{x}\right) \quad (6)$$

The total wavefunction Ψ in this approximation is then expanded as

$$\Psi = a_1 \varphi_1 \exp\left[-i \left(E_1 + \frac{1}{8} v^2\right) t\right] + b_j \varphi_j \exp\left[-i \left(E_j + \frac{1}{8} v^2\right) t\right] \quad (7)$$

and substituted into the conditions

$$\left[\varphi_1, \left(H - i \frac{\partial}{\partial t}\right) \Psi\right] \exp\left[i \left(E_1 + \frac{1}{8} v^2\right) t\right] = 0 \quad (8)$$

and

$$\left[\varphi_j, \left(H - i \frac{\partial}{\partial t}\right) \Psi\right] \exp\left[i \left(E_j - \frac{1}{8} v^2\right) t\right] = 0 \quad (9)$$

where $H = T + V_a + V_b$ is the total Hamiltonian. The equations of the two-state model then follow

$$\begin{aligned} i \dot{a}_1 + i S_{1j} \exp[i(E_1 - E_j)t] \dot{b}_j &= h_{11} a_1 + h_{1j} \exp[i(E_1 - E_j)t] b_j \\ i S_{j1} \exp[i(E_j - E_1)t] \dot{a}_1 + i \dot{b}_j &= h_{j1} \exp[i(E_j - E_1)t] a_1 + h_{jj} b_j \end{aligned} \quad (10)$$

where

$$S_{1j} = (\varphi_1, \varphi_j), \quad h_{1j} = (\varphi_1, V_a \varphi_j), \quad \text{and} \quad h_{j1} = (\varphi_j, V_b \varphi_1) \quad (11)$$

The initial conditions for Equation (1) are that, say, $a_1 = 1$, $b_j = 0$. At the end of the trajectory $|b_j|^2$ will be the capture probability for that impact parameter.

$$c(\rho) = |b_j(+\infty)|^2 \quad (12)$$

and the cross section is

$$Q = 2\pi \int_0^\infty c(\rho) \rho \, d\rho \quad (13)$$

Normalization ($= |a_1|^2 + |b_j|^2$) will remain at unity if

$$h_{j1}^* - h_{1j} = i \frac{d S_{1j}}{dt} - (E_1 - E_j) S_{1j} \quad (14)$$

which replaces Equation (12) of reference 1.

Equations (10) are equivalent to the following form:

$$\begin{aligned} \dot{a}_i &= -i K_{ij} b_j \exp\left[i \int^t g(t') dt'\right] \exp(i(E_i - E_j)t] \\ \dot{b}_j &= -i K_{ji} a_i \exp\left[i \int^t g(t') dt'\right] \exp[i(E_j - E_i)t] \end{aligned} \quad (15)$$

where

$$K_{kl} = \frac{h_{kl} - S_{kl} h_{ll}}{1 - |S_{kl}|^2} \quad (16)$$

and the distortion term is

$$g = \frac{h_{ii} - h_{jj} - S_{ij} h_{ji} + S_{ji} h_{ij}}{1 - |S_{ij}|^2} \quad (17)$$

The wavefunction models and the appropriate techniques for calculating the matrix elements (11) have been reported in detail in reference 1. The method of integrating Equations (10), the set solved in practice, is also described in reference 1. The wavefunction parameter in the 1s model employed is the present set of calculations, and others available for further calculations are listed in Table I.

TABLE I

IONIZATION POTENTIALS AND 1s MODEL PARAMETERS

Element	Ionization Potential (au)	α	$2\alpha^{3/2}$
Al	0.22009	0.66347	1.08083
Fe	0.29039	0.76209	1.33058
U	0.22463	0.67027	1.09750
N	0.53435	1.03378	2.10219
O	0.50072	1.00072	2.00215
Ar	0.57946	1.07653	2.23390

2. Exchange and Distortion Refinements

Two methods are described below by which it is believed that the basic ls or ns model could be improved should further calculations of this type be undertaken.

a. Electron Exchange

Let μ represent certain matrix elements that occur in Equations (10) ($\mu = S_{ij}, h_{ij},$ or h_{ji}). For convenience, the complex exponentials in Equations (10) are included in the definition of the elements in this analysis. The various approximations to μ are denoted as follows:

- μ : matrix elements calculated by using exact many-electron fully antisymmetrized combinations of atomic wavefunctions.
- μ^0 : matrix elements calculated by neglecting atom-atom electron exchange but otherwise exact.
- $\bar{\mu}$: matrix elements adopted for inclusion in the two-state calculation.
- $\bar{\mu}^0$: matrix elements calculated directly from the one-electron model.

It was established in an earlier final report (Ref. 4) that at sufficiently large internuclear distances where second and higher order overlap terms may be neglected

$$\mu = F \mu^0 \quad (18)$$

where F is the geometric mean of the numbers of active electrons in the initial state of the target and the final state of the projectile. An active electron could be defined arbitrarily as one with a binding energy not more than twice that of the most loosely bound electron. Because the matrix elements $\bar{\mu}^0$ are an approximation to the μ^0 , we might write analogously to Equation (18), as an approximation:

$$\bar{\mu} = F \bar{\mu}^0 \quad (19)$$

but at the smaller internuclear distance $F \bar{\mu}^0$ will not represent $\bar{\mu}$ well because of the overlap approximation inherent in F and because of the shortcomings of the one-electron model itself. Therefore, Equation (19) is modified by inserting an additional factor G and adding a correction, δ

$$\bar{\mu} = G F \bar{\mu}^0 + \delta \quad (20)$$

where G departs from unity only to prevent $\bar{\mu}$ from becoming unphysical (i.e., when $|F \bar{S}_{ij}^0|$ exceeds unity). The correction δ ensures that normalization is conserved so that [compare Equation (14)]:

$$\bar{h}_{ij} - \bar{h}_{ji}^* = i \frac{d \bar{S}_{ij}^0}{dt} \quad (21)$$

The $\bar{\mu}^0$ elements automatically satisfy:

$$\bar{h}_{ij}^0 - \bar{h}_{ji}^{0*} = i \frac{d \bar{S}_{ij}^0}{dt} \quad (22)$$

and Equation (20) is applied by assuming

$$\begin{aligned} \bar{S}_{ij} &= G F \bar{S}_{ij}^0 \\ \bar{h}_{ij} &= G F \bar{h}_{ij}^0 + \frac{1}{2} \Delta \\ \bar{h}_{ji} &= G F \bar{h}_{ji}^0 - \frac{1}{2} \Delta^* \end{aligned} \quad (23)$$

Substitution of Equations (23) and (22) into Equation (21) yields:

$$\Delta = \frac{1}{2} \frac{dG}{dt} F \bar{S}^0 \quad (24)$$

Now the limit is imposed

$$|\bar{S}_{ij}| \leq L \quad (25)$$

where L might be, say, 0.9. Then, either

$$G = 1; \Delta = 0 \quad (26)$$

or

$$G = \frac{L}{F |\bar{s}_{ij}^0|} ; \Delta = -1 \frac{L \bar{s}^0}{|\bar{s}^0|} \frac{d}{dt} |\bar{s}^0| \quad (27)$$

This extension of the basic model contains the arbitrary limit L and the validity of the scheme requires demonstrated insensitivity of the cross section to L . Clearly, at sufficiently large velocities so that Equation (26) holds, the effect of the scheme is simply to multiply the cross section by F^2 .

b. Distortion

At large internuclear distances, the rate at which the distortion g diminishes is controlled by $h_{ii} - h_{jj}$ [see Equation (17)]. The basic one-electron model has the flaw that $h_{ii} - h_{jj} \sim (Z_B - Z_A)/R$, assuming singly charged ions in both channels, whereas in fact $h_{ii} - h_{jj}$ should diminish faster than R^{-1} . In the hope of improving the accuracy of the results at low impact energies, the program has the capability of calculating h_{ii} and h_{jj} with the Coulombic term of each potential set equal to the net charge of the appropriate positive ion. In the calculation of h_{ij} and h_{ji} the original form of the potential is retained. This has been applied to $Ar^+ + Ar$ and has the effect of reducing the cross sections somewhat at all energies; however, this does not constitute a clear improvement in the results of the calculation. It has been established in other papers (Ref. 5 and 6) that distortion has a great effect on the cross section at lower energies.

3. Capture into Excited States

The rate of energy loss of a beam of heavy particles in gases is dependent on the cross sections for the numerous inelastic scattering processes that can occur. The contribution to the rate of energy loss from charge transfer processes into excited states is different than that for the capture into the ground state of the projectile system. Capture into excited states can produce excited or metastable species that behave sufficiently different than ground-state systems in subsequent processes so as to complicate the interpretation of many experimental studies of heavy-body collision processes. In addition, though capture into excited states and possible excitations of the target system, energy can appear in the radiation field rather than in the potential and kinetic energy of the nuclei and electrons. The majority of experimental studies of charge transfer processes give information on the sum of the cross sections for transfer into all of the bound projectile states with the target left in the ground state or excited states, while the theoretical studies usually consider specific states of the final target and projectile system.

A considerable body of theoretical and experimental literature on charge transfer cross sections for capture into excited states is available, however it is almost exclusively concerned with proton projectiles on various target gases, so that generalizations to more complex projectile systems must be performed with care. The large amount of data for the case of the proton projectile indicates quite clearly, however, that the cross section for capture into an excited state is usually much smaller than the cross section for capture in the ground state, and that the dominant contribution to the total capture cross section usually arises from capture into the ground state.

If the cross section for capture from a state with principle quantum number n_i and orbital angular momentum quantum number l_i into a state with quantum numbers n_f and l_f is denoted as $Q(n_i l_i | n_f l_f)$, Oppenheimer (Ref. 7) showed that $Q(1s | n_f s)$ falls off as n_f^{-3} at high energies by using the Oppenheimer-Brinkman-Kramers (Ref. 7 and 8) approximation, which neglects the nucleon-nucleon interaction in a Born-type approximation. Generalizing this, Bates and Dalgarno (Ref. 9) and Bates and McCarroll (Ref. 3) argue that $Q(n_i s | n_f s)$ falls off as $(n_f n_i)^{-3}$ at high energies and $Q(n_i l_i | n_f l_f)$ for $l_i, l_f \neq 0$ falls off rather more slowly. Mapleton (Ref. 10), in full Born approximation calculations for protons on atomic hydrogen and helium obtains numerical results that confirm the rules given above. In an experiment involving



Hughes, et al. (Ref. 11) obtain results that approach Mapleton's results at high energy, but are much lower at low energies as is expected from Born approximation results. Jaecks, et al. (Ref. 12) have studied the capture into the metastable 2s state of hydrogen for protons incident on the rare gases. Considerable work on capture into excited projectile states was reported at the 1967 Leningrad conference (Ref. 13), however, the choice of projectile still appears to be protons.

The two-state ns model discussed in reference 1 and in Section II-1 is employed to estimate the cross section for capture into excited states for several systems. The final projectile states considered are the lowest few s states in lithium. 1s-model wavefunctions are used for the target systems of atomic nitrogen and neon. The ns states of the projectile are represented by the corresponding ns hydrogenic wavefunction with the effective charge adjusted to reproduce the experimental ionization energy of the given projectile state.

The results of the explicit calculations for lithium ions in atomic oxygen and neon target gases are shown in Figures 1 and 2. Attempts were made to extend the calculations to the capture into s states with higher values of the quantum number n, and for capture into n = 4 states of sodium (results for the capture into the n = 3 ground state of sodium are

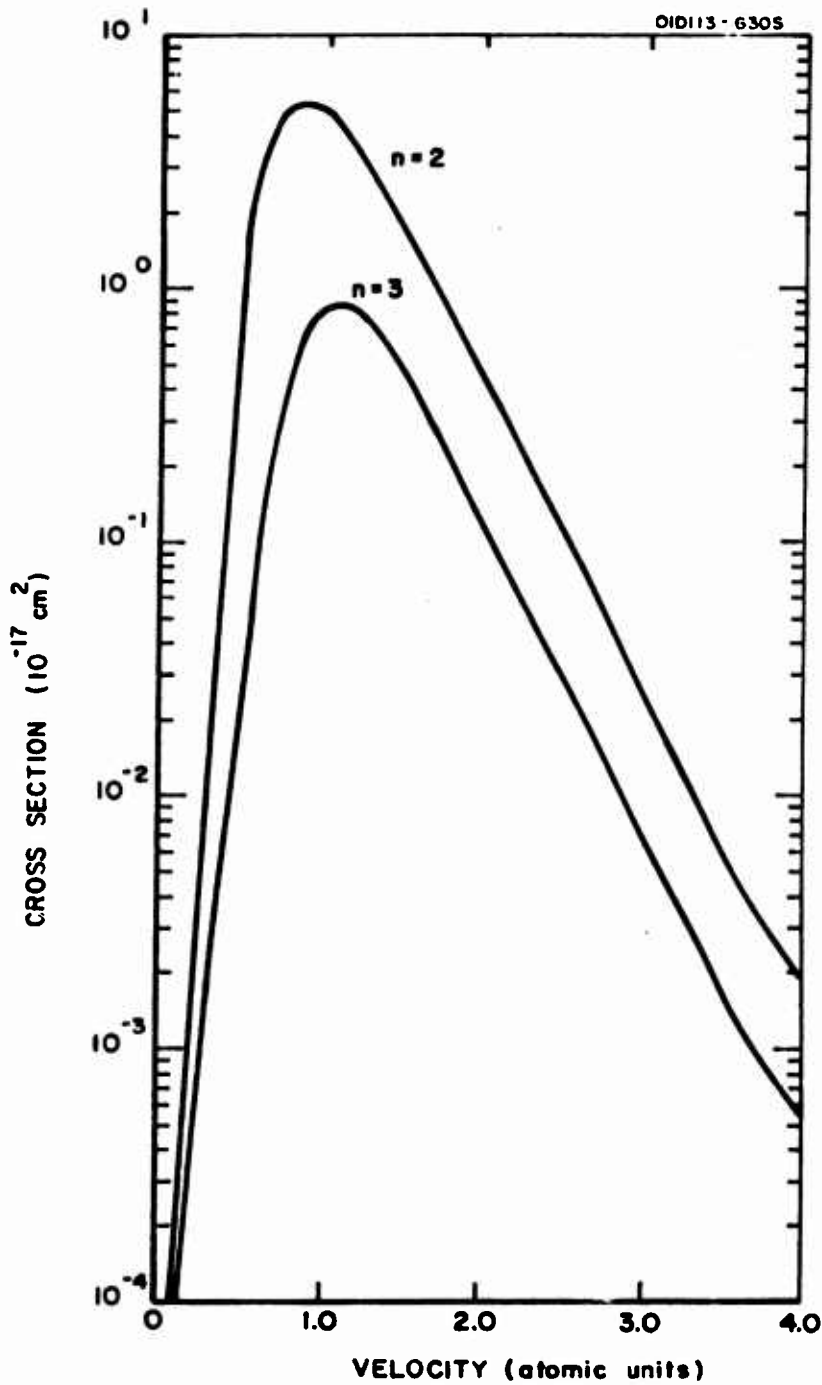


Figure 1. Charge Exchange Cross Sections for Capture into the n=2 and n=3 States of Lithium from Atomic Oxygen.

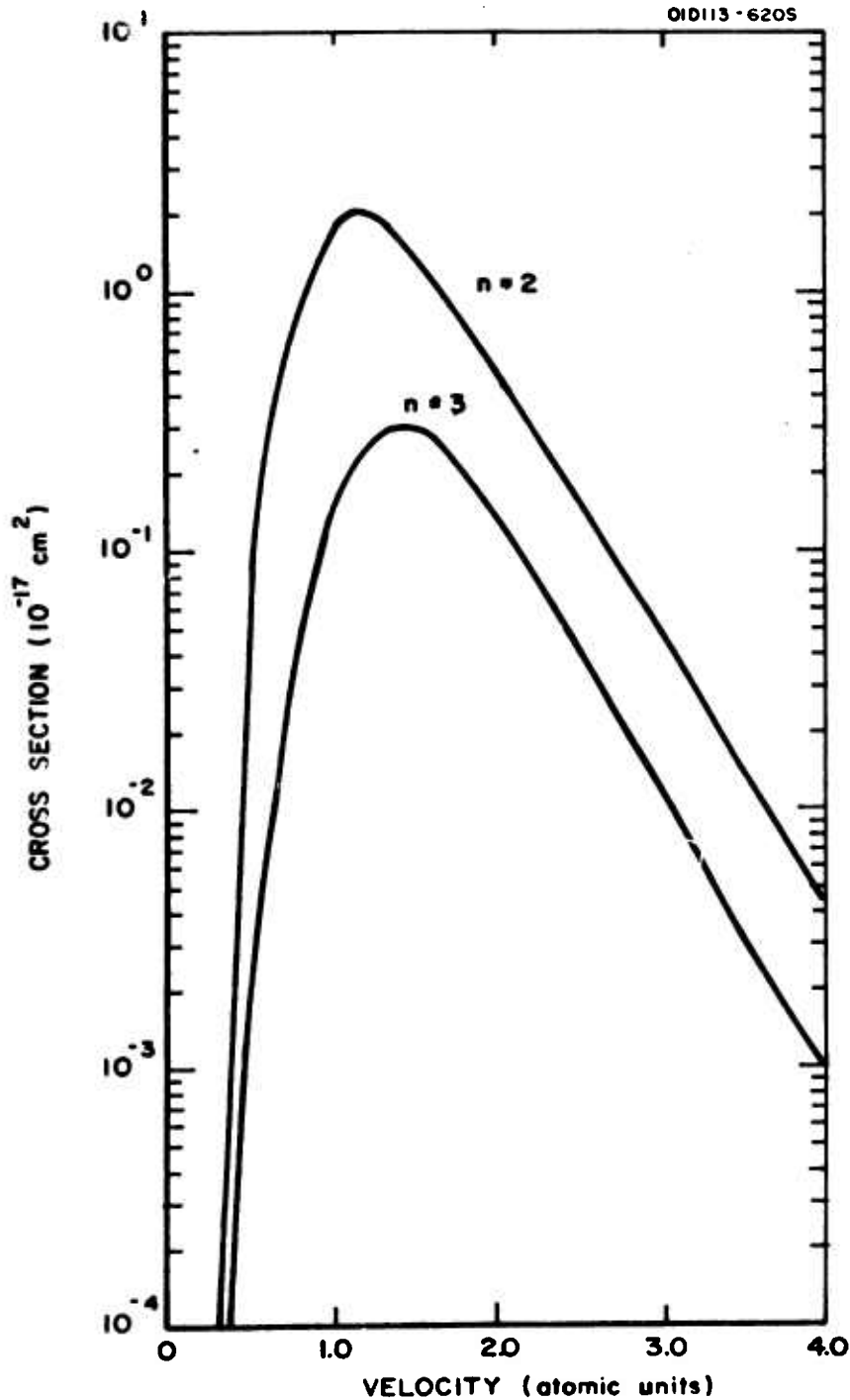


Figure 2. Charge Exchange Cross Sections for Capture into the n=2 and n=3 States of Lithium from Neon.

presented in Figures 3 and 4). The attempts have been unsuccessful since the number of nodes in an ns wavefunction increases with n , which introduces enough additional oscillations into the required matrix elements so that the present numerical procedures are not adequate. It may be possible to calculate capture cross sections into excited states with larger n than in the present case by using the existing programs and carefully adjusting those input parameters that control the integration step length and the quadrature formulae for the matrix elements. An alternate approach is to represent the higher excited states by ns model wavefunctions with lower values of n but with the effective charge selected to reproduce the experimental value of the excited state energy. Such a procedure can be expected to yield reliable results only if the dominant part of the capture cross section comes from those values of the impact parameter for which the incorrect representation of the inner nodes of the model wavefunction are not important. While such objections also can be made about the use of the $1s$ -model wavefunctions for the target and projectile systems in the calculation of the cross section for capture into the ground state, it must be remembered that the mean radius of an excited state orbital is much larger than the mean radius of the corresponding ground-state orbital. From the above discussion, it is clear that the accurate calculation of cross sections into highly excited states requires more careful study.

According to the Oppenheimer rule, the ratio of the cross section for capture at high energies into the $3s$ state of lithium to the cross section for capture into the $2s$ state should be $(2/3)^3 = 0.2963$. At the impact velocity of 3.0 atomic units, the calculated ratio is 0.27 for collisions with atomic oxygen and 0.26 for collisions with neon. The model calculations show that the impact velocity at which the cross section obtains its maximum value increases somewhat for the excited states and that the maximum cross sections depart significantly from the ratio of the cubes of the quantum numbers n . For the lithium-oxygen cross sections, the ratio of the maximum cross section for capture into the ground $2s$ state to the maximum cross section for capture into the $3s$ state is about 4.7, and the corresponding ratio for the neon target gas is 6.9.

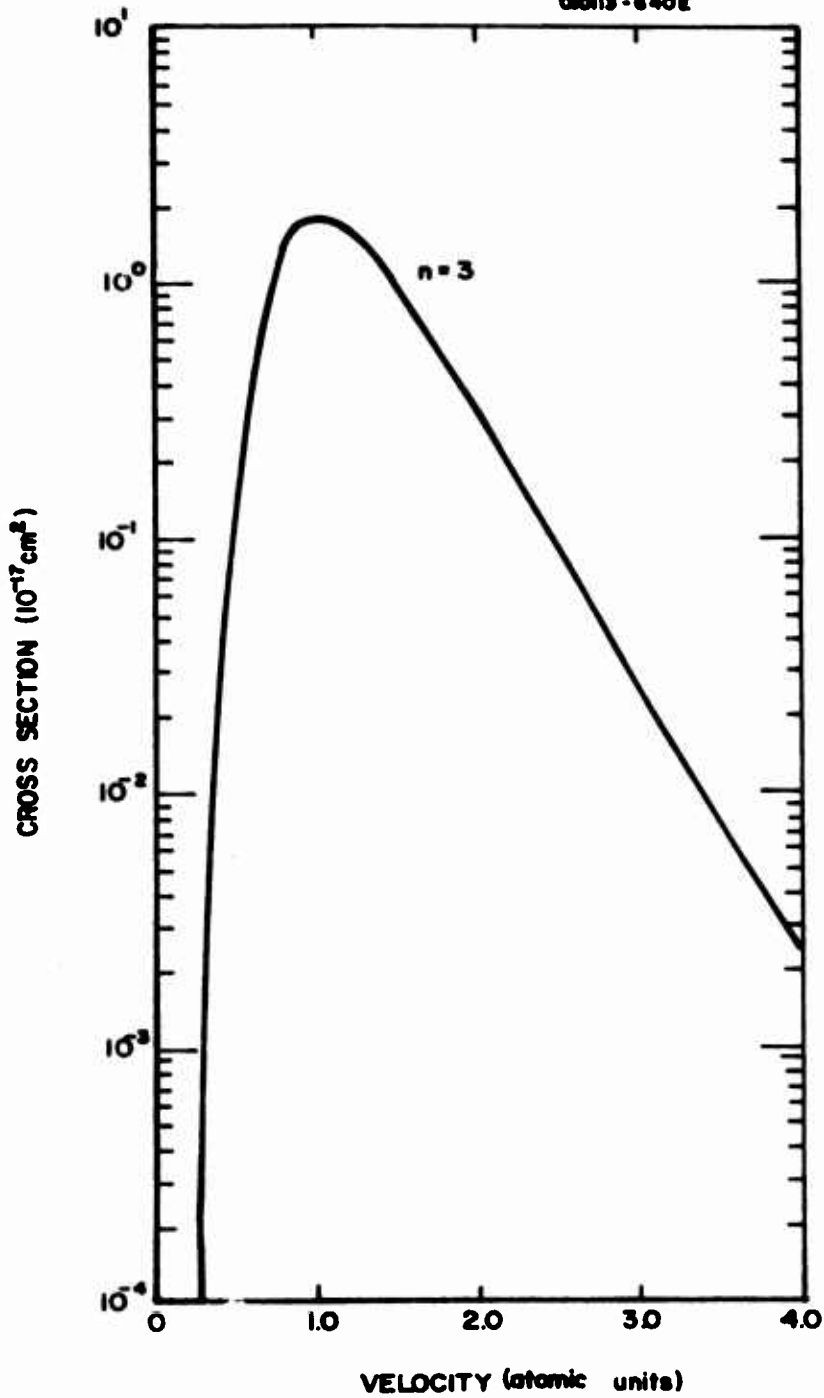


Figure 3. Charge Exchange Cross Section for Capture into the n=3 State of Sodium from Atomic Oxygen.

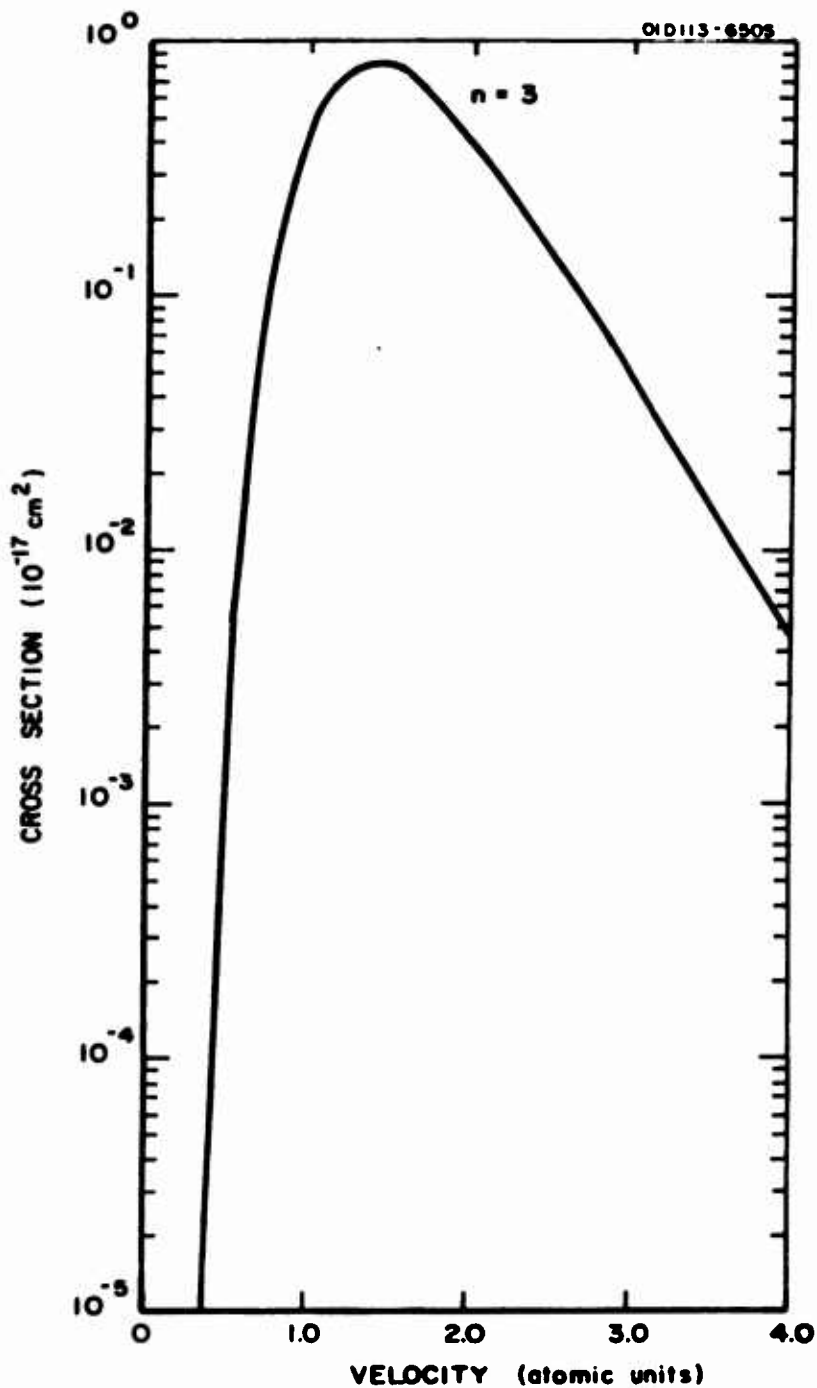


Figure 4. Charge Exchange Cross Section for Capture into the $n=3$ State of Sodium from Neon.

SECTION III

QUANTUM THEORY OF ELECTRON LOSS IN HEAVY-BODY COLLISIONS

1. Introduction

The collision processes of interest are of the type



where A and B are neutral or charged atoms and molecules. System A, which loses an electron during the collision, is termed the projectile, and system B is called the target system. It is assumed that either the target or projectile system is electrically neutral in the initial channel so that the problem is not complicated by a long-range Coulomb interaction among the reactants in the initial channel.

Ionization processes during very low-velocity heavy-body collisions have received some attention in the past few years. The low-energy theoretical treatments have involved a model based on a statistical treatment of the "evaporation" of electrons from an excited system created by the mutual interaction of the target and projectile charge distributions, or are based on the consideration of auto-ionization or Auger processes. Some relevant papers on low-energy ionization processes include Russek (Ref. 14), Fano and Lichten (Ref. 15), Kessel and Everhart (Ref. 16), and Demkov and Komarov (Ref. 17), while Smirnov and Firsov (Ref. 18) have considered negative ion-atom systems at low velocities. The details of the low-velocity theories will not be reviewed because it is unlikely that they can be meaningfully extended to treat moderate and high-energy collisions.

For high-energy heavy-body collisions involving ionization, the Belfast group (Ref. 19 through 21) have performed extensive calculations, using the Born approximation for light ions and atoms. Although the Born approximation results show good agreement with the experimental results at high energies, complete Born approximation calculations for many-electron projectile and target systems become involved and have not been attempted. Dmitriev and Nikolaev (Ref. 2) have proposed a model to describe stripping in high-energy collisions based on a free-collision approximation in which the Born approximation was used for the electron-target system scattering. They have performed explicit calculations for light target and projectile systems and find that the model yields results identical to the Born approximation at high energies. Calculations based on the free-collision approximation can be extended readily to many-electron target and projectile systems, with little computational difficulties.

2. Theory

Let k_0 be the magnitude of the initial momentum vector \underline{k}_0 of the electron incident on a spherically symmetric atom with Z electrons. Let \underline{k}_f be the final scattered electron momentum, and K be the magnitude of the momentum transfer vector $\underline{K} = \underline{k}_f - \underline{k}_0$. For elastic scattering,

$$e + B \rightarrow e + B \quad (29)$$

the cross section in momentum space from the Born approximation (Ref. 22) is

$$d\sigma_{e1} = \frac{8\pi}{k_0^2 K^3} |Z - F(K)|^2 dK \quad (30)$$

where $F(K)$ is the elastic form factor given by the ground state expectation value

$$F(K) = \sum_{j=1}^Z \langle \exp(i \underline{K} \cdot \underline{r}_j) \rangle \quad (31)$$

the sum being over the target electrons. For sufficiently large K , use can be made of the closure properties of the target eigenfunctions (Ref.22) and the sum of the cross sections of all contributing inelastic processes of the type

$$e + B \rightarrow e + B(n) \quad (32)$$

where n indicates excited target states, including the continuum, can be written in the Born approximation as

$$d\sigma_{in} = \frac{8\pi}{k_0^2 K^3} Z S_{in}(K) dK \quad (33)$$

where $S_{in}(K)$ is the incoherent scattering factor given by

$$S_{in}(K) = \frac{1}{Z} \left\{ \sum_{j,k=1}^Z \langle \exp[i \underline{K} \cdot (\underline{r}_j - \underline{r}_k)] \rangle - |F(K)|^2 \right\} \quad (34)$$

The evaluation of $S_{in}(K)$ is complicated by the occurrence of the expectation value of a two-electron operator. In order to use the closure relationship to obtain Equation (33), the momentum transfer must be much larger than the momentum required to supply the excitation energy for all significantly contributing inelastic processes. If the important momentum transfer values are not large enough to justify using the closure properties, it would be necessary to calculate the differential scattering cross section for all of the many significant inelastic excitation and ionization processes. Such calculations, on a large scale for many-electron targets, are impractical because of the need for accurate excited and continuum wavefunctions for the many-electron target system.

In the free-collision approximation, the projectile system is assumed to be composed of n electrons, each with a binding energy I_i required to remove the i -th electron, and each moving with an incident momentum k_0 , corresponding to the relative velocity between the two nuclei. These incident electrons are assumed to suffer elastic and inelastic collisions as free electrons with the target system. For the elastic scattering, the electron is assumed to be removed from the projectile system if the momentum transfer it acquires in the collision is sufficient to increase its energy by an amount greater than its binding energy I_i . For the inelastic scattering, the electron is assumed to be removed if it acquires enough energy through the momentum transfer to exceed both the binding energy of the electron to the projectile and the excitation energy required to excite the target. The total stripping cross section is given by

$$\sigma = \sum_{i=1}^n \left\{ \int_{k_{1i}}^{k_{2i}} d\sigma_{el} + \int_{k_{3i}}^{k_{4i}} d\sigma_{in} \right\} \quad (35)$$

where the sum is taken over the projectile electrons and the limits of integration are determined by the kinematics. The lower limit for the elastic contribution, k_{1i} is given by

$$k_{1i} = \sqrt{2 I_i} \quad (36)$$

and the upper limit is given by

$$k_{2i} = 2 k_0 \quad (37)$$

The lower limit for the inelastic contribution is the greater of the two quantities

$$\sqrt{2 I_i} \quad \text{and} \quad k_0 \left[1 - (1 - 2\Delta E/k_0^2)^{1/2} \right]$$

where the first quantity represents the minimum momentum transfer required to increase the energy of the i -th target electron by I_1 , and the second quantity is the minimum momentum transfer needed to transfer an excitation energy ΔE to the target system. Dmitriev and Nikolaev (Ref. 2) suggest using I_0 , the first ionization potential of the target system as ΔE . At high values of the incident momentum k_0 , i.e., $k_0^2 \gg \Delta E$, the choice of ΔE is unimportant because the first quantity is independent of k_0 and the second decreases as $\Delta E/k_0$ so that for large k_0 , the lower limit is determined entirely by $\sqrt{2 I_1}$, except possibly for inner shell electrons, which make little contribution to the sum in Equation (35). For processes in which $\Delta E > I_1$, for example the stripping of the loosely bound electron from a negative ion, the value of ΔE is important because the lower limit is determined by the expression containing ΔE for a considerable range of initial momentum k_0 . For this energy range, the use of Equation (33) is not valid because the conditions necessary for the use of the closure properties is not justified. It has been assumed that ΔE is given by the logarithmic mean energy, which enters in the Bethe (Ref. 23) theory for the stopping of fast heavy particles in matter, so that

$$\ln \Delta E = \frac{\sum_j f_{oj} \ln(E_{oj})}{\sum_j f_{oj}} \quad (38)$$

where f_{oj} is the oscillator strength for excitation of the target system from the ground state to the level j , E_{oj} is the corresponding excitation energy, and the summations in Equation (38) include integrations over the continuum. The use of Equation (38) to determine the lower limit of the inelastic scattering integration can be considered as using an effective upper limit for ΔE . The upper limit for the inelastic scattering contribution must also be selected with care. From purely kinematical arguments, k_{41} for the inelastic electron-atom scattering would be about $2 k_0$. However, Equation (33) fails at very high energies and the maximum momentum transfer involved is the maximum momentum transfer in electron-electron scattering processes which is k_0 . According to Dmitriev and Nikolaev (Ref. 2), the following is used

$$k_{41} = k_0 \quad (39)$$

Both the form factor $F(K)$ and the incoherent scattering factor $S_{in}(K)$ are important in the field of X-ray physics, the former in elastic X-ray scattering and the latter in Compton scattering of X-rays, so that considerable work on the calculation of the scattering factors is available from the literature. Kim and Inokuti (Ref. 24) have calculated highly accurate values of $F(K)$ and $S_{in}(K)$ for helium by using the accurate correlated wavefunction of Hart and Herzberg (Ref. 25). For systems with more electrons, Hartree-Fock calculations have been performed for the scattering

factors, a recent tabulation being reference 26. Many of the values of the scattering factors given in reference 26 are taken from the work of Freeman (Ref. 27), who considers systems with other than S ground-state symmetry. Cromer and Mann (Ref. 28) have recently published incoherent scattering factor calculations for most closed shell systems, using Hartree-Fock wavefunctions. For the target systems of interest in this study, it is not necessary to calculate scattering factors because the values have been tabulated in the literature. For nonspherical target systems, the spherical target systems, the spherical average scattering factors have been employed to be consistent with the neglect of the symmetry properties of the projectile system. For all atomic systems, the elastic scattering factor is a monotonically decreasing function of K, having the value Z for K = 0 and decreasing to zero for large K. The incoherent scattering factor is a monotonically increasing function of K, assuming the value 0 at K = 0, and increasing to Z for large values of K. The integrands for both the elastic and inelastic contributions to Equation (35) are smooth functions of K so that the integrals are performed simply by standard numerical methods. The integrands for helium, using the calculations of Kim and Ionkuti (Ref. 24), are shown in Figure 5. From the behavior of the inelastic integrand for low values of momentum transfer, it can be seen that the inelastic contribution is more sensitive to the value of the lower limit of integration than the elastic contribution.

Both integrands decrease rapidly for large K, so that the large k_0 , the upper limits may be replaced by ∞ and the high energy behavior of the stripping cross section becomes

$$\sigma = a/k_0^2 \quad (40)$$

where

$$a = 8\pi \sum_{i=1}^{n_i} \int_{\sqrt{2} I_i}^{\infty} \frac{dK}{K^3} \left\{ |Z - F(K)|^2 + Z S_{in}(K) \right\} \quad (41)$$

The E^{-1} high-energy dependence of the stripping cross section is consistent with experimental data (see Section IV-2).

The information needed for the projectile system is the number of electrons in each shell and the one-electron energies required to remove the electron from the individual shells. For neutral and positive ion projectiles, the energy needed to remove the outermost electron is the ionization potentials, which are taken from the experimental tabulations of Moore (Ref. 29). For the inner shells, the estimates of Slater (Ref. 30) are used. Results of detailed calculations and comparison with experimental results are presented in Section IV-2.

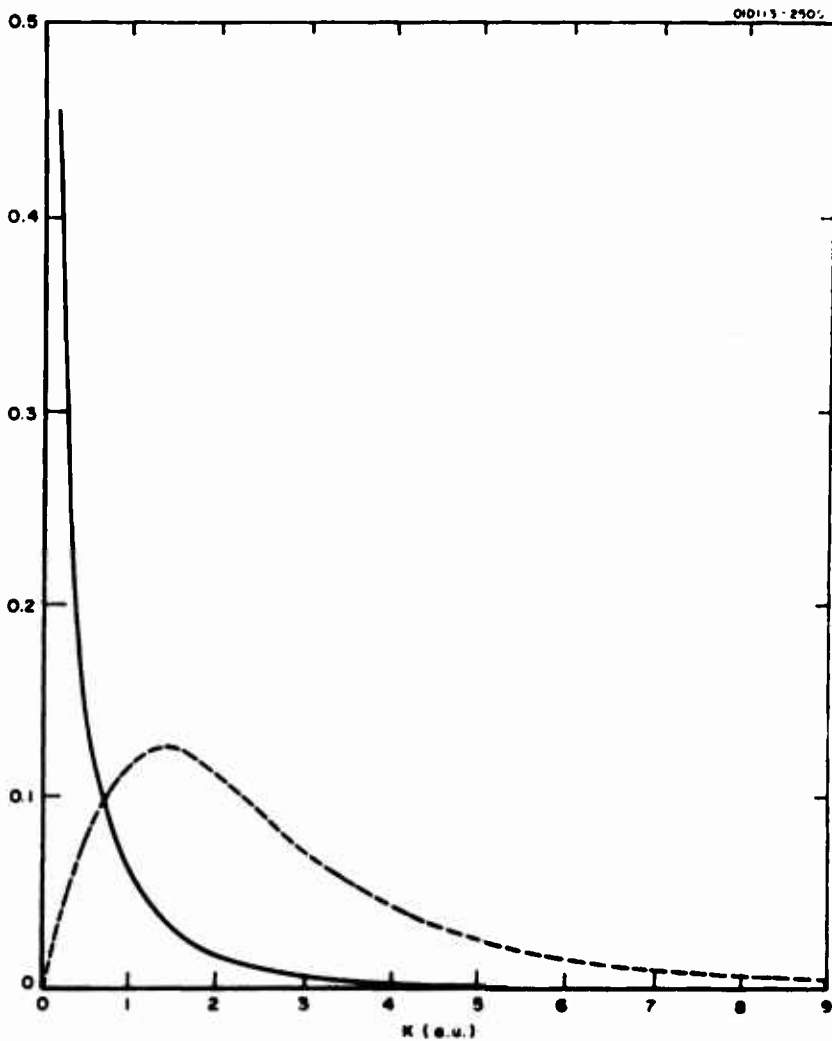


Figure 5. The Integrands, in Atomic Units, of Equation (35) for Helium Using the Scattering Factors of Reference 24. The Solid Curve is the Inelastic Integrand, the Dashed Curve the Elastic Integrand.

SECTION IV

RESULTS

1. Charge Exchange

The results of using the basic $1s$ model are presented in Tables II through VIII and graphed in Figures 6 through 46 where the experimental results of Layton and Fite (Ref. 31) are also shown. The calculated cross sections, as might be expected from such a simple model, share the same general shape although the predicted maximum cross sections vary through several orders of magnitude for different reactions. In the case of molecular O_2 and N_2 targets, these have been treated as single systems with approximately the same ionization potentials as the atomic systems, thus a factor of two has not been applied to the calculated cross sections in these cases.

The $1s$ model cross sections are usually smaller than the experimentally measured values. Where a comparison with the experimental results is possible, the $1s$ model yields a sharper maximum than the former, from there falling off much too rapidly as the energy diminishes and somewhat more rapidly in some cases as the energy increases. Use of the n^* model may give a less rapid fall-off at the high-velocity end, as may be seen from Figure 47. At a sufficiently high energy, the exchange correction will certainly operate in the favorable sense.

TABLE II

CROSS SECTIONS σ_{10} (UNITS OF 10^{-17} cm^2) CALCULATED FOR K^+ PROJECTILES (1s MODEL)

VELOCITY (10^8 cm sec^{-1})	ENERGY (keV)	TARGETS*					
		H	He	Ne	Ar	N	O
0.314	20	7.93(-3)	1.50(-5)	2.98(-5)	1.20(-3)	3.46(-3)	7.80(-3)
0.444	40	6.50(-2)	3.78(-4)	8.09(-4)	1.15(-2)	2.98(-2)	6.39(-2)
0.544	60	4.86(-1)	1.38(-3)	4.81(-3)	1.28(-1)	2.68(-1)	4.80(-1)
0.628	80	1.31(0)	1.10(-2)	3.70(-2)	4.78(-1)	8.35(-1)	1.29(0)
0.737	110	2.15(0)	6.39(-2)	1.61(-1)	9.97(-1)	1.51(0)	2.13(0)
0.875	155	3.22(0)	1.71(-1)	3.22(-1)	1.36(0)	2.13(0)	3.19(0)
1.217	300	9.87(0)	2.62(-1)	5.95(-1)	4.50(0)	7.00(0)	9.80(0)
1.571	500	1.19(1)	8.53(-1)	1.80(0)	7.33(0)	9.67(0)	1.19(1)
2.048	850	7.72(0)	1.63(0)	2.59(0)	5.92(0)	6.90(0)	7.71(0)
2.629	1400	3.26(0)	1.42(0)	1.86(0)	2.89(0)	3.10(0)	3.25(0)
3.142	2000	1.39(0)	9.07(-1)	1.07(0)	1.34(0)	1.38(0)	1.39(0)
3.369	2300	9.49(-1)	7.11(-1)	8.09(-1)	9.44(-1)	9.51(-1)	9.50(-1)
4.713	4500	1.05(-1)	1.37(-1)	1.35(-1)	1.17(-1)	1.11(-1)	1.05(-1)

*The number in parentheses is the power of 10 by which the entries are to be multiplied.

TABLE III

CROSS SECTIONS σ_{10} (UNITS OF 10^{-17} cm²) CALCULATED FOR I⁺ PROJECTILES (1s MODEL)

VELOCITY (10^8 cm sec ⁻¹)	ENERGY (keV)	TARGETS*						
		H	He	Ne	Ar	N	O	
0.174	20	1.63(0)	1.33(-5)	1.47(-5)	4.01(-2)	3.00(-1)	1.57(0)	
0.247	40	3.64(0)	7.97(-5)	7.42(-4)	3.52(-1)	1.27(0)	3.55(0)	
0.302	60	1.74(1)	5.82(-4)	2.35(-3)	1.66(0)	6.11(0)	1.71(1)	
0.349	80	2.29(1)	5.27(-3)	4.64(-2)	3.06(0)	8.93(0)	2.25(1)	
0.409	110	3.00(1)	7.57(-3)	5.21(-2)	3.92(0)	1.21(1)	2.95(1)	
0.485	155	4.86(1)	7.18(-2)	3.07(-1)	1.01(1)	2.45(1)	4.80(1)	
0.675	300	7.52(1)	4.25(-1)	1.56(0)	2.80(1)	5.00(1)	7.46(1)	
0.872	500	7.82(1)	2.21(0)	5.62(0)	4.11(1)	6.01(1)	7.78(1)	
1.137	850	7.88(1)	4.73(0)	1.08(1)	5.09(1)	6.61(1)	7.86(1)	
1.459	1400	6.43(1)	9.79(0)	1.83(1)	5.00(1)	5.82(1)	6.42(1)	
1.744	2000	4.52(1)	1.27(1)	1.98(1)	3.89(1)	4.27(1)	4.52(1)	
2.616	4500	1.15(1)	8.14(0)	9.57(0)	1.15(1)	1.15(1)	1.15(1)	
3.899	10000	1.48(0)	1.82(0)	1.82(0)	1.63(0)	1.55(0)	1.48(0)	

*The number in parentheses is the power of 10 by which the entries are to be multiplied.

TABLE IV

CROSS SECTIONS σ_{10} (UNITS OF 10^{-17} cm^2) CALCULATED FOR Ct^+ PROJECTILE ($1s$ MODEL)

VELOCITY (10^8 cm sec^{-1})	ENERGY (keV)	TARGETS*						
		H	He	Ne	Ar	N	O	
0.275	20	9.04(-3)	1.26(-5)	5.90(-5)	5.98(-4)	1.62(-3)	8.72(-3)	
0.387	40	4.84(-1)	5.19(-4)	2.61(-3)	9.45(-2)	2.28(-1)	4.77(-1)	
0.475	60	1.46(0)	2.86(-3)	9.88(-3)	3.24(-1)	7.38(-1)	1.44(0)	
0.548	80	3.21(0)	6.57(-3)	3.10(-2)	7.73(-1)	1.67(0)	3.17(0)	
0.642	110	7.65(0)	3.79(-2)	1.45(-1)	2.32(0)	4.46(0)	7.56(0)	
0.765	155	1.28(1)	2.31(-1)	6.06(-1)	4.85(0)	8.21(0)	1.27(1)	
1.065	300	2.69(1)	7.83(-1)	1.64(0)	1.20(1)	1.89(1)	2.67(1)	
1.371	500	3.34(1)	1.86(0)	4.24(0)	2.00(1)	2.69(1)	3.33(1)	
1.786	850	2.41(1)	4.24(0)	7.22(0)	1.82(1)	2.14(1)	2.40(1)	
2.292	1400	1.17(1)	4.47(0)	6.14(0)	1.02(1)	1.11(1)	1.16(1)	
2.436	1600	9.06(0)	4.10(0)	5.38(0)	8.19(0)	8.71(0)	9.05(0)	
2.739	2000	5.65(0)	3.28(0)	4.01(0)	5.36(0)	5.55(0)	5.65(0)	
3.336	3000	2.04(0)	1.73(0)	1.91(0)	2.09(0)	2.07(0)	2.04(0)	
4.307	5000	4.25(-1)	5.26(-1)	5.26(-1)	4.70(-1)	4.47(-1)	4.26(-1)	

*The number in parentheses is the power of 10 by which the entries are to be multiplied.

TABLE V

CROSS SECTIONS σ_{10} (UNITS OF 10^{-17} cm^2) CALCULATED FOR Li^+ PROJECTILE ($1s$ MODEL)

VELOCITY (10^8 cm sec^{-1})	ENERGY (keV)	TARGETS*						
		H	He	Ne	Ar	N	O	
0.219	1.72	9.03(-4)	-----	1.13(-5)	1.05(-4)	3.13(-4)	7.50(-4)	
0.273	2.69	5.00(-3)	-----	5.11(-5)	4.82(-4)	1.76(-3)	5.22(-3)	
0.320	3.87	6.46(-2)	6.97(-5)	1.70(-4)	1.04(-2)	2.40(-2)	5.83(-2)	
0.547	10.8	1.11(0)	-----	9.41(-3)	2.82(-1)	5.99(-1)	1.09(0)	
1.09	43.0	1.46(1)	4.67(-1)	8.89(-1)	6.22(0)	1.00(1)	1.44(1)	
1.64	96.8	1.83(1)	1.89(0)	3.66(0)	1.22(1)	1.54(1)	1.82(1)	
2.19	172.0	9.43(0)	2.79(0)	4.09(0)	7.83(0)	8.75(0)	9.46(0)	
4.38	688.0	2.72(-1)	3.31(-1)	3.32(-1)	2.99(-1)	2.85(-1)	2.72(-1)	
6.56	1548.0	1.12(-2)	2.24(-2)	1.98(-2)	1.37(-2)	1.23(-2)	1.12(-2)	

* The number in parentheses is the power of 10 by which the entries are to be multiplied.

TABLE VI

CROSS SECTIONS σ_{10} (UNITS OF 10^{-17} cm^2) CALCULATED FOR Na^+ PROJECTILE ($1s$ MODEL)

VELOCITY (10^8 cm sec^{-1})	ENERGY (keV)	TARGETS*						
		H	He	Ne	Ar	O	N	
0.219	5.70	6.05(-4)	1.11(-5)	1.37(-5)	8.83(-5)	6.02(-4)	2.11(-4)	
0.273	8.91	4.05(-3)	2.33(-5)	4.39(-5)	3.62(-4)	3.97(-3)	1.15(-3)	
0.328	12.8	2.90(-2)	6.63(-5)	1.64(-4)	6.68(-3)	2.90(-2)	1.69(-2)	
0.547	35.6	9.20(-1)	3.27(-4)	9.03(-3)	2.36(-1)	9.08(-1)	5.00(-1)	
1.09	142.0	1.25(1)	4.10(-1)	7.61(-1)	5.29(0)	1.25(1)	8.57(0)	
1.64	321.0	1.66(1)	1.64(0)	3.22(0)	1.10(1)	1.65(1)	1.39(1)	
2.19	570.0	8.73(0)	2.50(0)	3.69(0)	7.16(0)	8.72(0)	8.04(0)	
4.38	2280.0	2.50(-1)	3.02(-1)	3.04(-1)	2.75(-1)	2.50(-1)	2.62(-1)	
6.56	5130.0	1.02(-2)	2.04(-2)	1.80(-2)	1.25(-2)	1.02(-2)	1.12(-2)	

*The number in parentheses is the power of 10 by which the entries are to be multiplied.

TABLE VII

CROSS SECTIONS σ_{10} (UNITS OF 10^{-17} cm^2) CALCULATED FOR Rb^+ PROJECTILE (1s MODEL)

VELOCITY (10^8 cm sec^{-1})	ENERGY (keV)	TARGETS*						
		H	He	Ne	Ar	O	N	
0.219	21.2	1.74(-4)	1.33(-5)	1.26(-5)	4.86(-5)	1.73(-4)	1.05(-4)	
0.273	33.1	8.35(-4)	1.98(-5)	3.49(-5)	1.91(-4)	8.04(-4)	4.39(-4)	
0.328	47.7	1.14(-2)	6.35(-5)	1.45(-4)	2.37(-3)	-----	5.91(-3)	
0.547	132.0	4.62(-1)	2.17(-3)	5.93(-3)	1.24(-1)	4.56(-1)	2.58(-1)	
1.09	530.0	6.55(0)	2.36(-1)	4.04(-1)	2.63(0)	6.50(0)	4.36(0)	
1.64	1192.0	1.07(1)	9.06(-1)	1.83(0)	6.80(0)	1.07(1)	8.80(0)	
2.19	2119.0	6.03(0)	1.54(0)	2.33(0)	4.80(0)	6.02(0)	5.48(0)	
4.38	8477.0	1.73(-1)	2.02(-1)	2.05(-1)	1.89(-1)	1.73(-1)	1.81(-1)	
6.56	19070.0	6.74(-3)	1.34(-2)	1.18(-2)	8.25(-3)	6.75(-3)	7.41(-3)	

*The number in parentheses is the power of 10 by which the entries are to be multiplied.

TABLE VIII

CROSS SECTIONS σ_{10} (UNITS OF 10^{-17} cm^2) CALCULATED FOR Cs^+ PROJECTILE (1s MODEL)

VELOCITY (10^3 cm sec^{-1})	ENERGY (keV)	TARGETS*				
		H	He	Ne	Ar	
0.219	32.9	1.32(-4)	1.12(-5)	1.39(-5)	4.35(-5)	1.29(-4)
0.273	51.5	6.53(-4)	1.92(-5)	3.53(-5)	1.75(-4)	6.34(-4)
0.328	74.1	6.07(-3)	6.05(-5)	1.34(-4)	1.83(-3)	7.09(-3)
0.547	205.0	3.79(-1)	2.69(-6)	5.57(-3)	1.04(-1)	3.74(-1)
1.09	824.0	5.25(0)	1.98(-1)	3.29(-1)	2.08(0)	5.20(0)
1.64	1853.0	9.18(0)	7.41(-1)	1.51(0)	5.76(0)	9.15(0)
2.19	3295.0	5.29(0)	1.31(0)	1.99(0)	4.18(0)	5.28(0)
4.38	13180.0	1.52(-1)	1.76(-1)	1.79(-1)	1.66(-1)	1.52(-1)
6.56	29655.0	5.84(-3)	1.16(-2)	1.02(-2)	7.15(-3)	5.85(-3)

*The number in parentheses is the power of 10 by which the entries are to be multiplied.

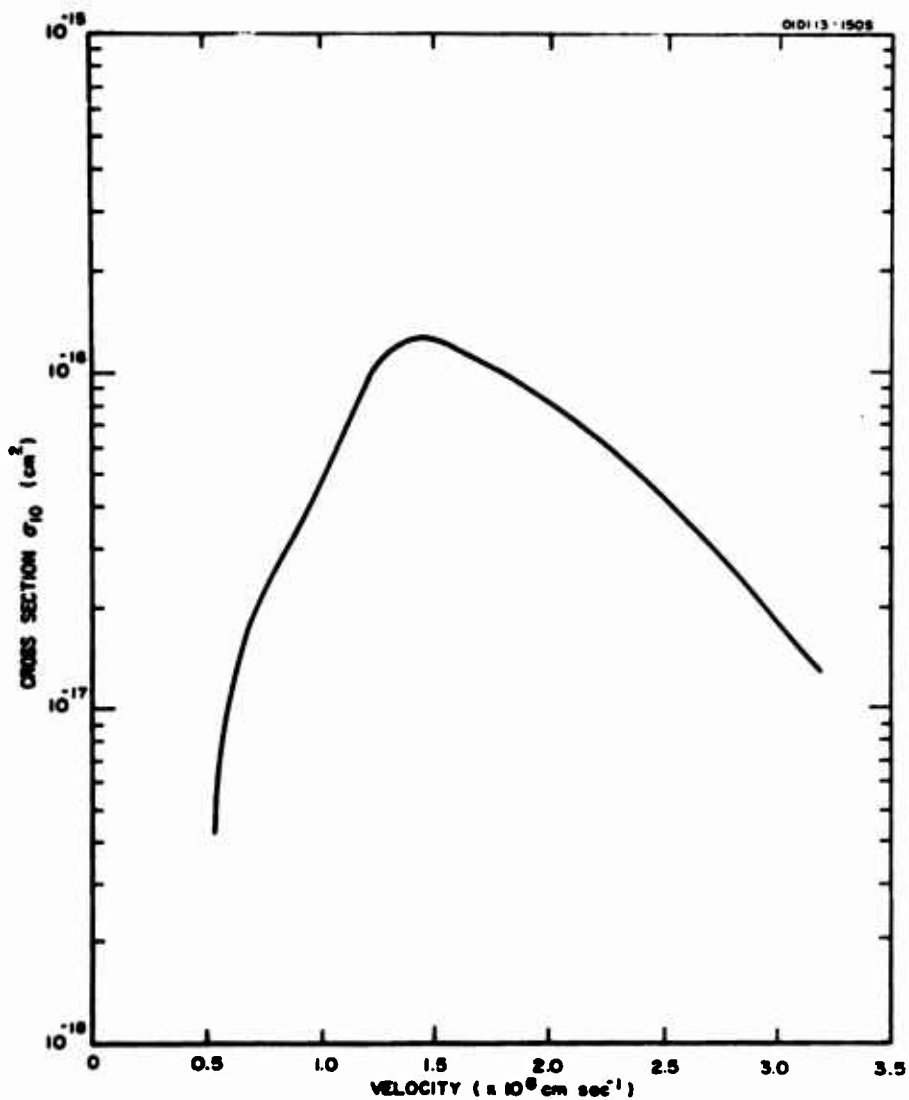


Figure 6. Charge Exchange Cross Section for Capture into the Ground State for Singly Charged Potassium in Atomic Hydrogen.

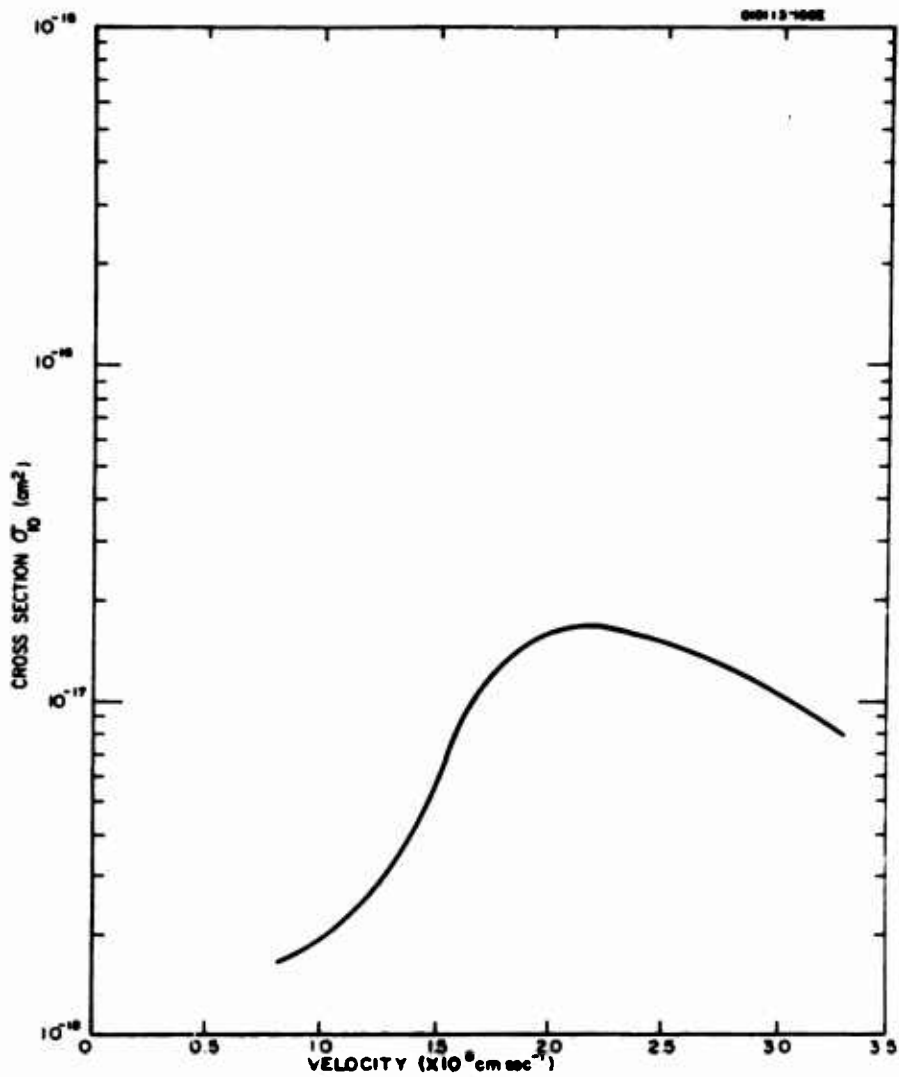


Figure 7. Charge Exchange Cross Section for Capture into the Ground State for Singly Charged Potassium in Helium.

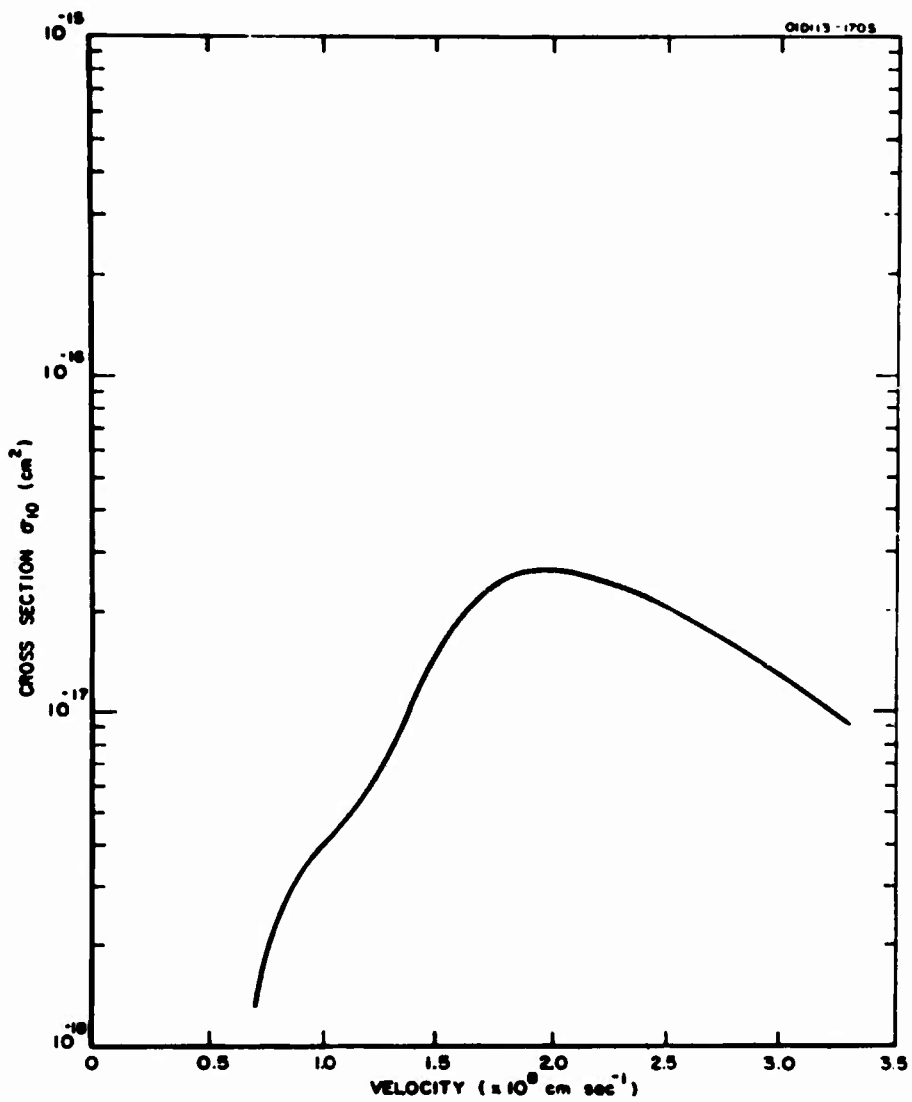


Figure 8. Charge Exchange Cross Section for Capture into the Ground State for Singly Charged Potassium in Neon.

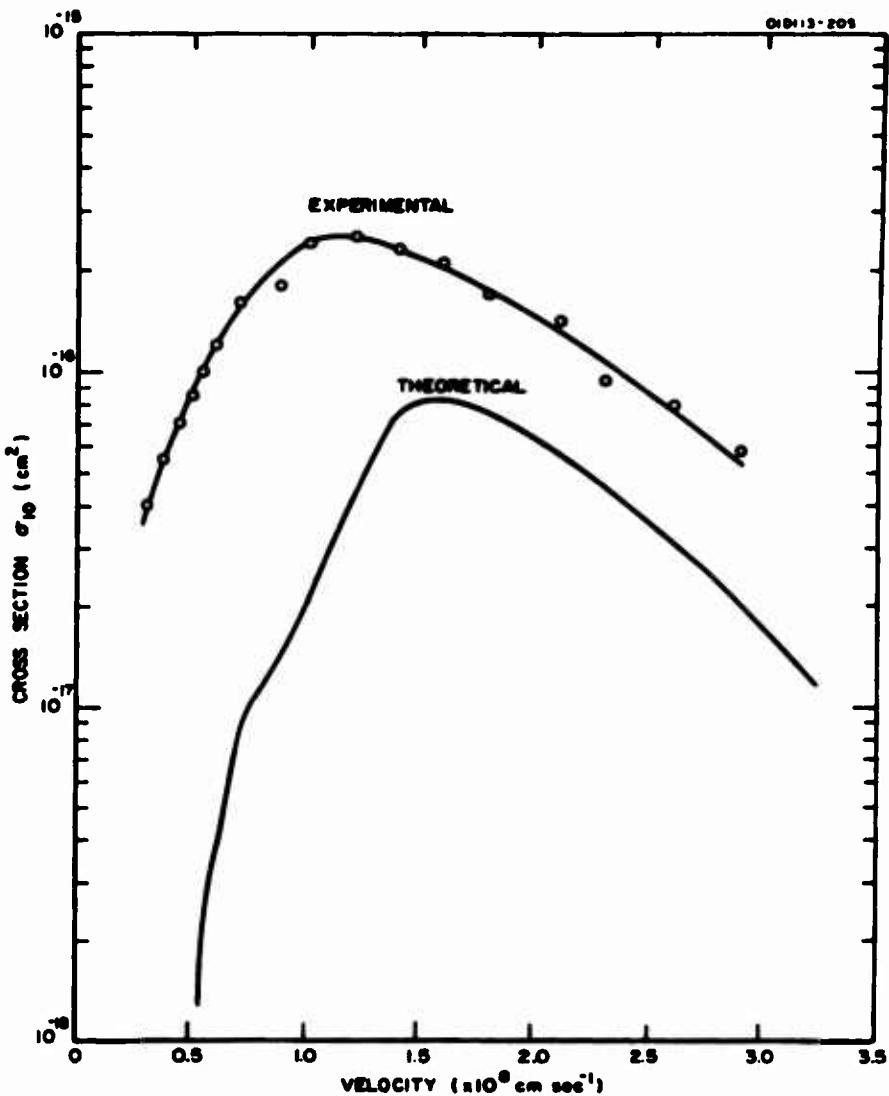


Figure 9. Charge Exchange Cross Section for Capture into the Ground State for Singly Charged Potassium in Argon. The Experimental Results are from Reference 31.

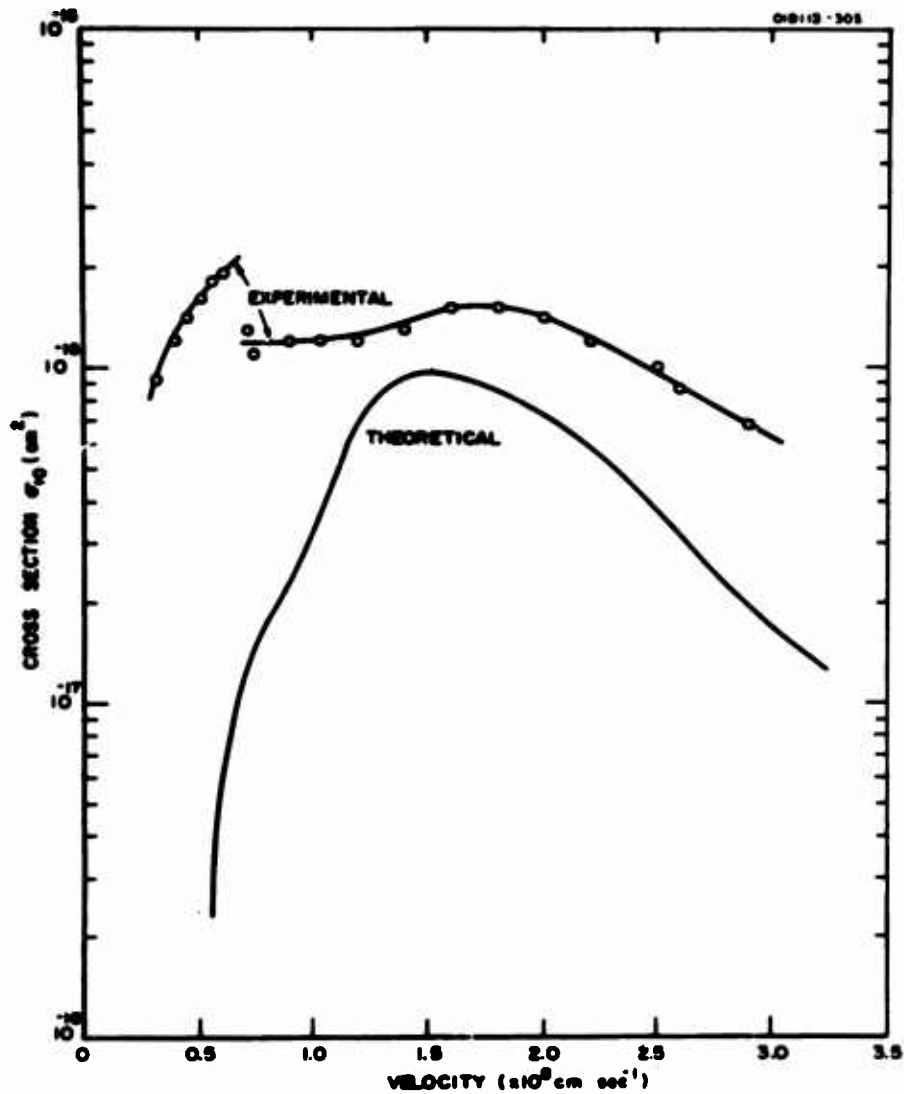


Figure 10. Charge Exchange Cross Section for Capture into the Ground State for Singly Charged Potassium in Atomic Nitrogen. The Experimental Results are from Reference 31.

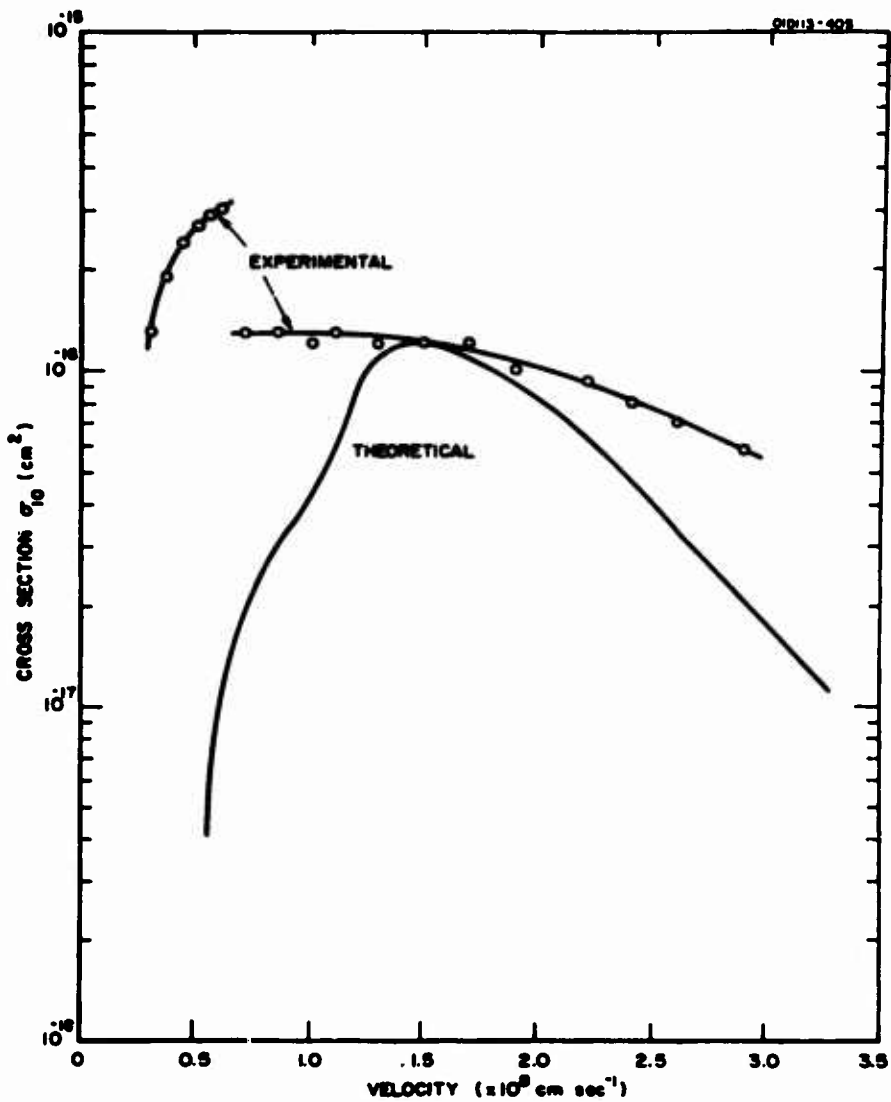


Figure 11. Charge Exchange Cross Section for Capture into the Ground State for Singly Charged Potassium in Atomic Oxygen. The Experimental Results are from Reference 31.

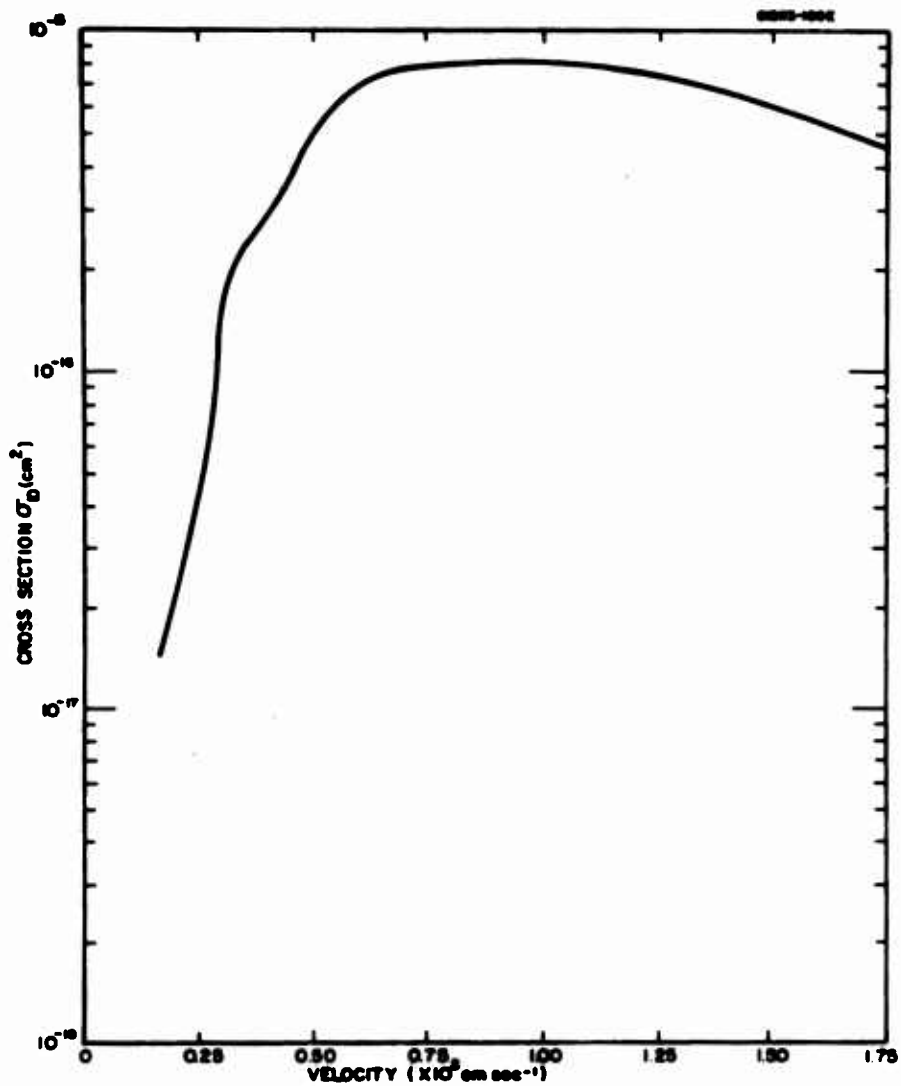


Figure 12. Charge Exchange Cross Section for Capture into the Ground State for Singly Charged Iodine in Atomic Hydrogen.

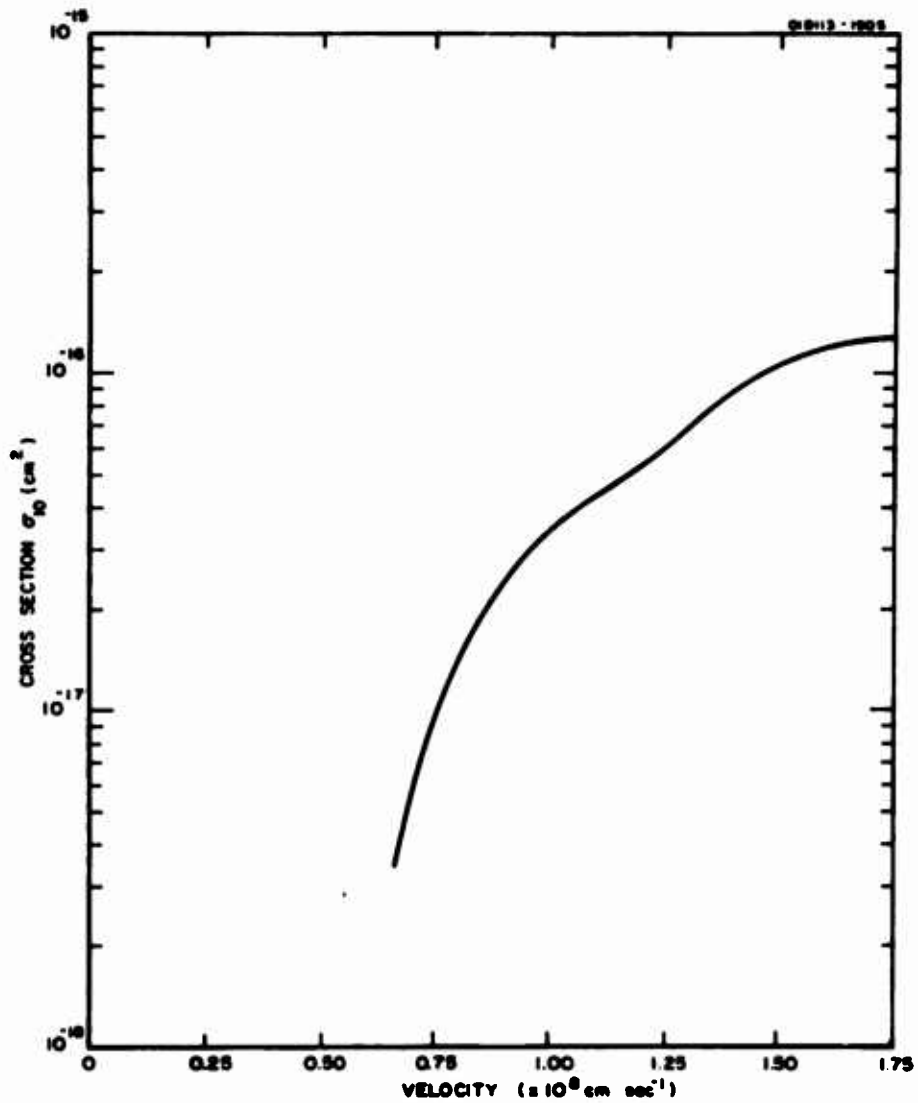


Figure 13. Charge Exchange Cross Section for Capture into the Ground State for Singly Charged Iodine in Helium.

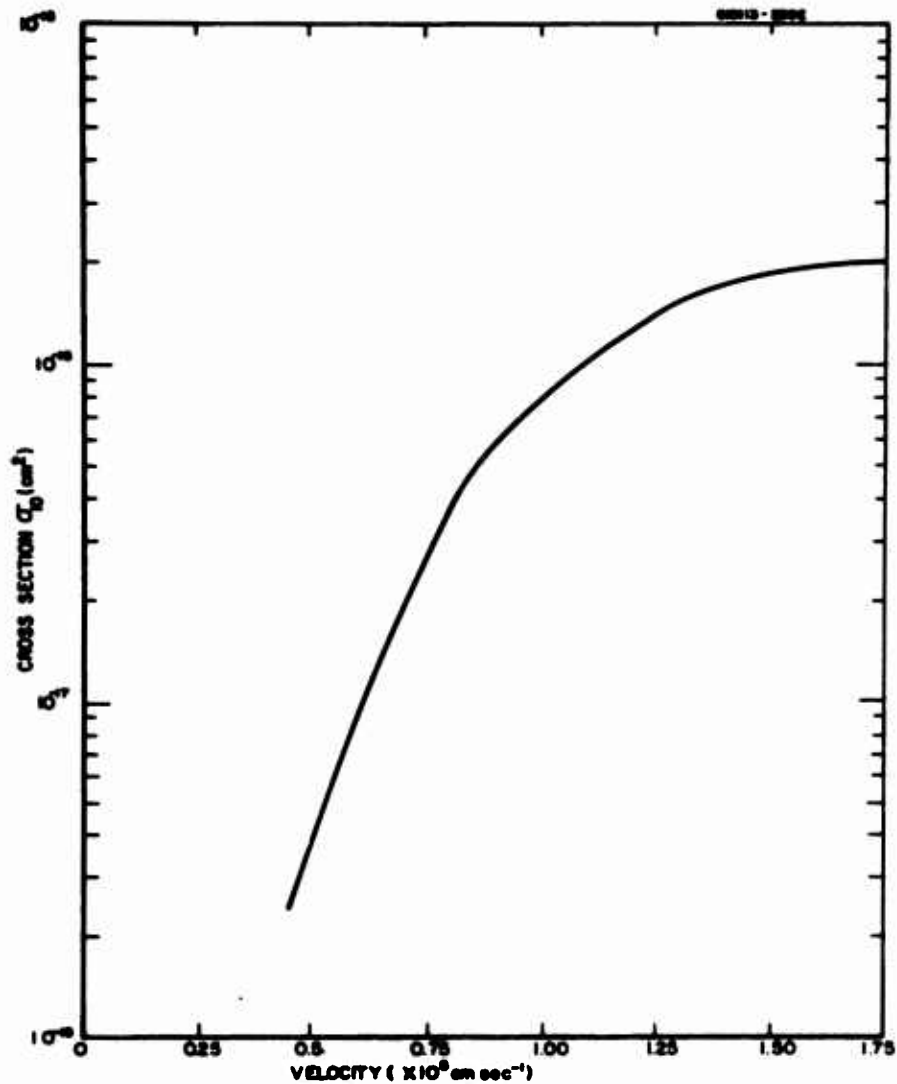


Figure 14. Charge Exchange Cross Section for Capture into the Ground State for Singly Charged Iodine in Neon.

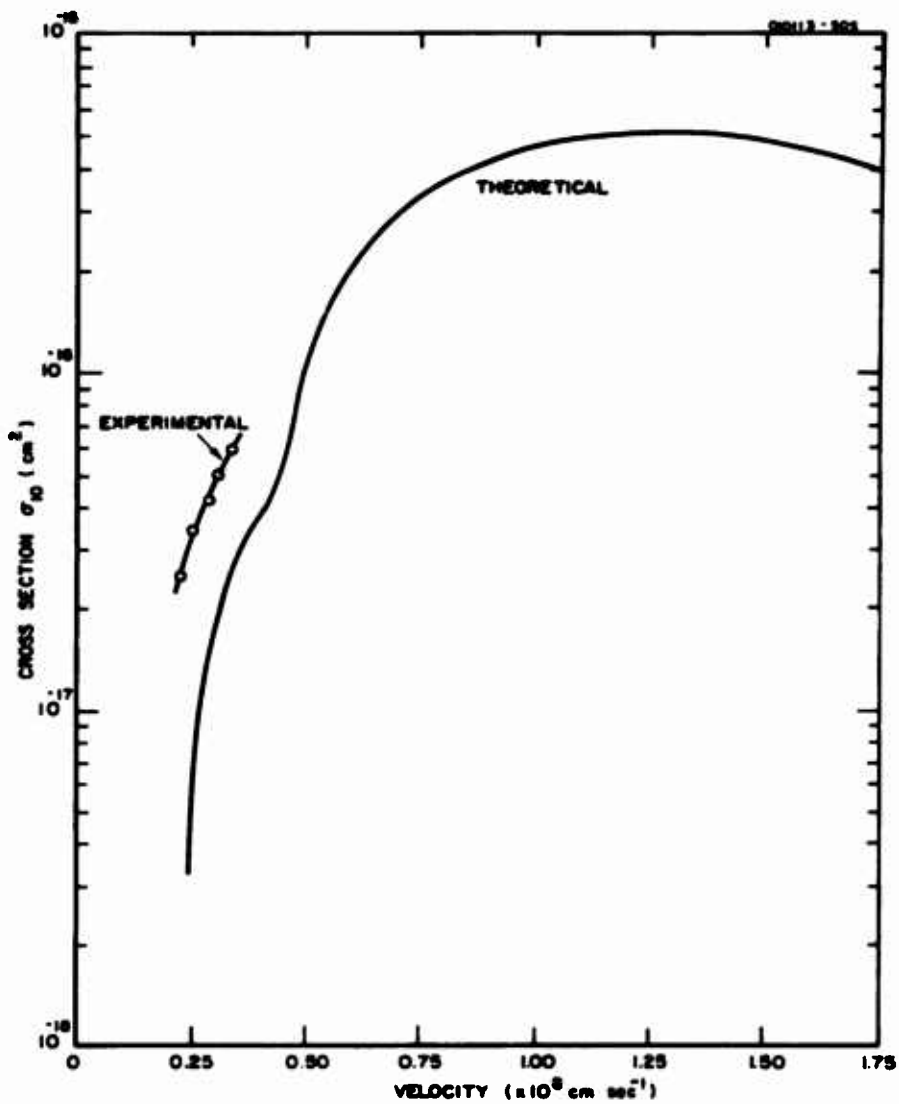


Figure 15. Charge Exchange Cross Section for Capture into the Ground State for Singly Charged Iodine in Argon. The Experimental Results are from Reference 31.

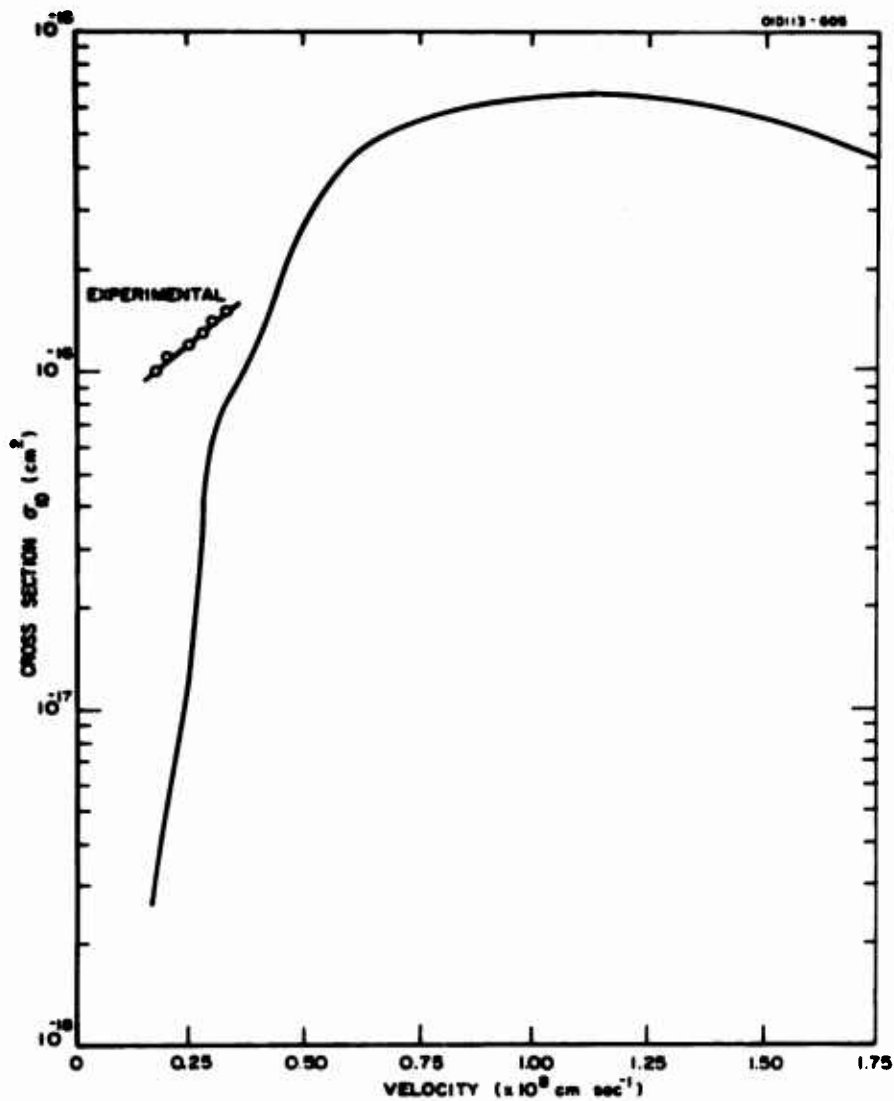


Figure 16. Charge Exchange Cross Section for Capture into the Ground State for Singly Charged Iodine in Atomic Nitrogen. The Experimental Results are from Reference 31.

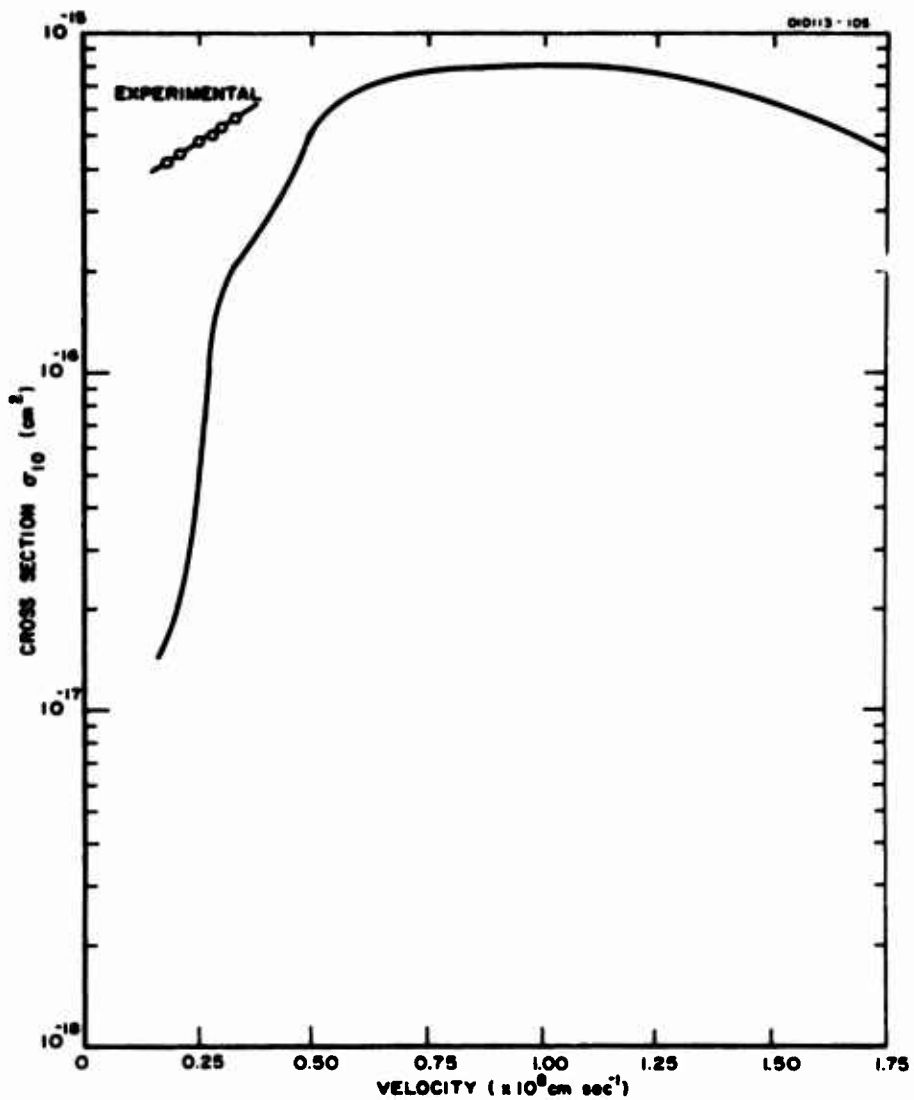


Figure 17. Charge Exchange Cross Section for Capture into the Ground State for Singly Charged Iodine in Atomic Oxygen. The Experimental Results are from Reference 31.

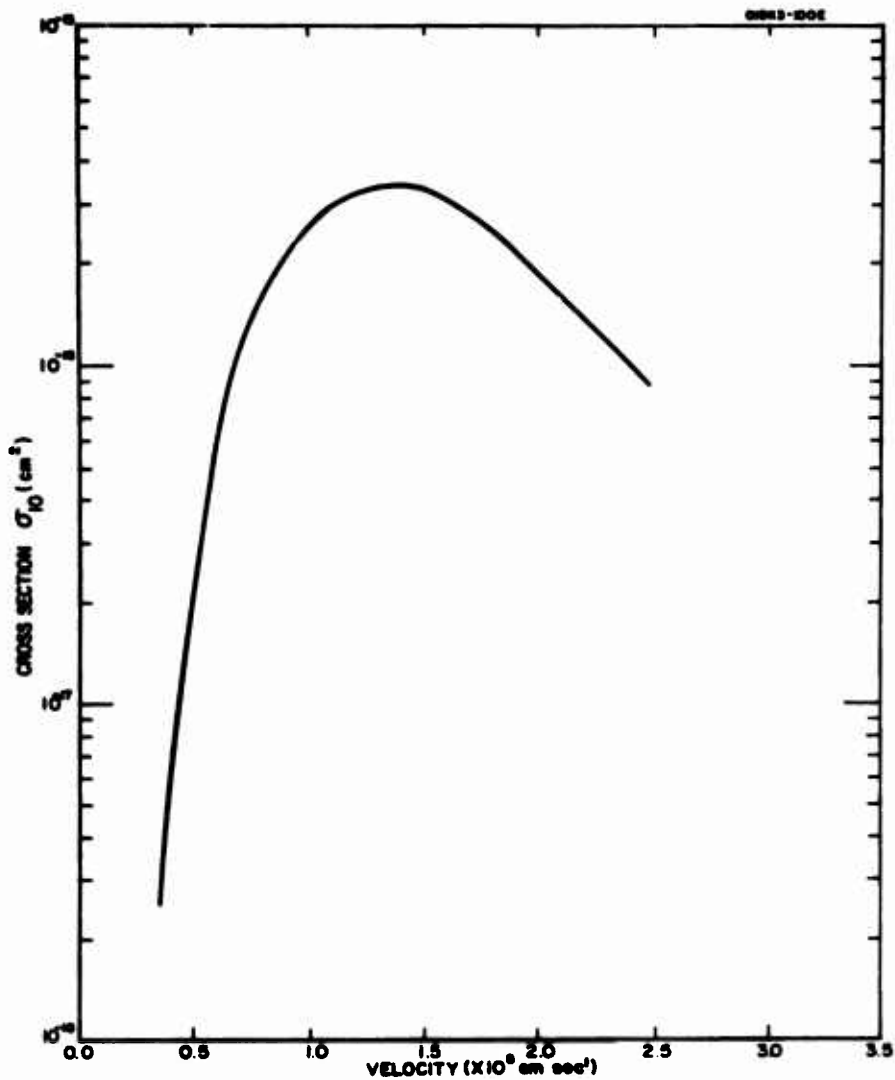


Figure 18. Charge Exchange Cross Sections for Capture into the Ground State for Singly Charged Chromium in Atomic Hydrogen.

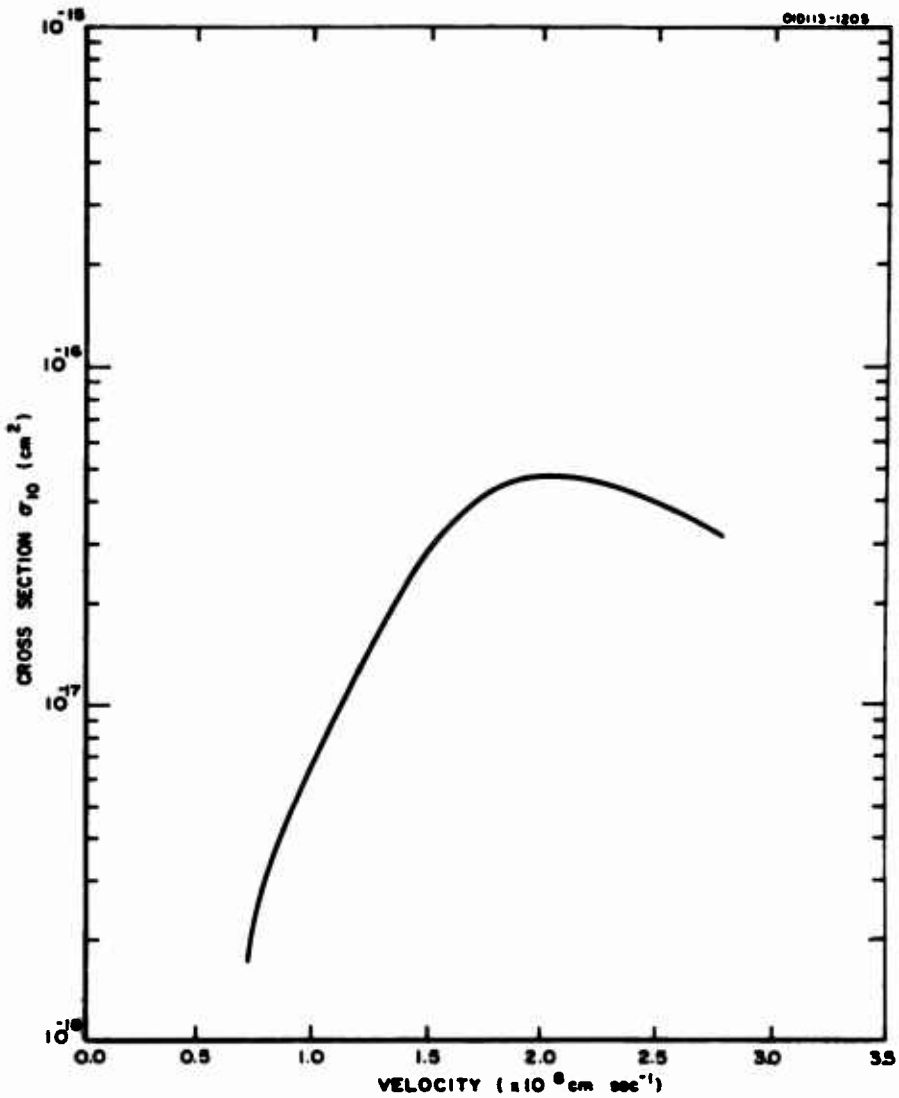


Figure 19. Charge Exchange Cross Section for Capture into the Ground State for Singly Charged Chromium in Helium.

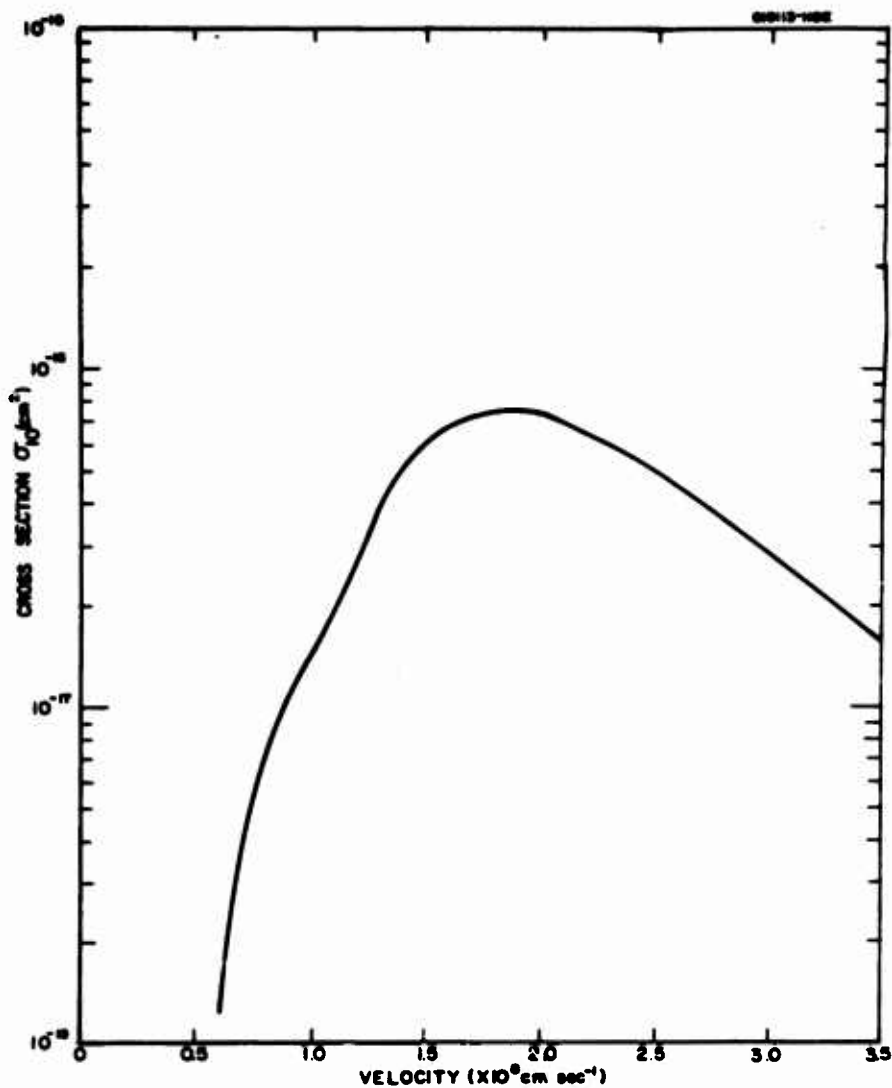


Figure 20. Charge Exchange Cross Section for Capture into the Ground State for Singly Charged Chromium in Neon.

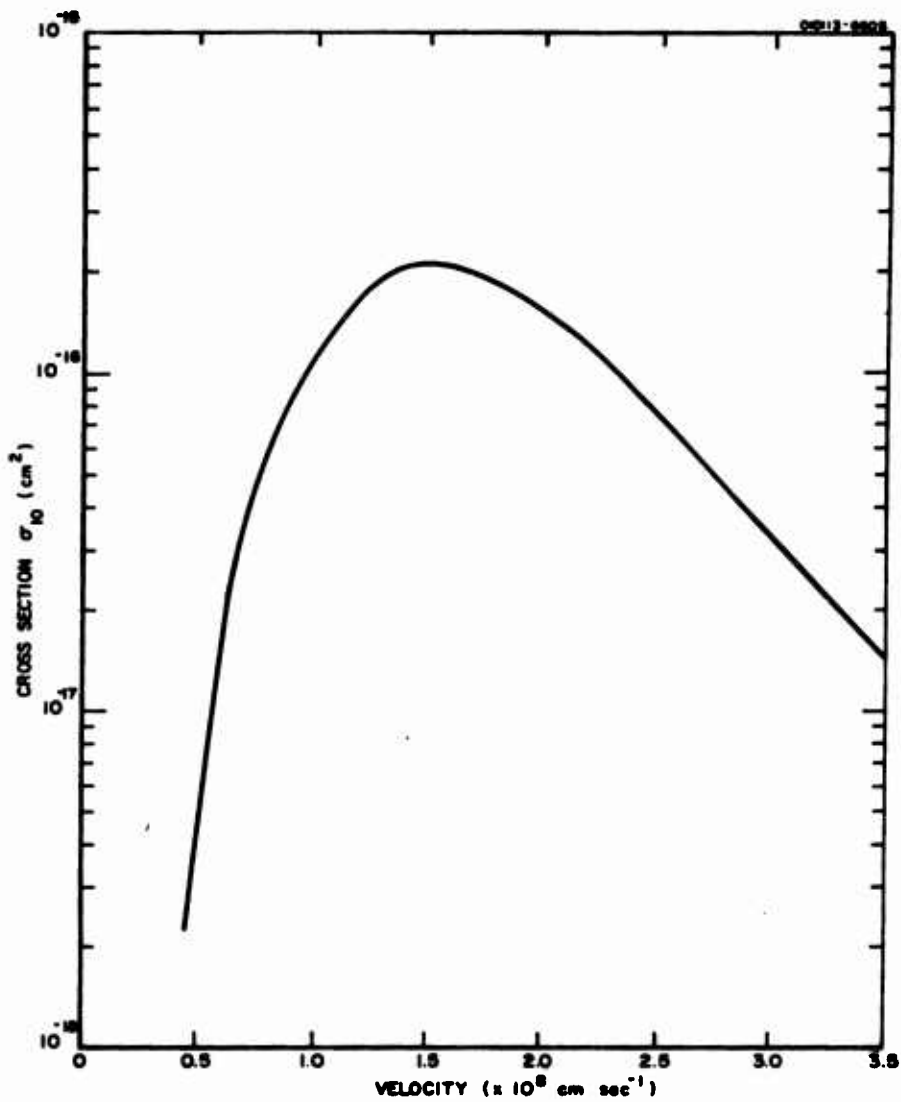


Figure 21. Charge Exchange Cross Section for Capture into the Ground State for Singly Charged Chromium in Argon.

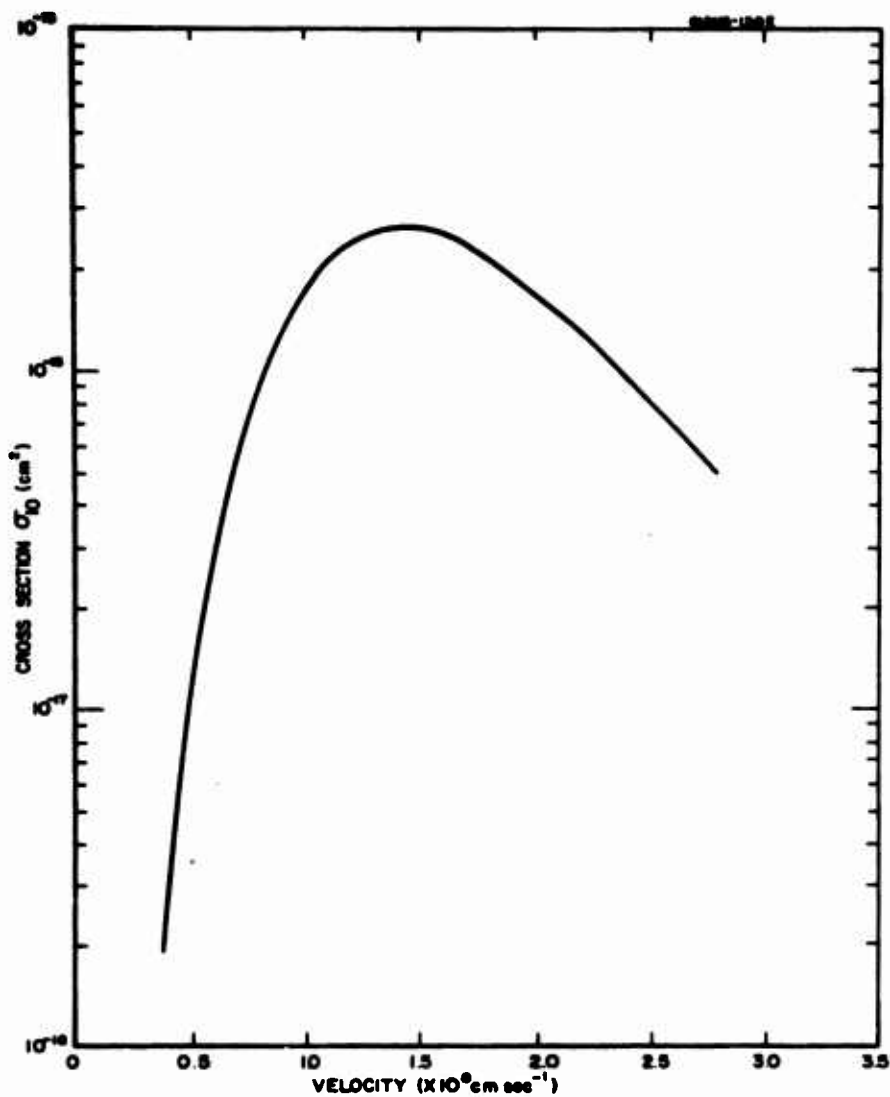


Figure 22. Charge Exchange Cross Section for Capture into the Ground State for Singly Charged Chromium in Atomic Nitrogen.

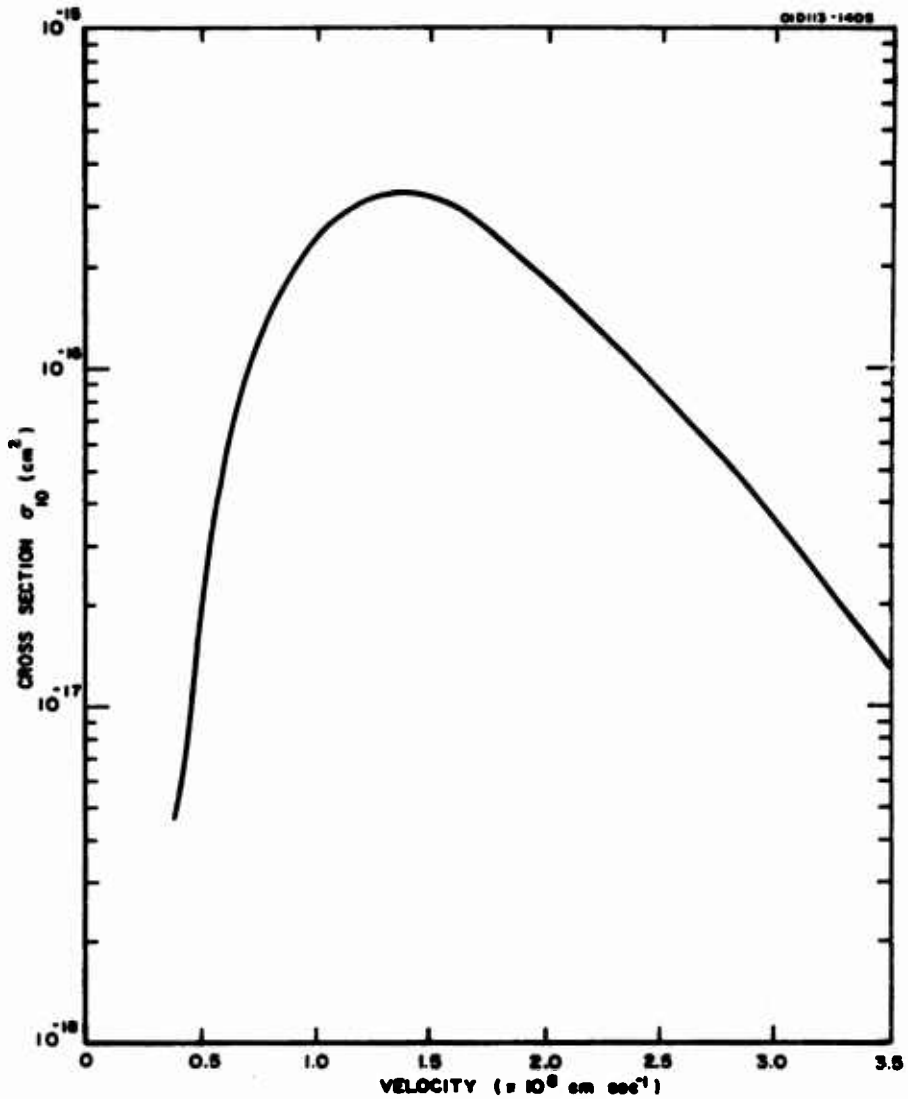


Figure 23. Charge Exchange Cross Section for Capture into the Ground State for Singly Charged Chromium in Atomic Oxygen.

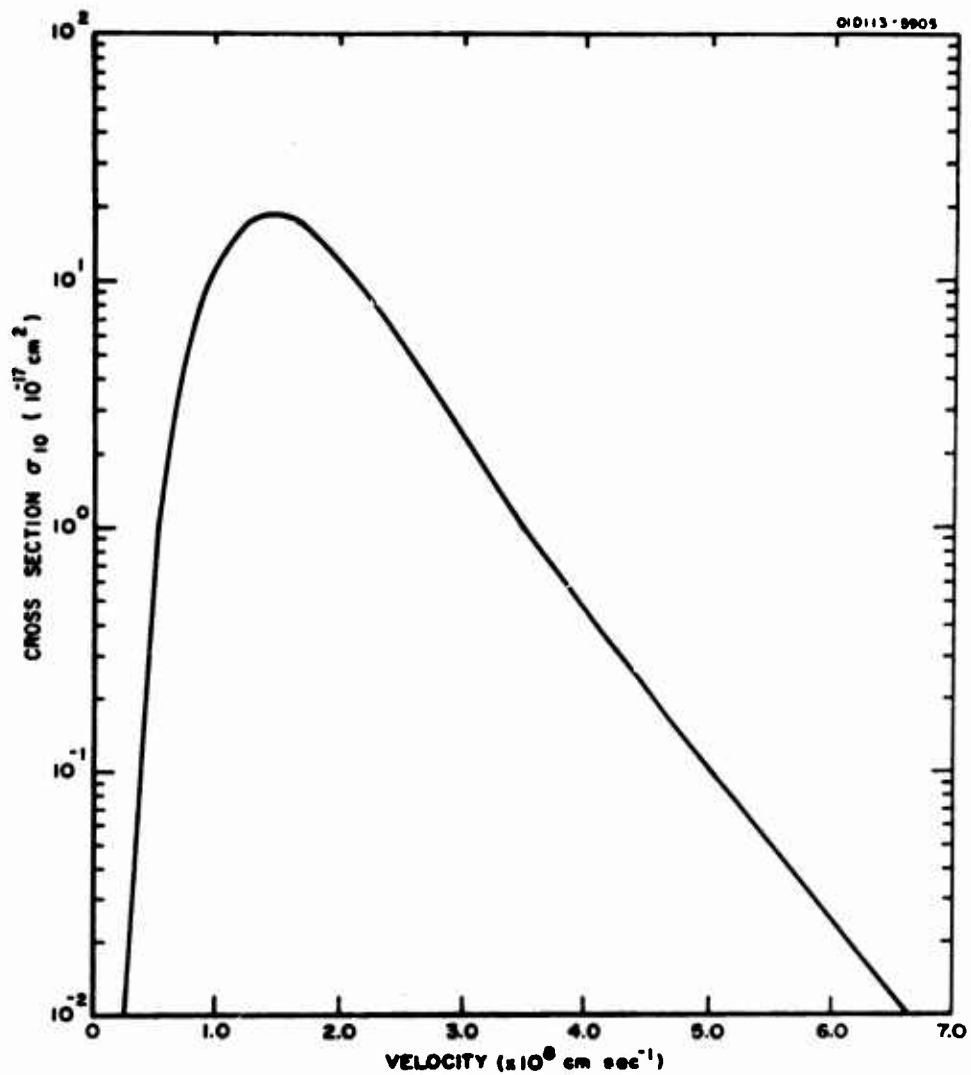


Figure 24. Charge Exchange Cross Section for Capture into the Ground State for Singly Charged Lithium in Atomic Hydrogen.

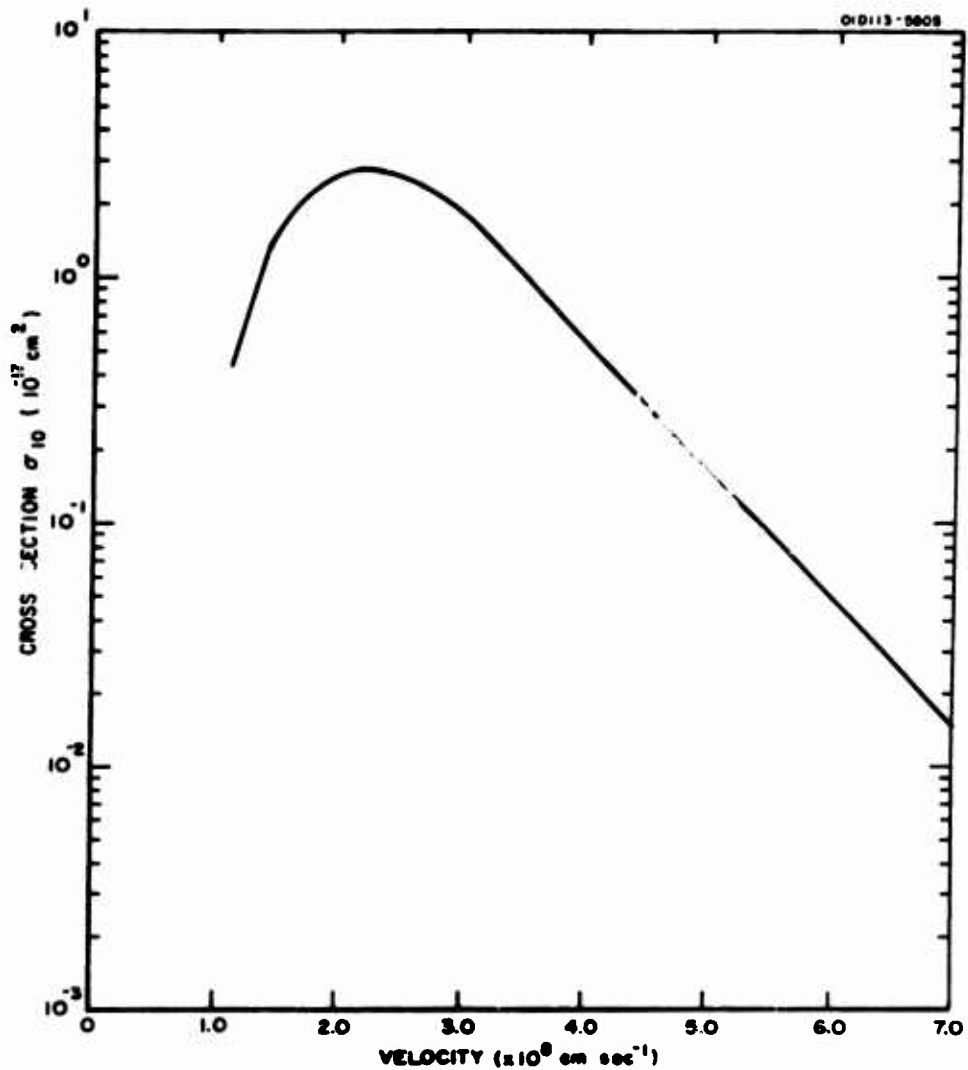


Figure 25. Charge Exchange Cross Section for Capture into the Ground State for Singly Charged Lithium in Helium.

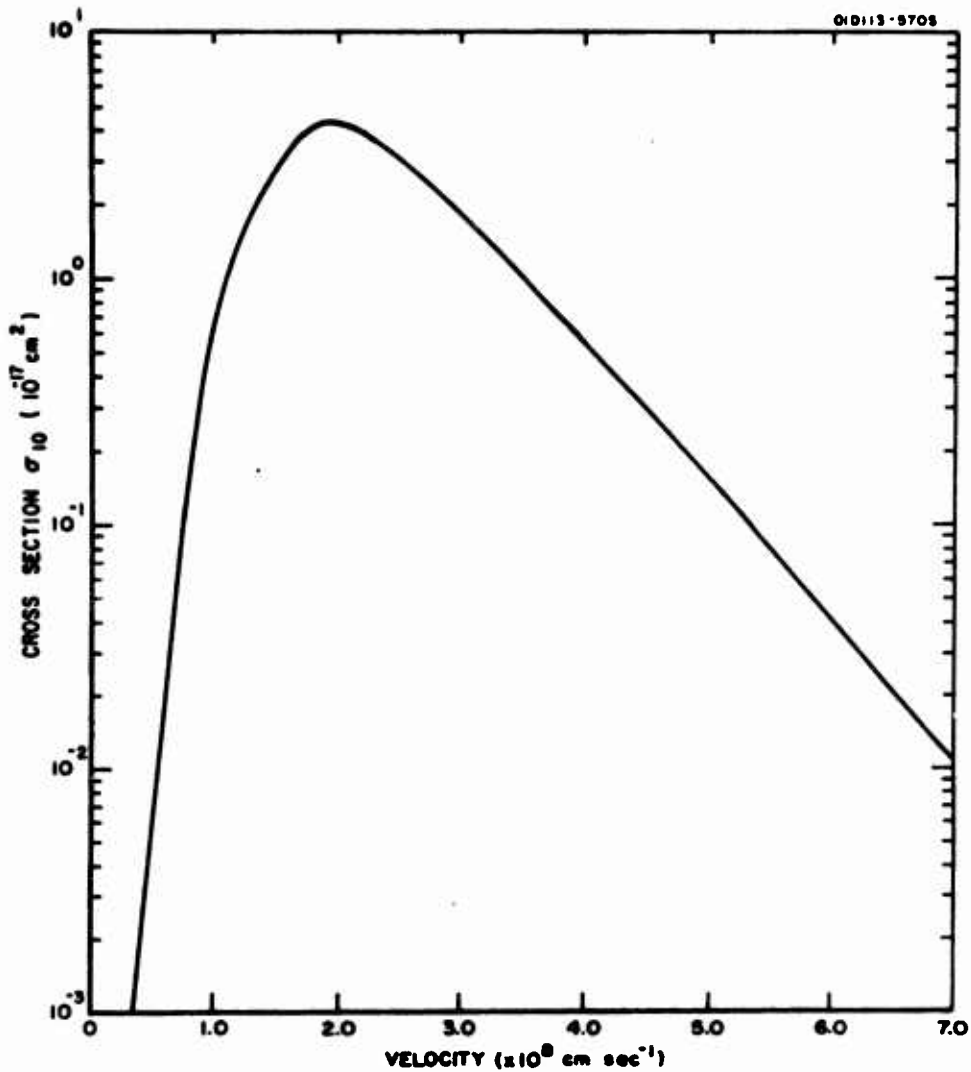


Figure 26. Charge Exchange Cross Section for Capture into the Ground State for Singly Charged Lithium in Neon.

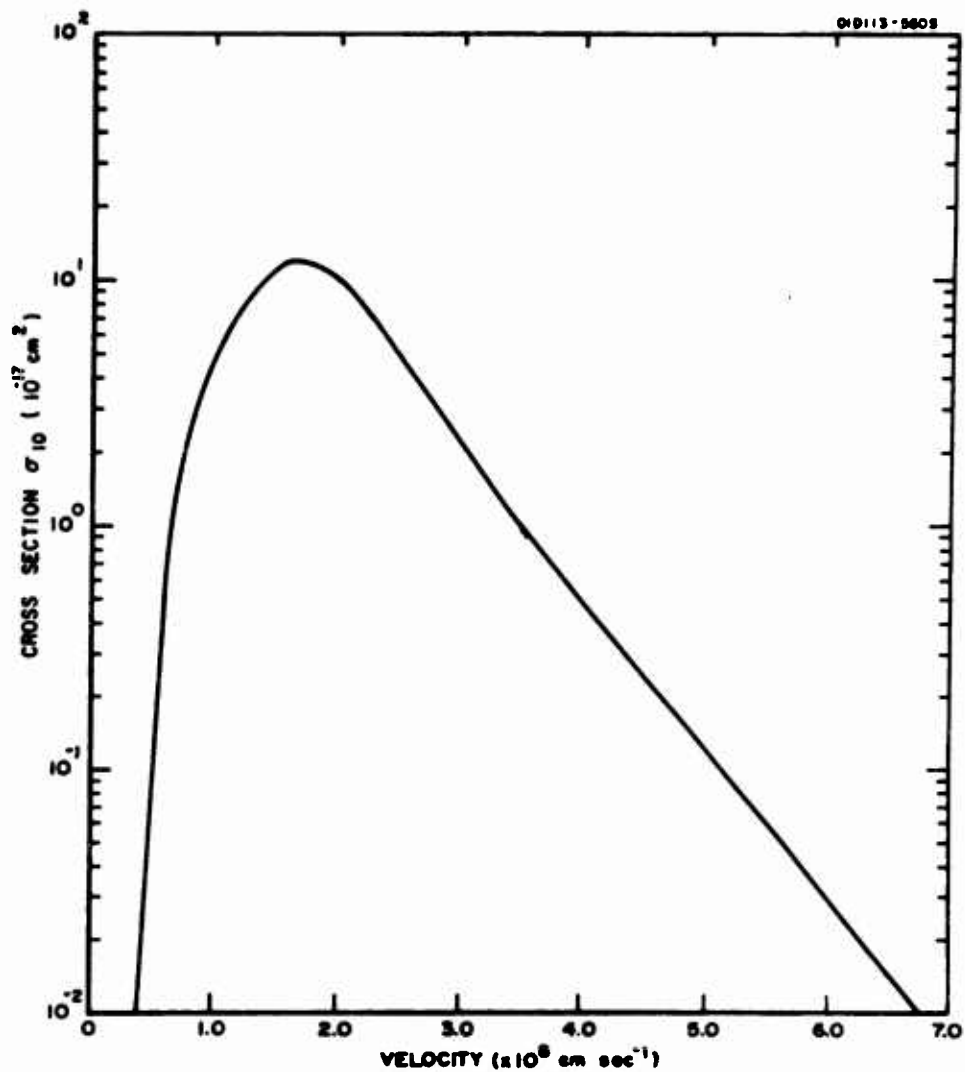


Figure 27. Charge Exchange Cross Section for Capture into the Ground State for Singly Charged Lithium in Argon.

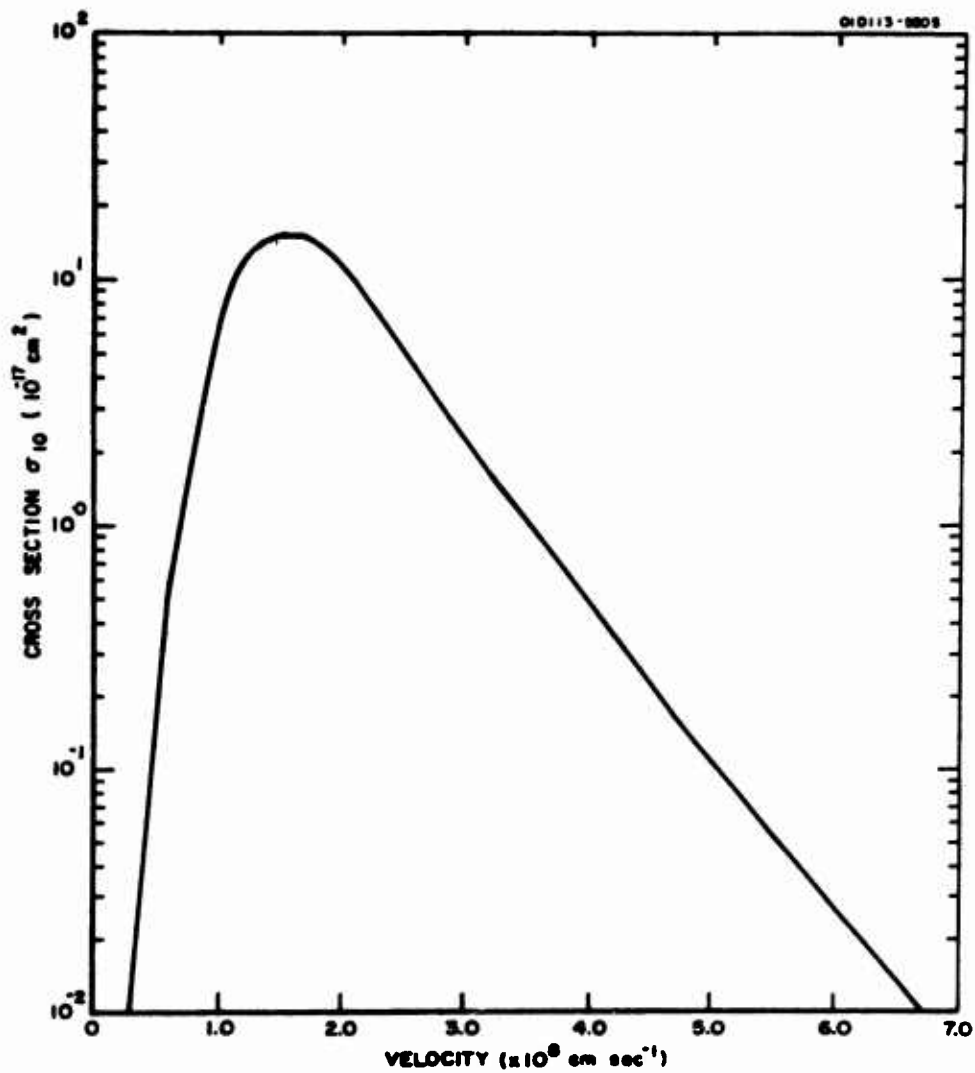


Figure 28. Charge Exchange Cross Section for Capture into the Ground State for Singly Charged Lithium in Atomic Nitrogen.

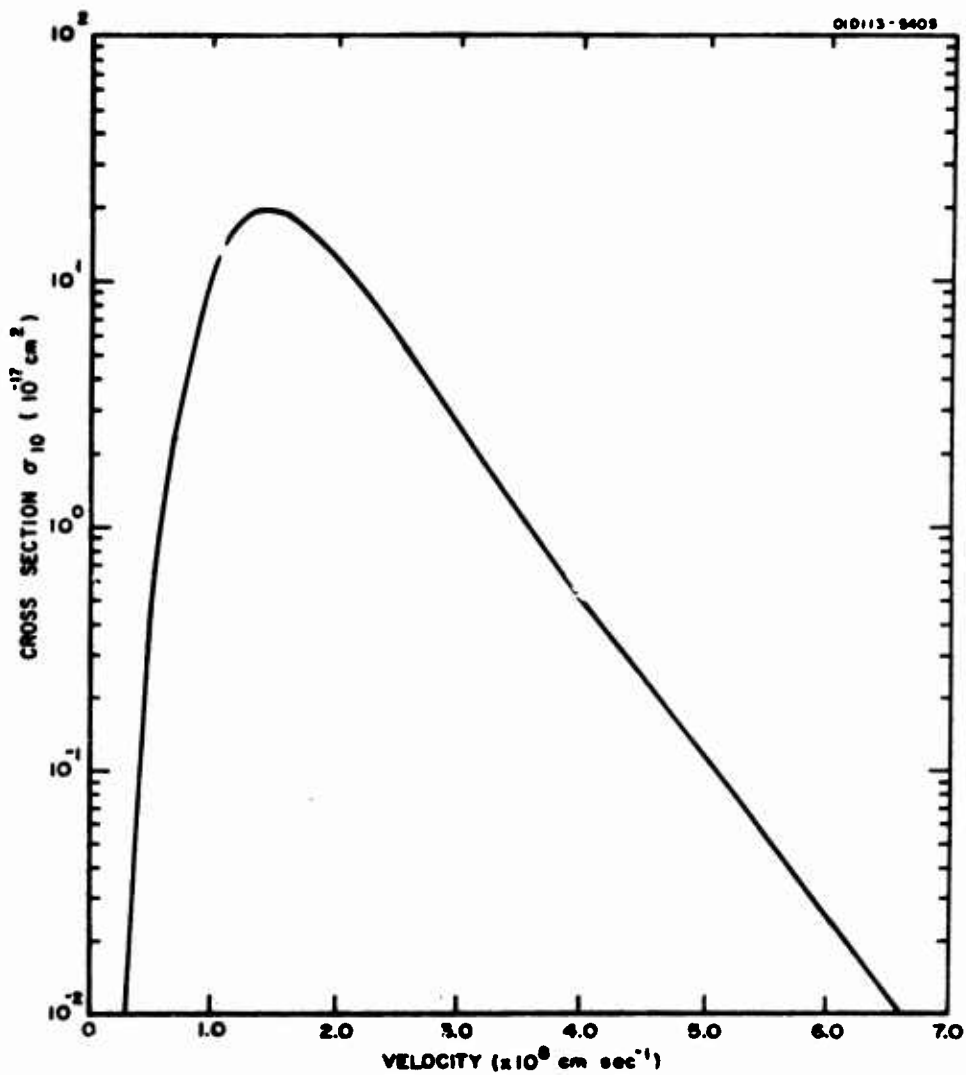


Figure 29. Charge Exchange Cross Section for Capture into the Ground State for Singly Charged Lithium in Atomic Oxygen.

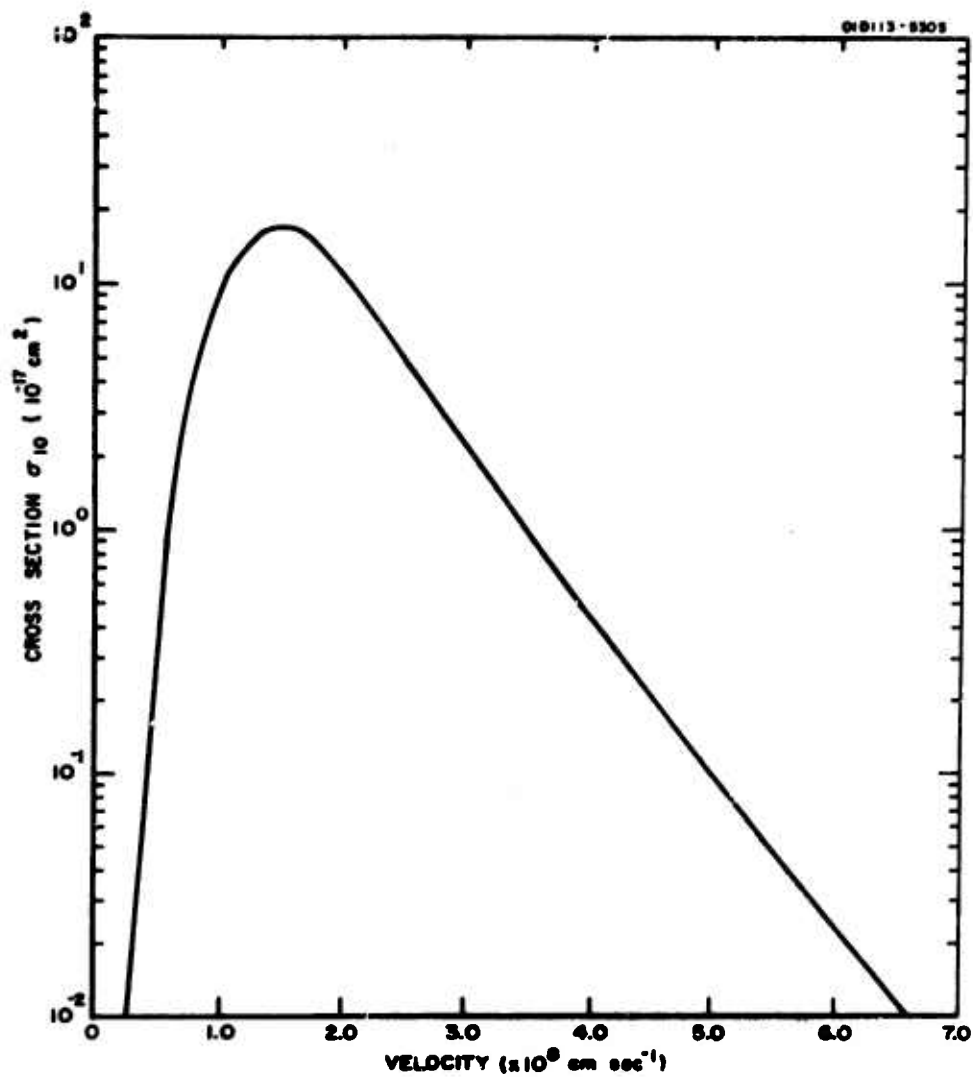


Figure 30. Charge Exchange Cross Section for Capture into the Ground State for Singly Charged Sodium in Atomic Hydrogen.

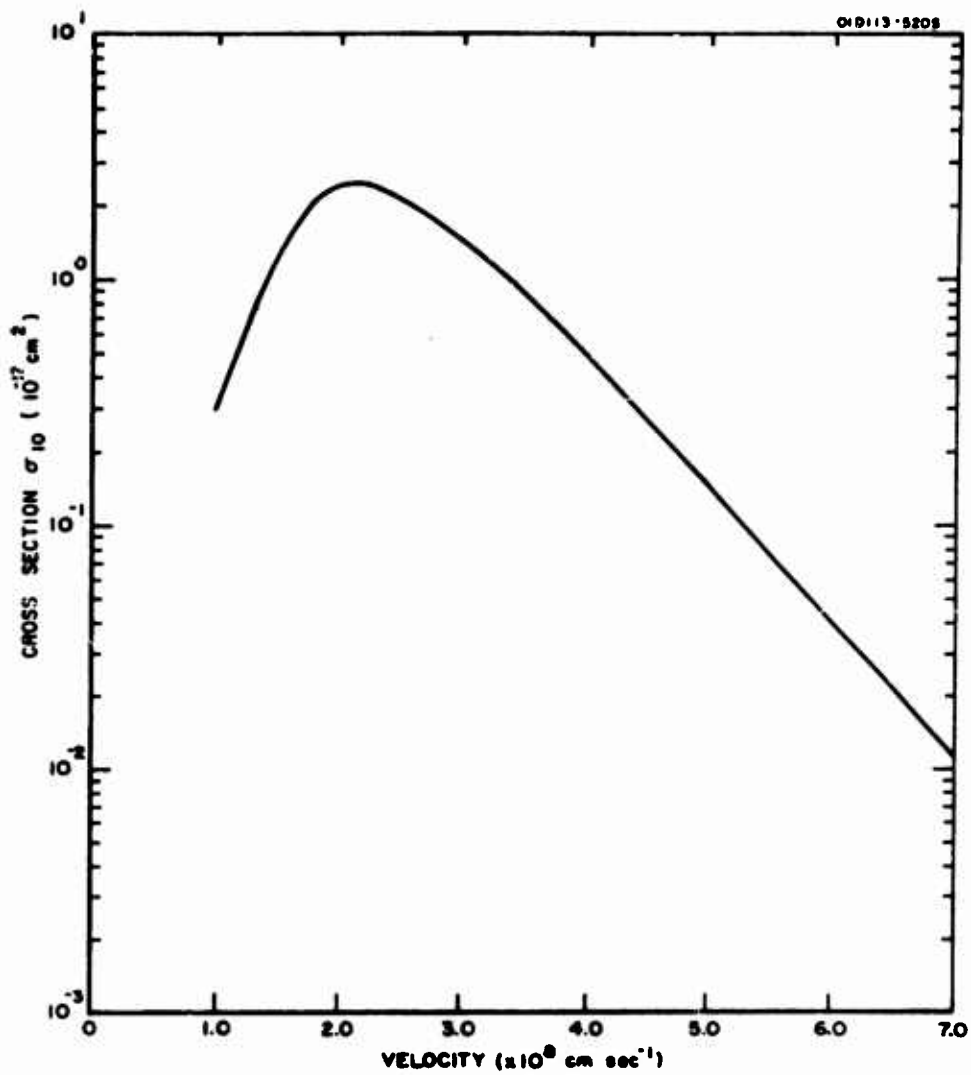


Figure 31. Charge Exchange Cross Section for Capture into the Ground State for Singly Charged Sodium in Helium.

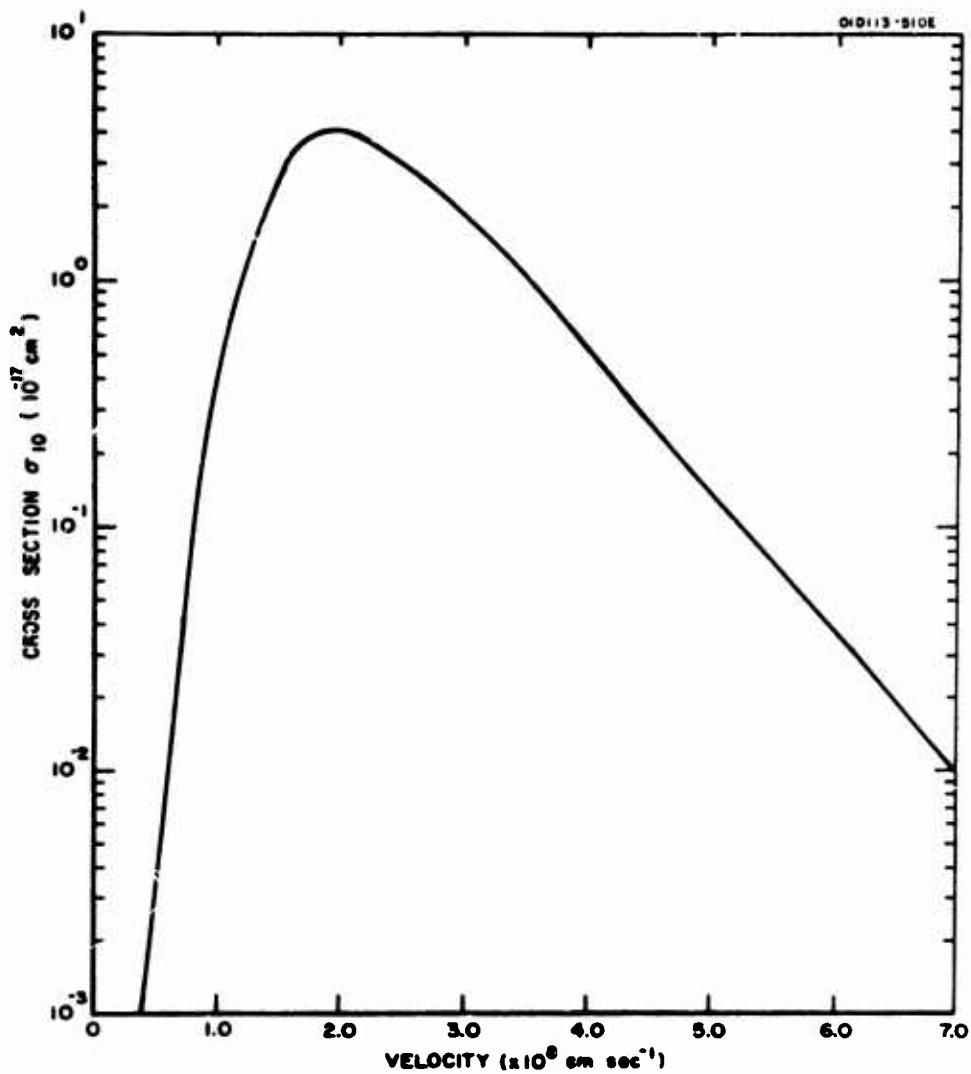


Figure 32. Charge Exchange Cross Section for Capture into the Ground State for Singly Charged Sodium in Neon.

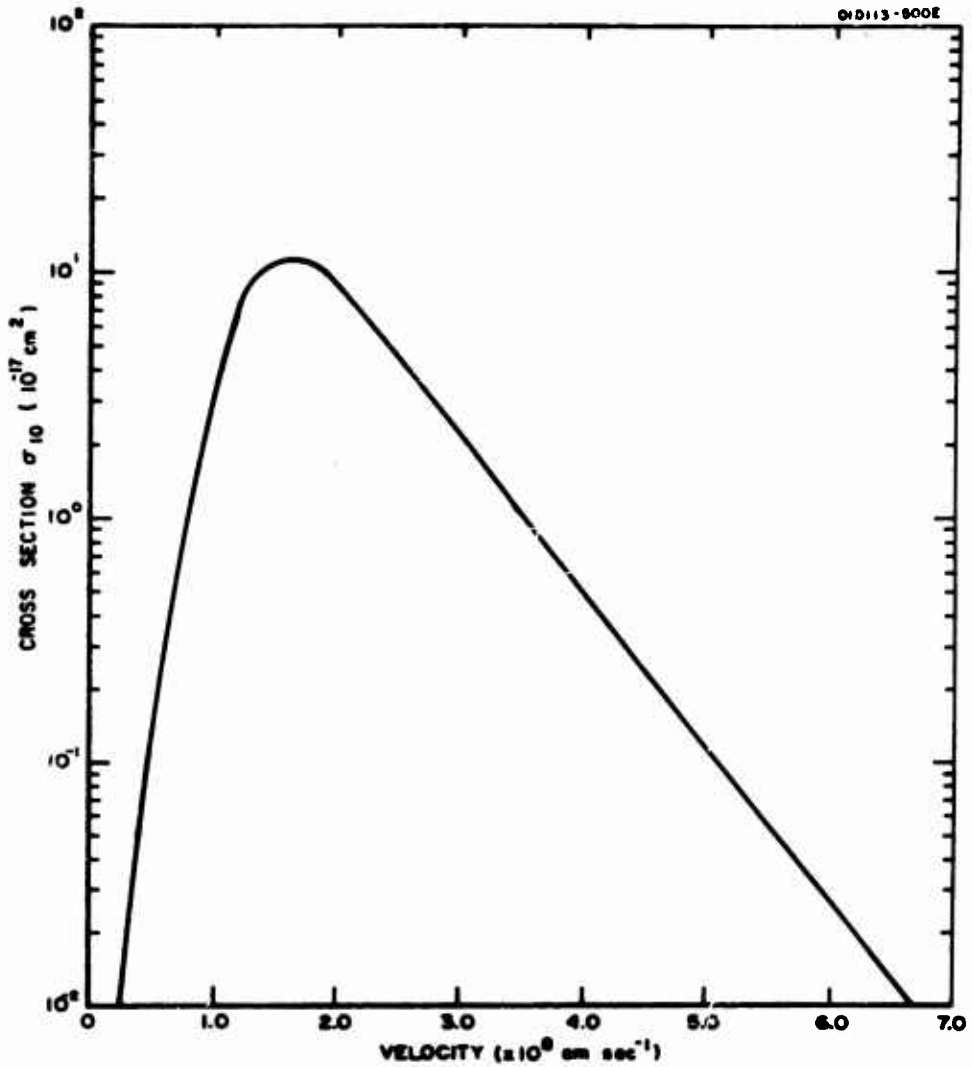


Figure 33. Charge Exchange Cross Section for Capture into the Ground State for Singly Charged Sodium in Argon.

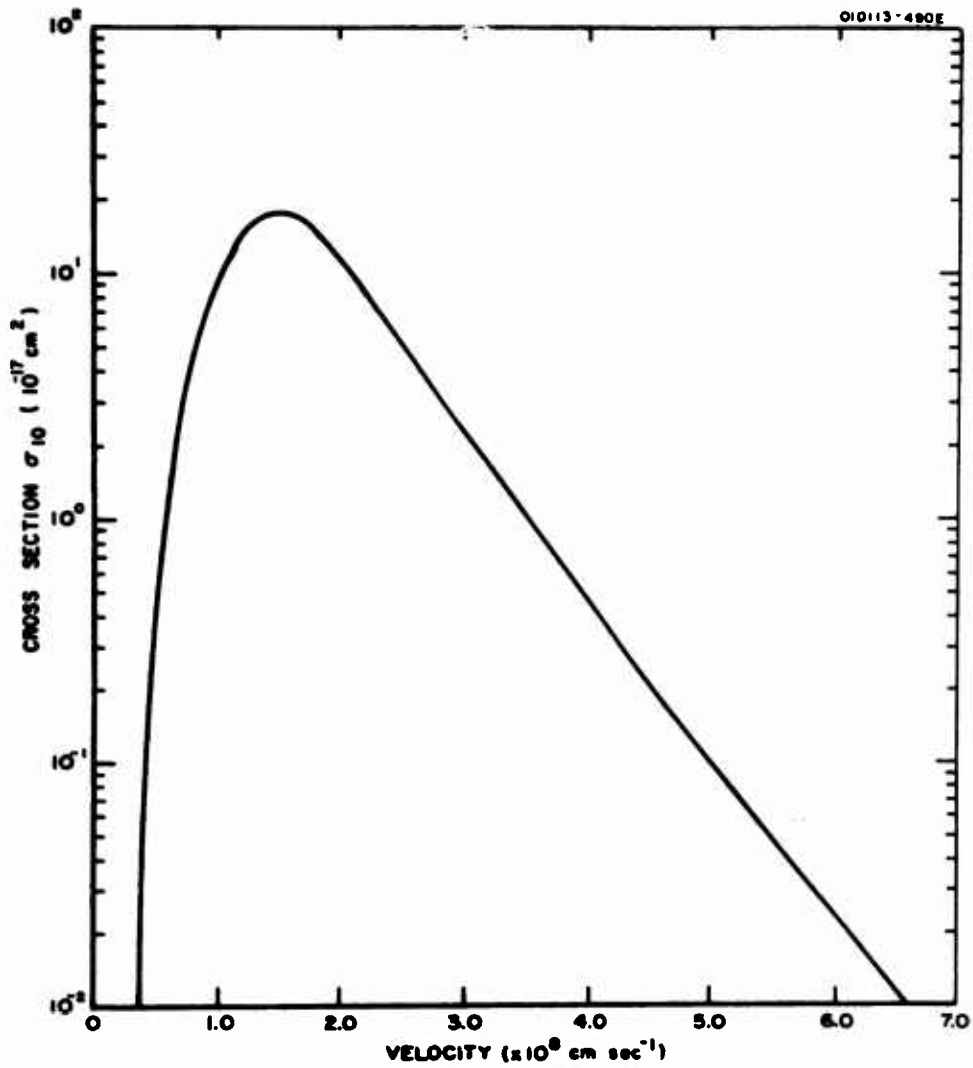


Figure 34. Charge Exchange Cross Section for Capture into the Ground State for Singly Charged Sodium in Atomic Oxygen.

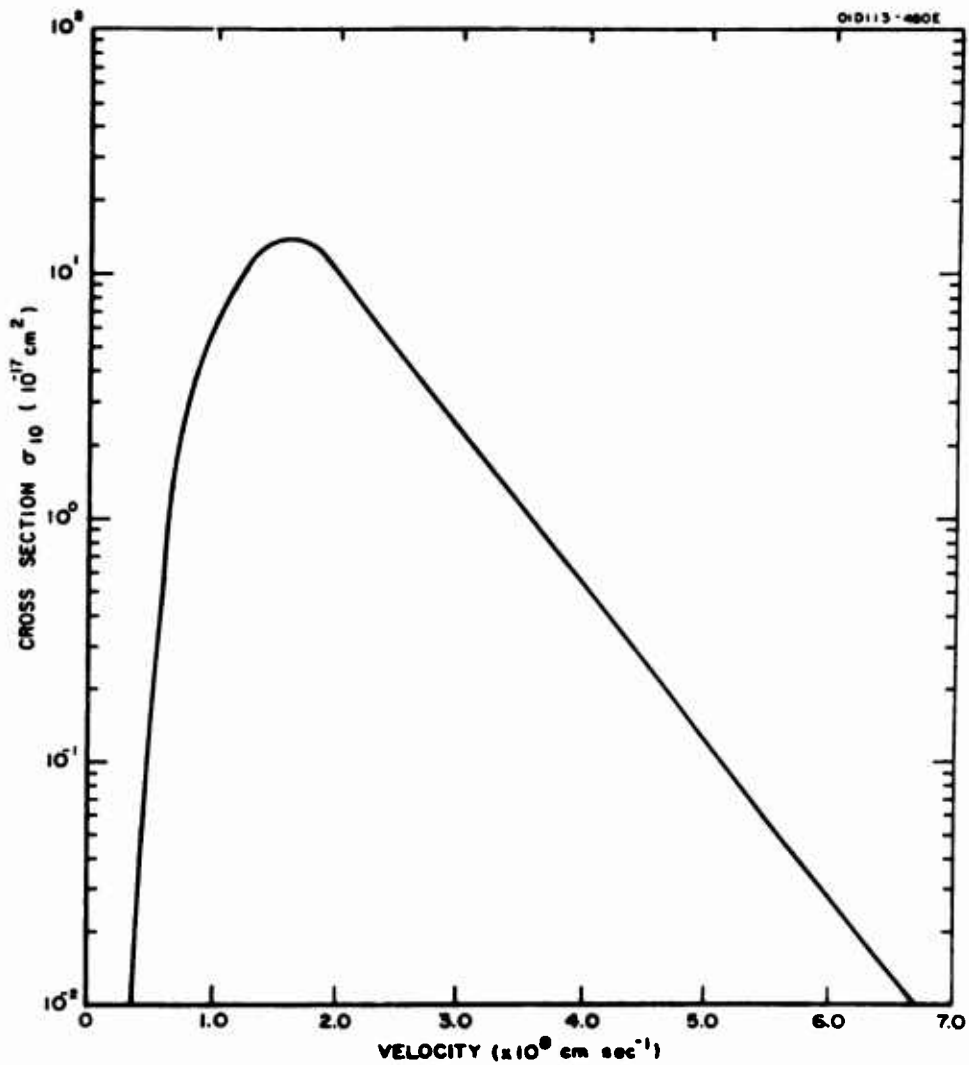


Figure 35. Charge Exchange Cross Section for Capture into the Ground State for Singly Charged Sodium in Atomic Nitrogen.

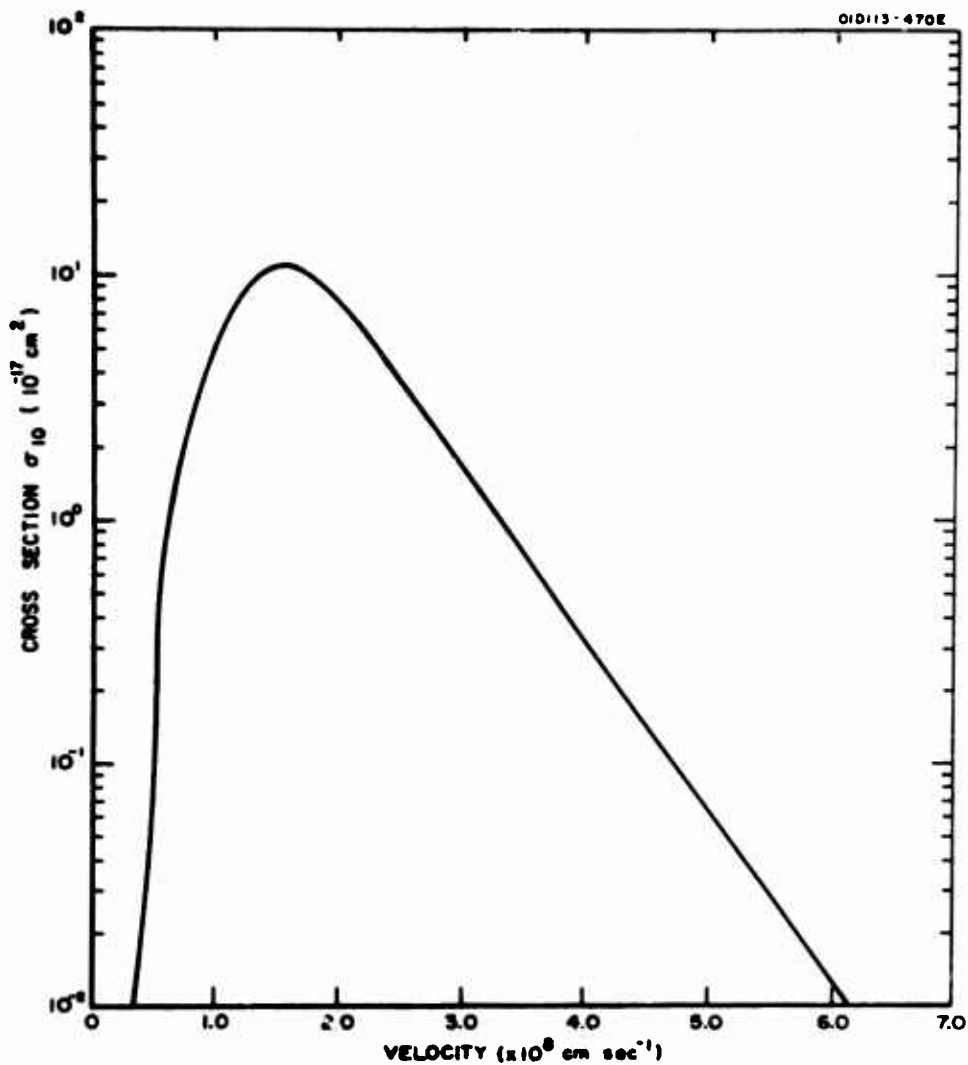


Figure 36. Charge Exchange Cross Section for Capture into the Ground State for Singly Charged Rubidium in Atomic Hydrogen.

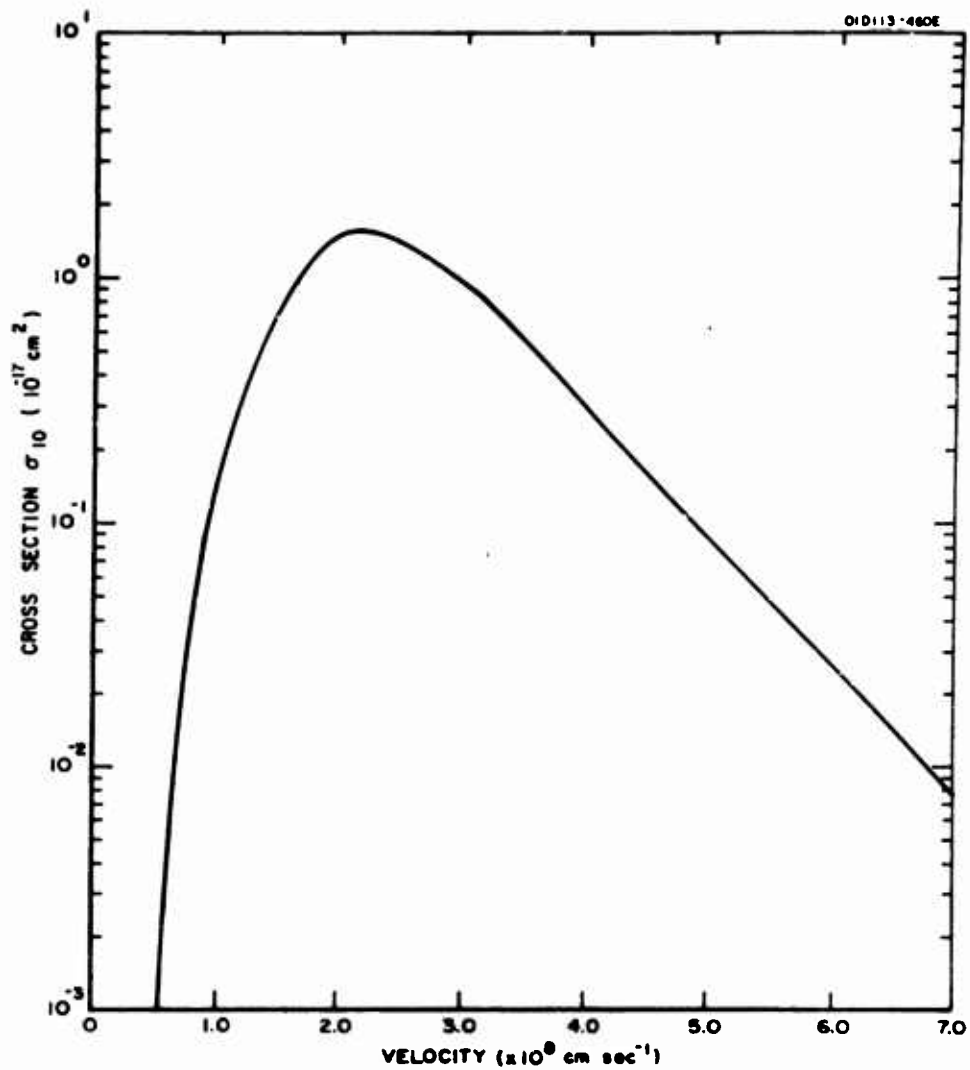


Figure 37. Charge Exchange Cross Section for Capture into the Ground State for Singly Charged Rubidium in Helium.

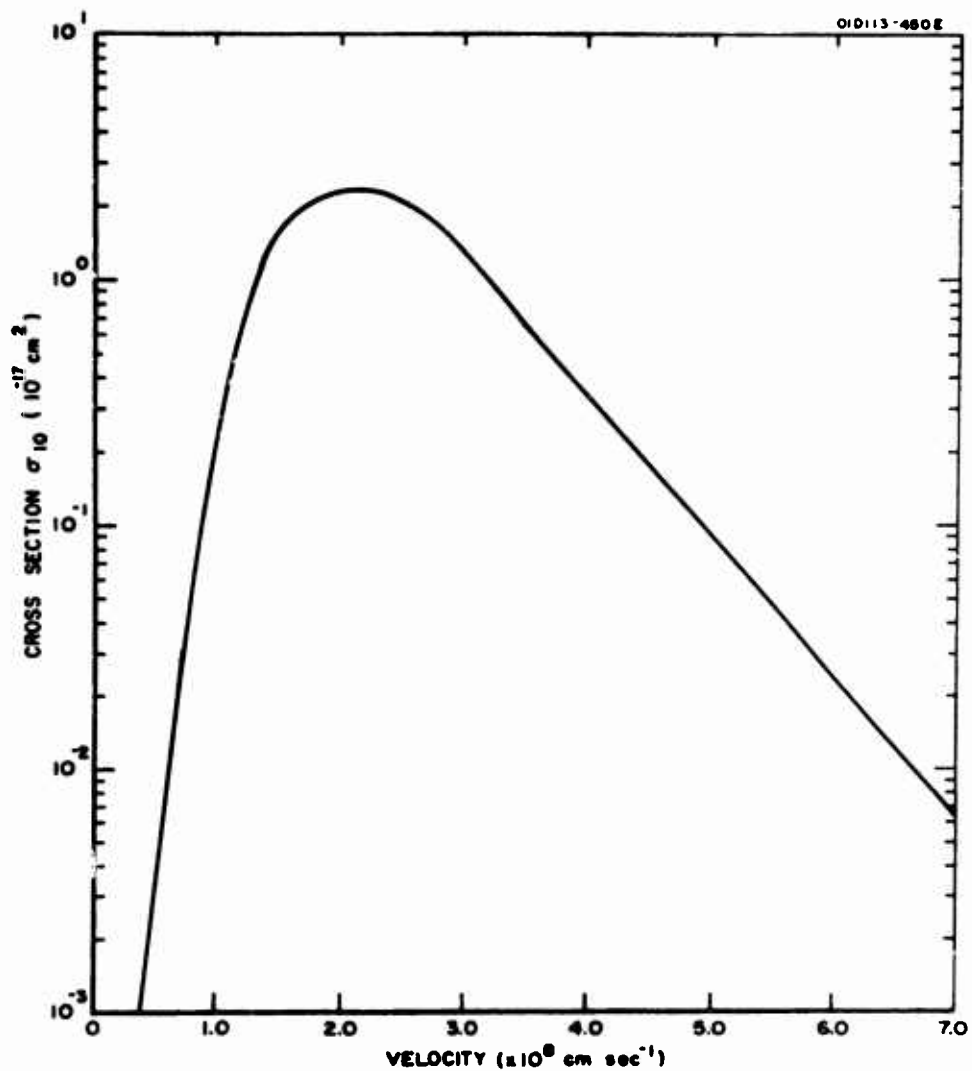


Figure 38. Charge Exchange Cross Section for Capture into the Ground State for Singly Charged Rubidium in Neon.

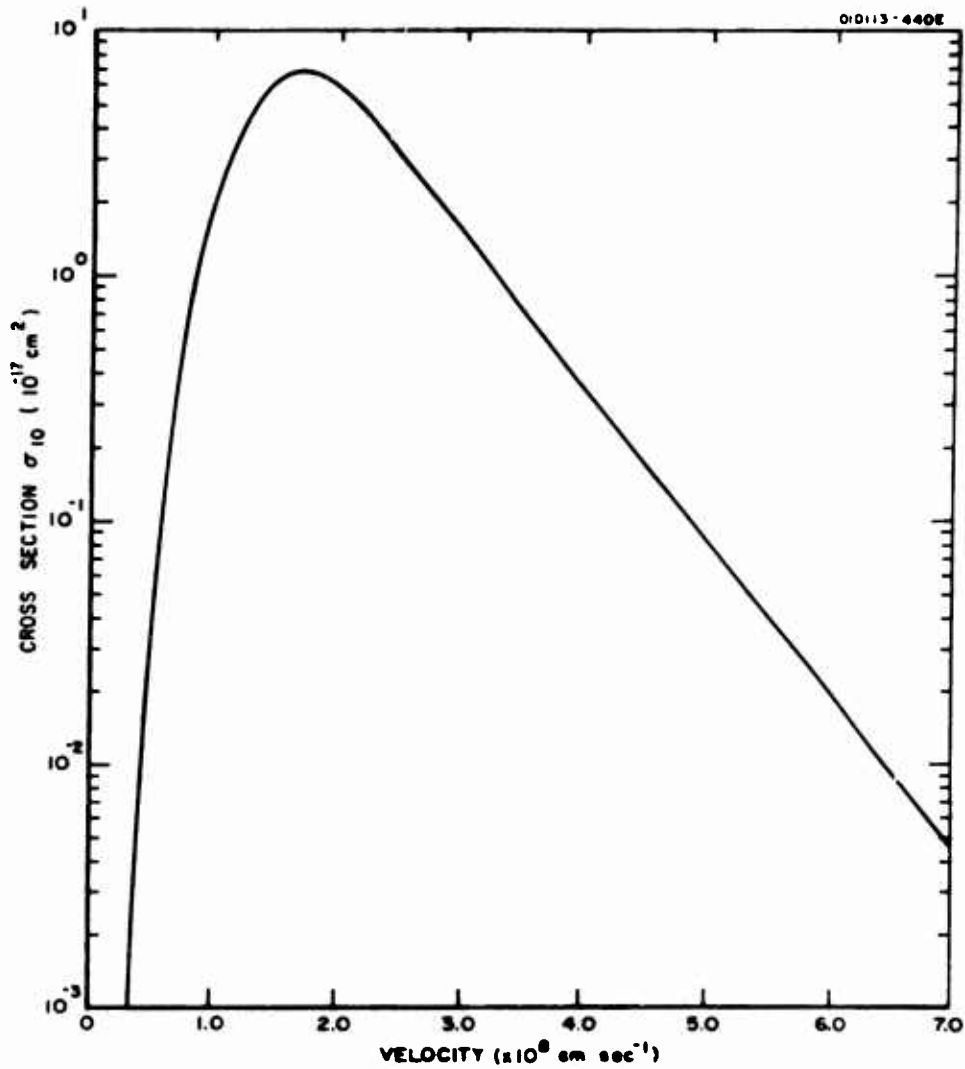


Figure 39. Charge Exchange Cross Section for Capture into the Ground State for Singly Charged Rubidium in Argon.

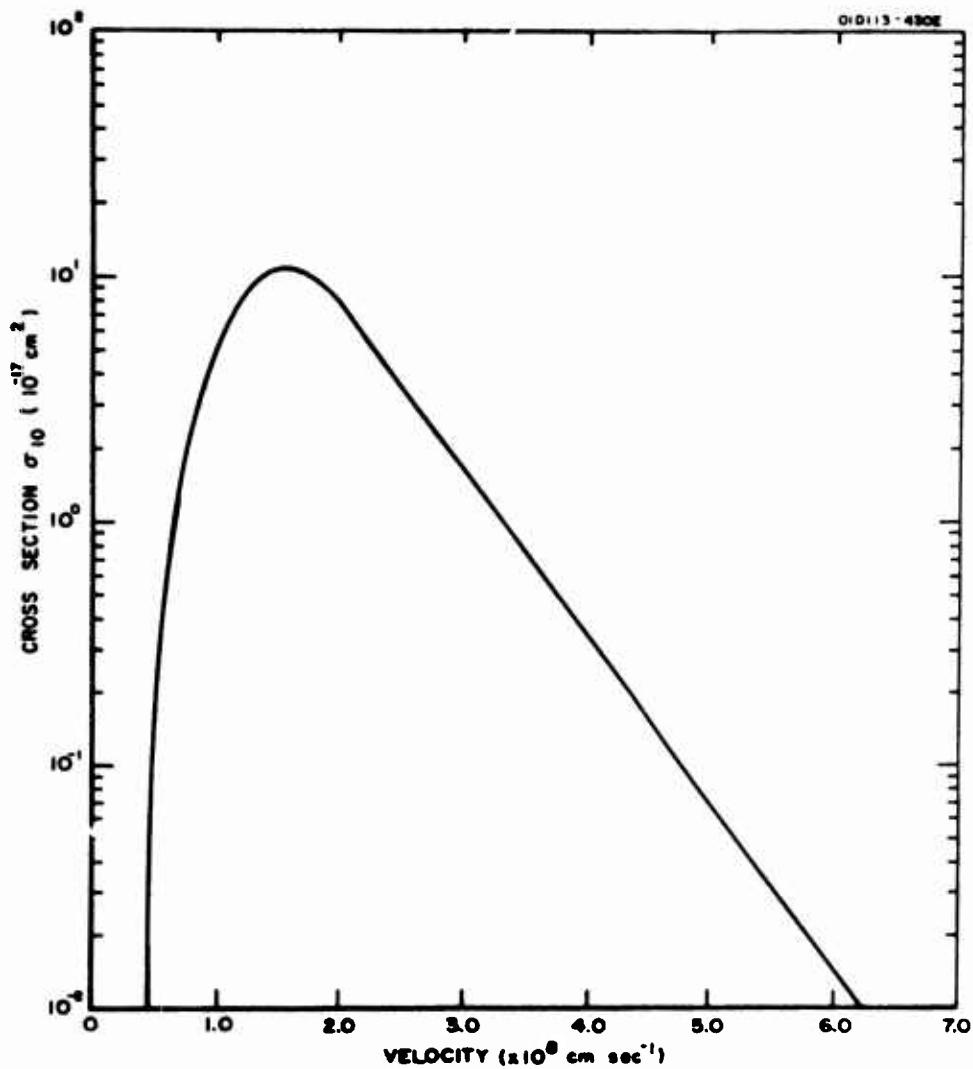


Figure 40. Charge Exchange Cross Section for Capture into the Ground State for Singly Charged Rubidium in Atomic Oxygen.

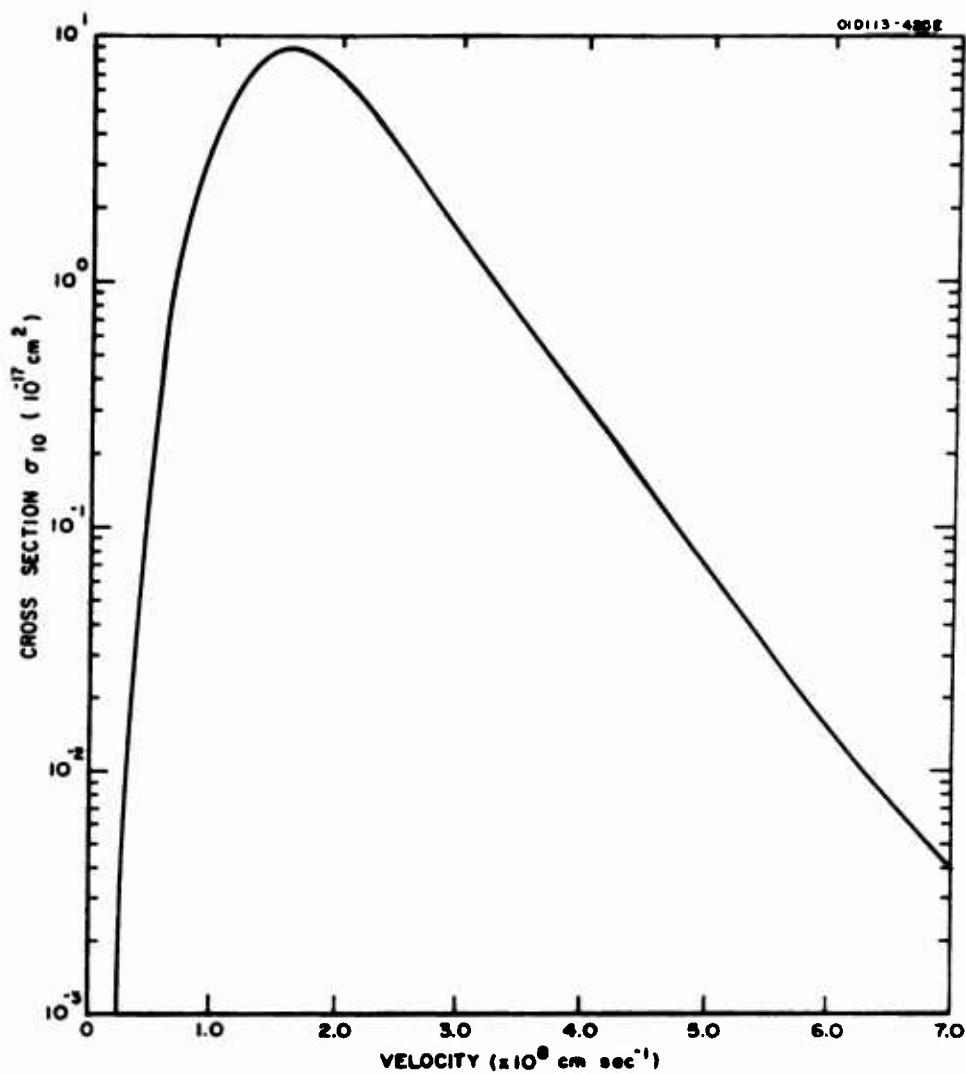


Figure 41. Charge Exchange Cross Section for Capture into the Ground State for Singly Charged Rubidium in Atomic Nitrogen.

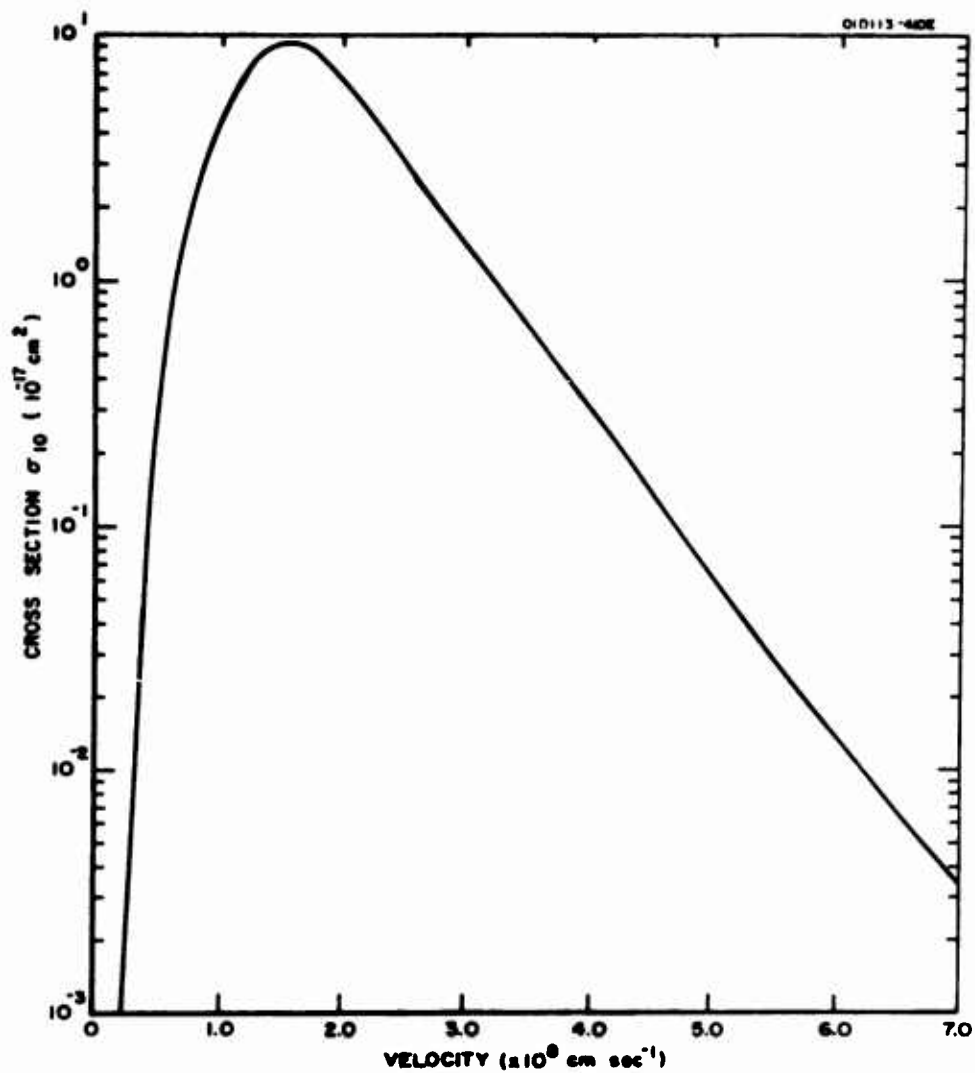


Figure 42. Charge Exchange Cross Section for Capture into the Ground State for Singly Charged Cesium in Atomic Hydrogen.

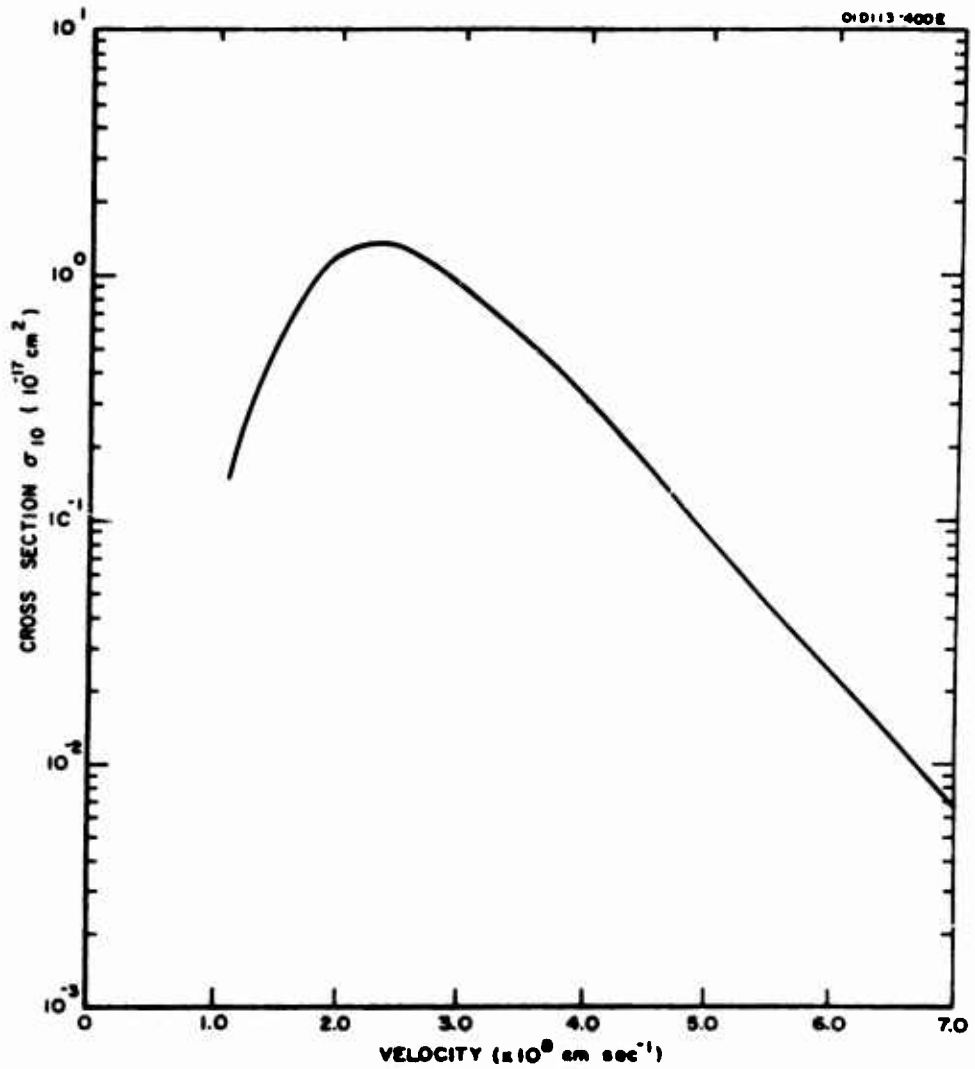


Figure 43. Charge Exchange Cross Section for Capture into the Ground State for Singly Charged Cesium in Helium.

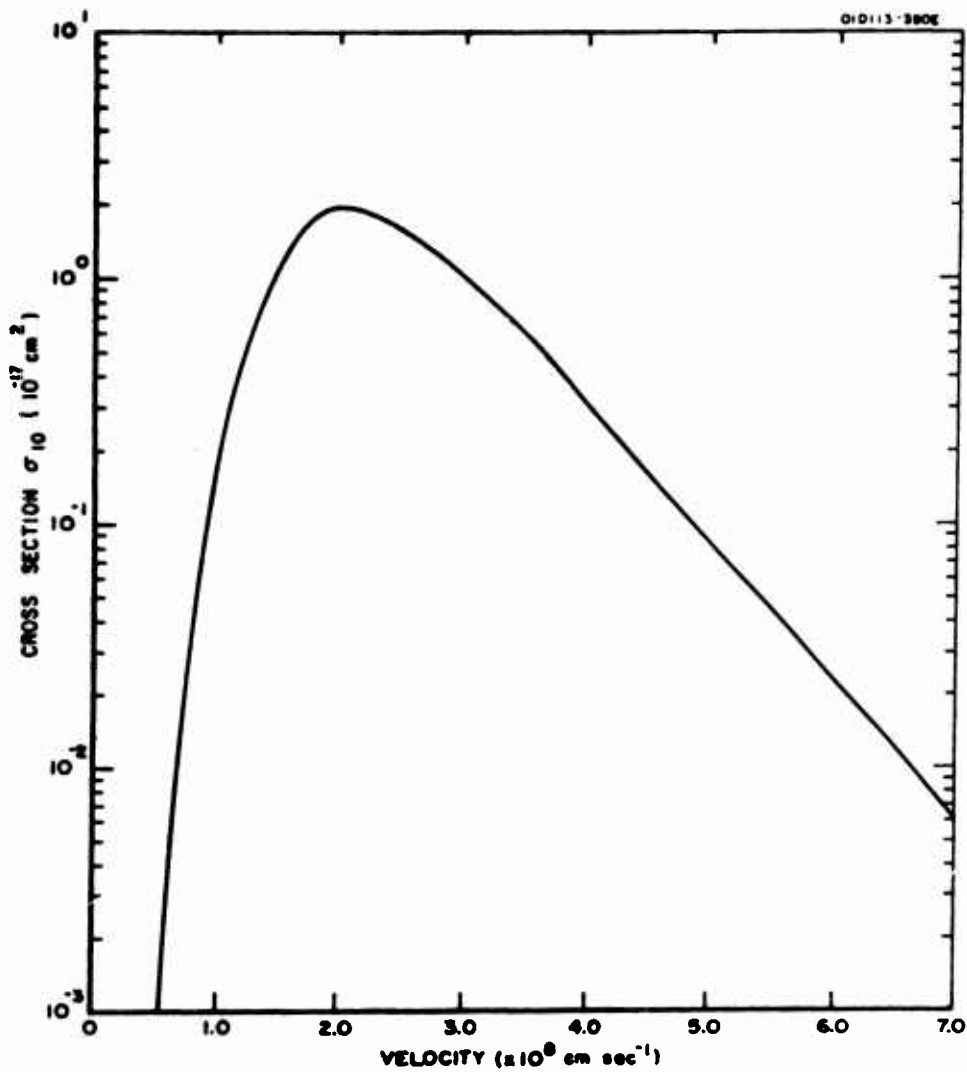


Figure 44. Charge Exchange Cross Section for Capture into the Ground State for Singly Charged Cesium in Neon.

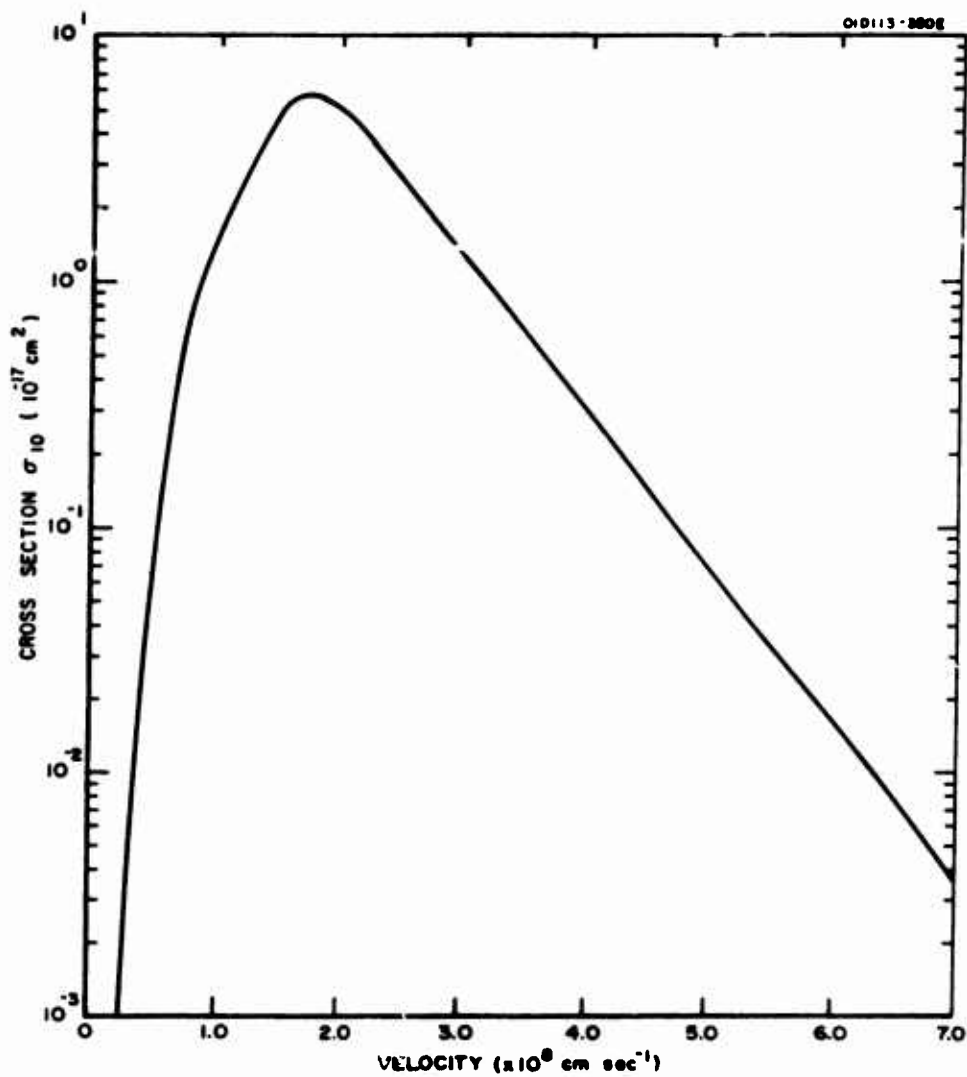


Figure 45. Charge Exchange Cross Section for Capture into the Ground State for Singly Charged Cesium in Argon.

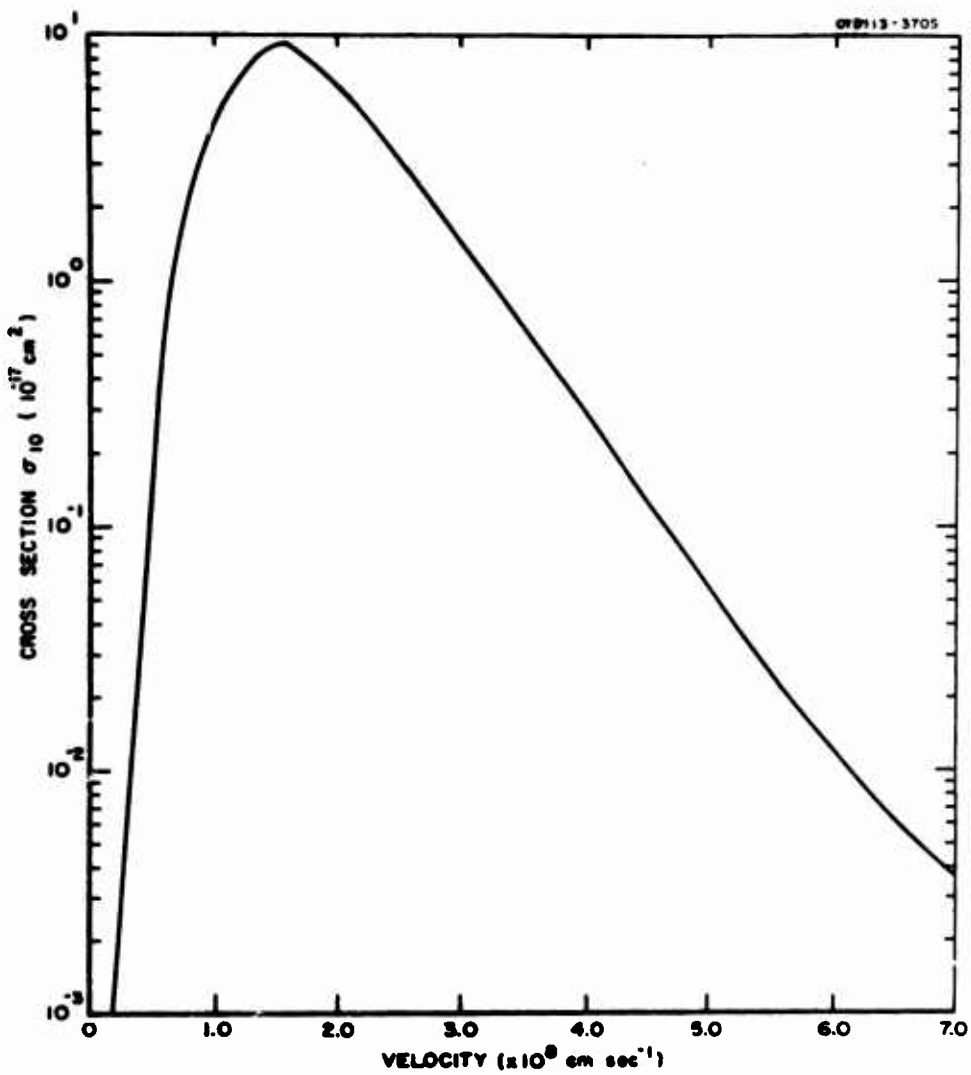


Figure 46. Charge Exchange Cross Section for Capture into the Ground State for Singly Charged Cesium in Atomic Oxygen.

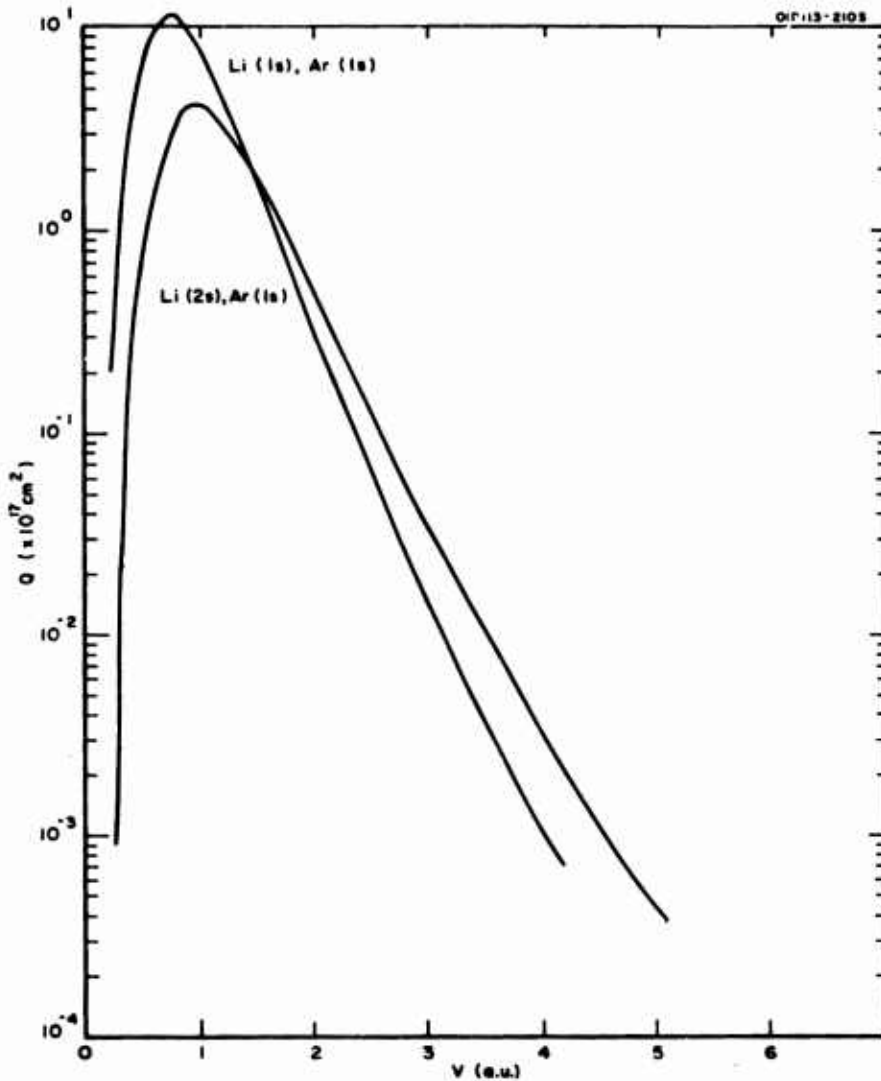
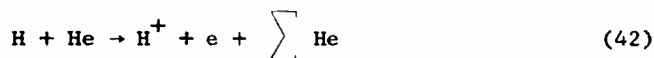


Figure 47. Charge Exchange Cross Section for Capture into Ground State of Lithium Using 1s and 2s Representations of the Lithium Wavefunction. The 1s Representation is used for the Argon Target Gas.

2. Electron Stripping Cross Sections

The theory developed in Section III has been employed to calculate the electron stripping cross sections for a variety of ions in several atomic gases. The projectile systems considered are H, H⁻, He He⁺, Li, Li⁻, N, O, Ne, F, Na, Mg, Al, Fe, Mn, and Cr. The target gases considered are He, N, O, Ne, and Ar. A wide range of impact energies are considered, however, as discussed in Section III, the theory is limited to high energy impacts. In this section, the results of these calculations are presented and the theoretical predictions are compared with experimental data.

In Figure 48, the stripping cross section is presented for the few-electron system process



where by $\sum He$ the elastic and inelastic processes is indicated including

ionization of the helium atom. The experimental data of Allison (Ref. 32), Berkner, et al. (Ref. 33), and Smythe and Toevs (Ref. 34) are shown for comparison. At high energies, the cross section is given by

$$\sigma = \frac{a}{E} \quad (43)$$

with $a = 1.595 \times 10^{-11} \text{ cm}^2 \text{ eV}$ and E is the projectile energy in the laboratory frame in electron volts. The agreement between theory and experiment is good over the energy range of 100 keV to 100 MeV, and is remarkable at the 10 MeV and 14.6 MeV data points. Figures 49 and 50 give the results for hydrogen atoms incident on the heavier system of atomic nitrogen and argon. For these target systems, the cross section at high energies can again be represented by Equation (43) with a assuming the values $4.237 \times 10^{-10} \text{ cm}^2 \text{ eV}$ and $4.706 \times 10^{-10} \text{ cm}^2 \text{ eV}$ for nitrogen and argon, respectively. The agreement between theory and experiment is not as good as for the H-He case. At 100 keV the theory overestimates the cross section by a factor of about 3 for the nitrogen target, where the per atom result for molecular nitrogen is used for the experimental data, and a factor of about 7 for the argon target. At higher energies, where the theory is valid, the agreement is better; the theory giving results about 10 and 20 percent higher than the experimental results for the nitrogen and argon targets, respectively.

Kim and Inokuti (Ref. 24) have used Hartree-Fock wavefunction as well as accurate correlated wavefunctions in their calculations of the atomic form factor and the incoherent scattering function. These results give an atomic form factor using the correlated wavefunction that is larger for large K values and smaller at small K values than the corresponding

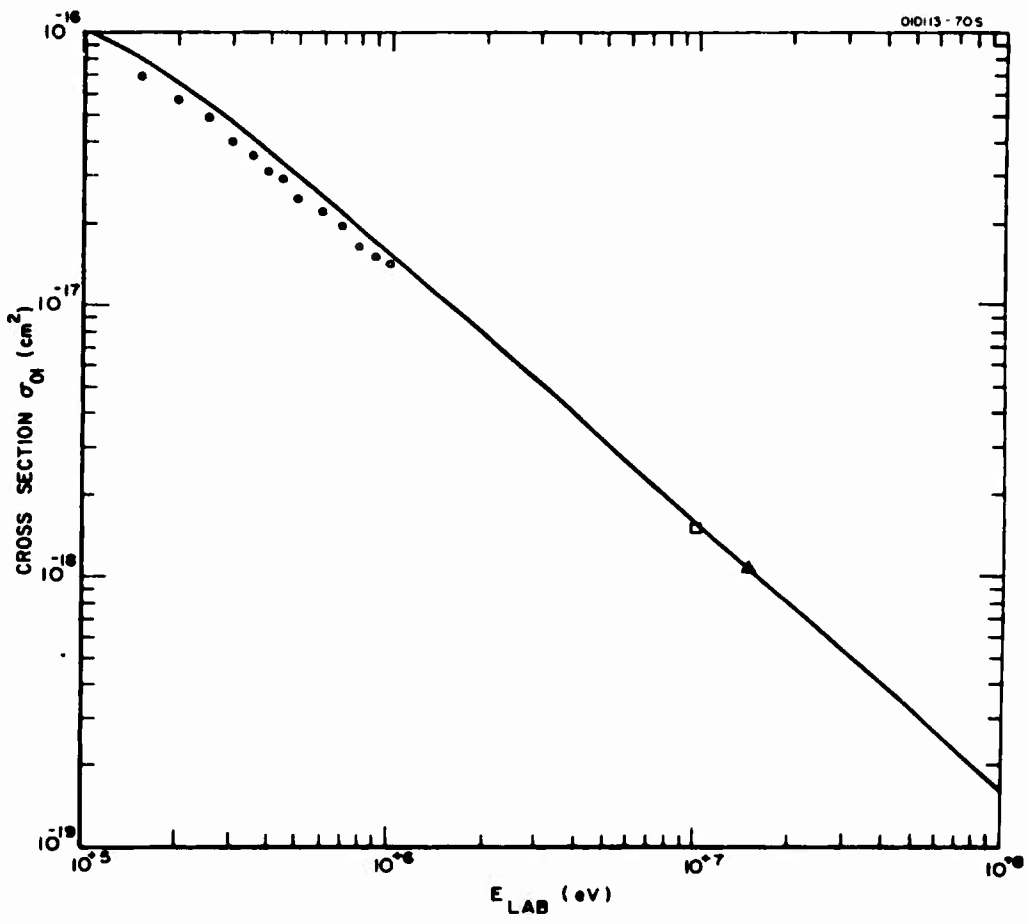


Figure 48. Electron Stripping Cross Section for Hydrogen Atoms Incident on Atomic Hydrogen. The Experimental Results are: \circ , Ref. 32; \square , Ref. 33; \triangle , Ref. 34.

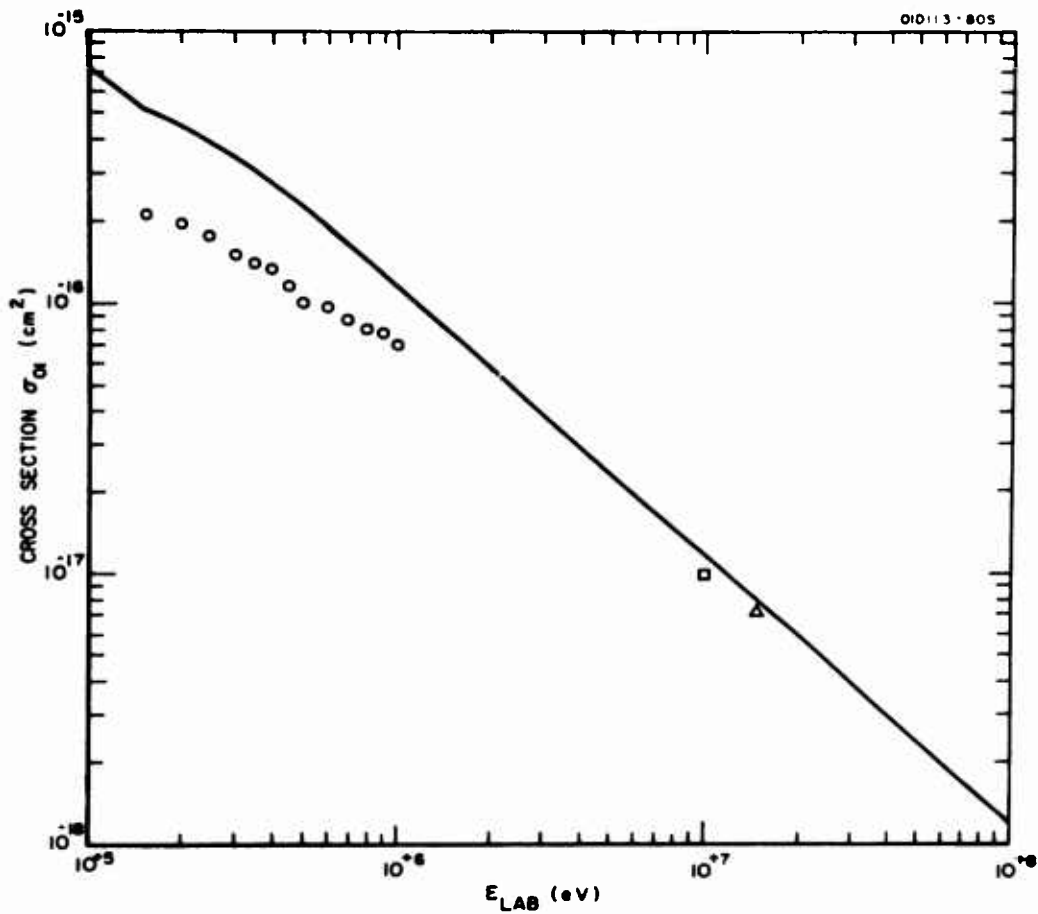


Figure 49. Electron Stripping Cross Section for Hydrogen Atoms Incident on Atomic Nitrogen. The Experimental Results are: ○, Ref. 32; □, Ref. 33; △, Ref. 34.

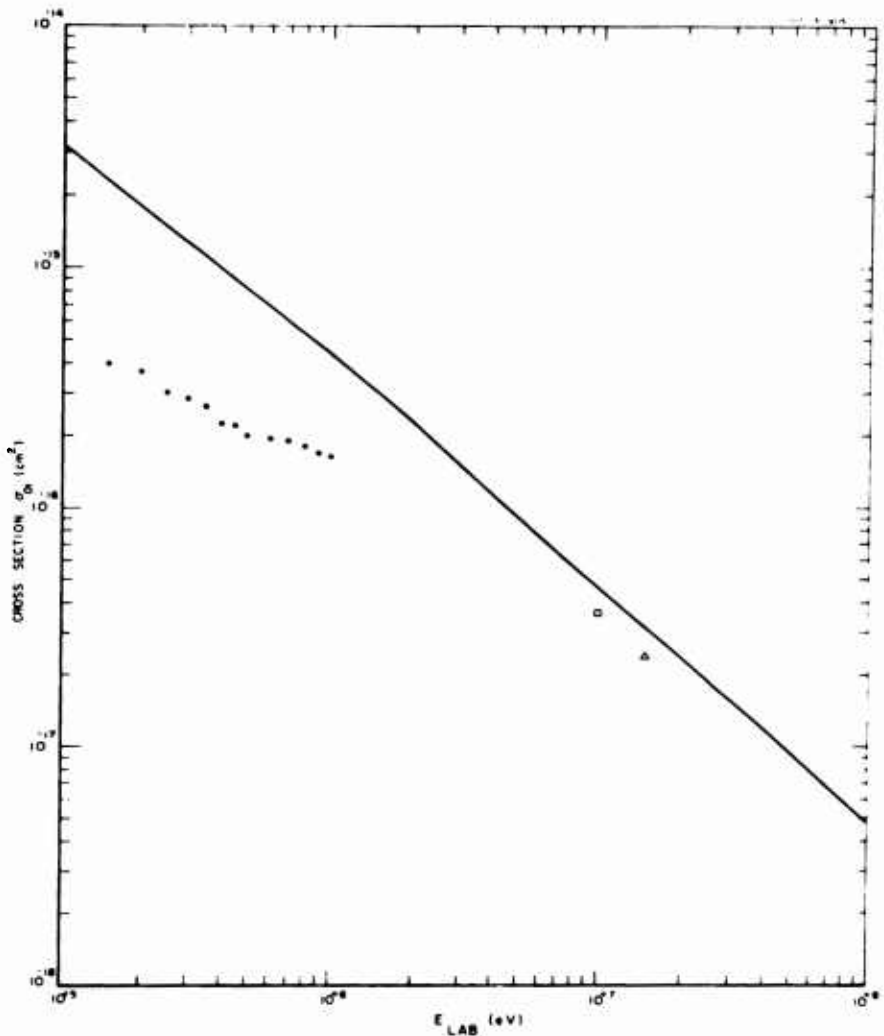


Figure 50. Electron Stripping Cross Section for Hydrogen Atoms Incident on Argon. The Experimental Results are: \circ , Ref. 32; \square , Ref. 33; \triangle , Ref. 34.

Hartree-Fock results. The more accurate calculations of the incoherent scattering factors using the correlated wavefunctions is smaller than the corresponding Hartree-Fock results for all values of the momentum transfer. It is expected that this behavior of the scattering factors is not limited to the helium system, but is true for larger systems. As the number of electrons in the system increases, the accuracy of the Hartree-Fock results decreases, especially for the incoherent scattering factor, which is a two-electron operator expectation value. Because the Hartree-Fock incoherent scattering factor is larger at all K than the accurate incoherent scattering factor, the integrand for the inelastic scattering contribution is overestimated by the use of Hartree-Fock incoherent scattering factors at all K , so that the contribution of inelastic processes to the high-energy stripping cross section is overestimated by the Hartree-Fock theory. For the elastic contribution, similar arguments show that for large K the use of Hartree-Fock form factors overestimates the integrand, but at small K it underestimates the integrand. The net effect on the elastic contribution can vary from system to system, but at high energies for projectile systems with large ionization potentials, where the lower limit of the elastic integration is large, the use of Hartree-Fock form factors will also lead to an overestimation of the stripping cross section. The extent to which the use of Hartree-Fock scattering factors contributes to the disagreement between theory and experiment for the high-energy H-N and H-Ar results cannot be resolved because it is dependent on the availability of more accurate nitrogen and argon wavefunctions, which must await considerable theoretical and computational advances. However, some of the discrepancy is caused by the use of Hartree-Fock wavefunctions in the scattering factor calculations.

Figure 51 compares the theoretical cross section for collisional detachment of the electron from the negative hydrogen ion upon impact with helium with the experimental data from Allison (Ref. 32). For these impact energies, the theory is not expected to apply so that the agreement to within a factor of about two may be accidental. The process is so efficient that the cross section has not been measured accurately at very high energies because the equilibrium fraction of negative ions in the beam becomes very small. It is interesting to note that here the theoretical results lie below the experimental results.

Figure 52 shows the electron stripping cross section for the many-electron projectile system of sodium incident on helium gas. The contributions of the various shells to the total cross section is shown. At high energies, it can be seen that the 2p shell contribution is significantly larger than the 3s shell contribution although the energy required to remove the 2p electrons is larger than the energy required to remove the 3s electrons. At high energies, the ratio of the 2p contribution to the 3s contribution is roughly 3:1, while the ratio of the number of 2p electrons to 3s electrons is 6, so that per electron, it is more efficient to remove the outer electron. The contribution of the 2s shell is negligible, as is the 1s contribution. The abrupt changes

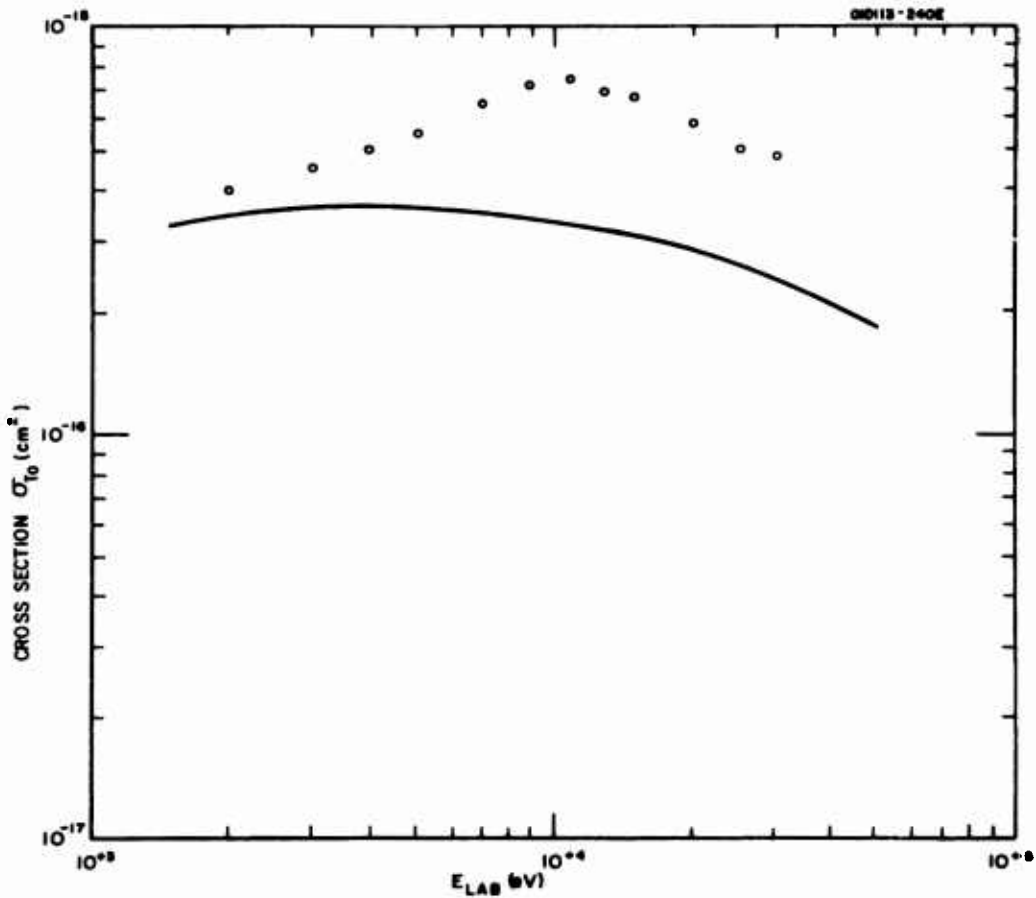


Figure 51. Collisional Detachment Cross Section for Negative Hydrogen Ions Incident on Helium. The Experimental Results are from Ref. 32.

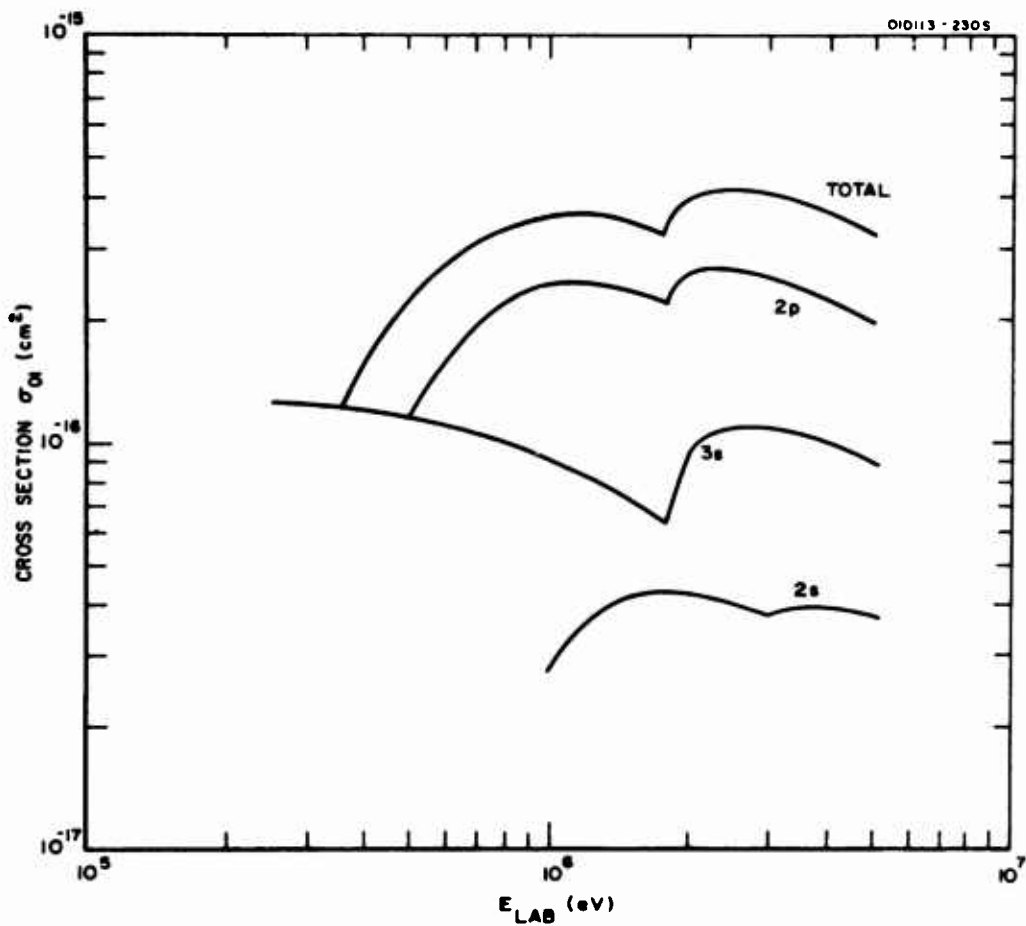


Figure 52. Electron Stripping Cross Section for Sodium Ions on Helium Showing the Total Cross Section and the Contributions of the Different Shells.

of the cross sections shown are not real and are only an artifact of the theory. At the cusps, the lower limit of the integration for the inelastic contribution changes from being dependent on k_0 and ΔE , to being a constant dependent only on the one electron energies of the electrons. However, the magnitude of the variation in the vicinity of the cusps show that the inelastic scattering contribution is large and is a sensitive function of the lower limit of the integration as discussed previously in Section III.

Some calculations of the electron stripping cross section for a more highly stripped projectile system have been performed involving an argon target and Cr, Cr^+ , Cr^{++} , Cr^{+3} , Cr^{+4} , and Cr^{+5} projectiles. The results are shown in Figure 53. At low energies, the cross section decreases rapidly with the stage of ionization of the projectile, but for higher energies the decrease in cross section is not nearly so rapid, and the highly stripped ions still have a large cross section for losing an additional electron. At these high energies, the equilibrium fraction of highly stripped ions in a beam is large. For the more highly stripped ions included in Figure 53, accurate values for the energy to remove one electron for the shells just below the valence shell are not available, so that estimates were employed. Accurate values of the valence electron ionization potentials (Ref. 29) are available, however, and in Figure 54 only the 3d valence shell contribution to the stripping cross section is shown. These results can be considered as lower limits to the stripping cross section in the free-electron scattering approximation. These values show a more rapid decrease of the stripping cross section as the stage of ionization of the projectile increases than the corresponding results when inner shell contributions are included.

The results of the calculations for the other systems, which are presented in Figures 55 through 64, will not be discussed in detail. Because of the limitations of the theory, only the results at very high energy are expected to be qualitatively reliable.

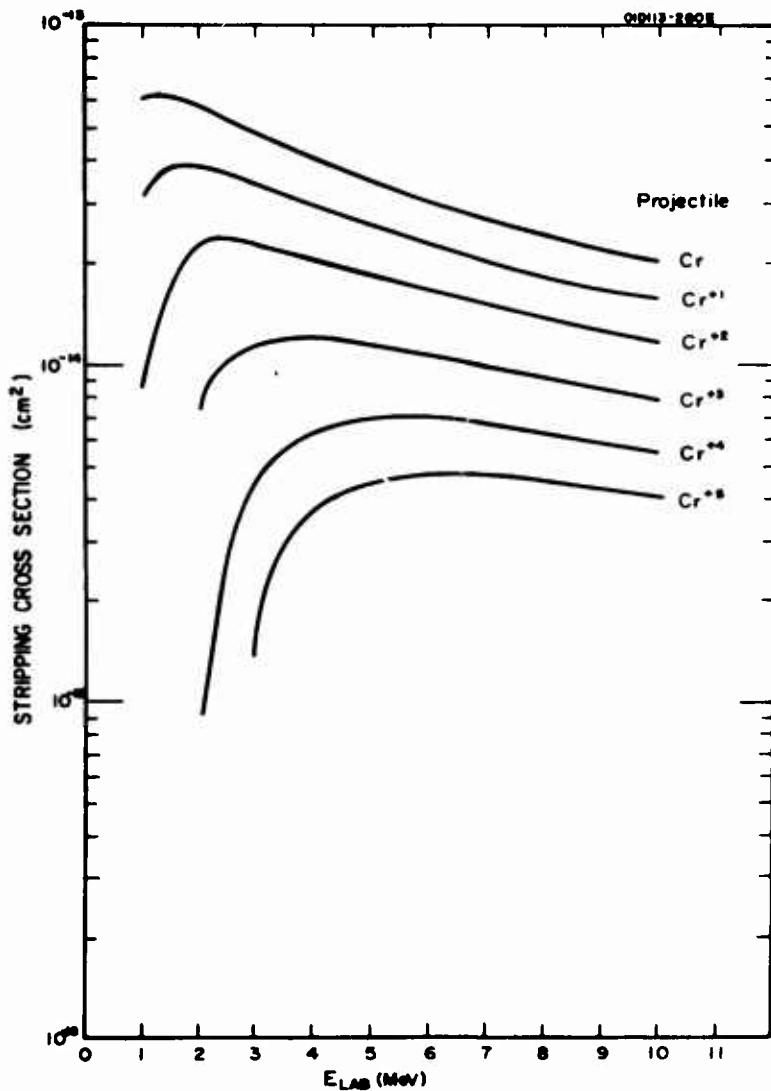


Figure 53. Electron Stripping Cross Sections for More Highly Stripped Chromium Ions Incident on Argon Including Inner Shell Contributions.

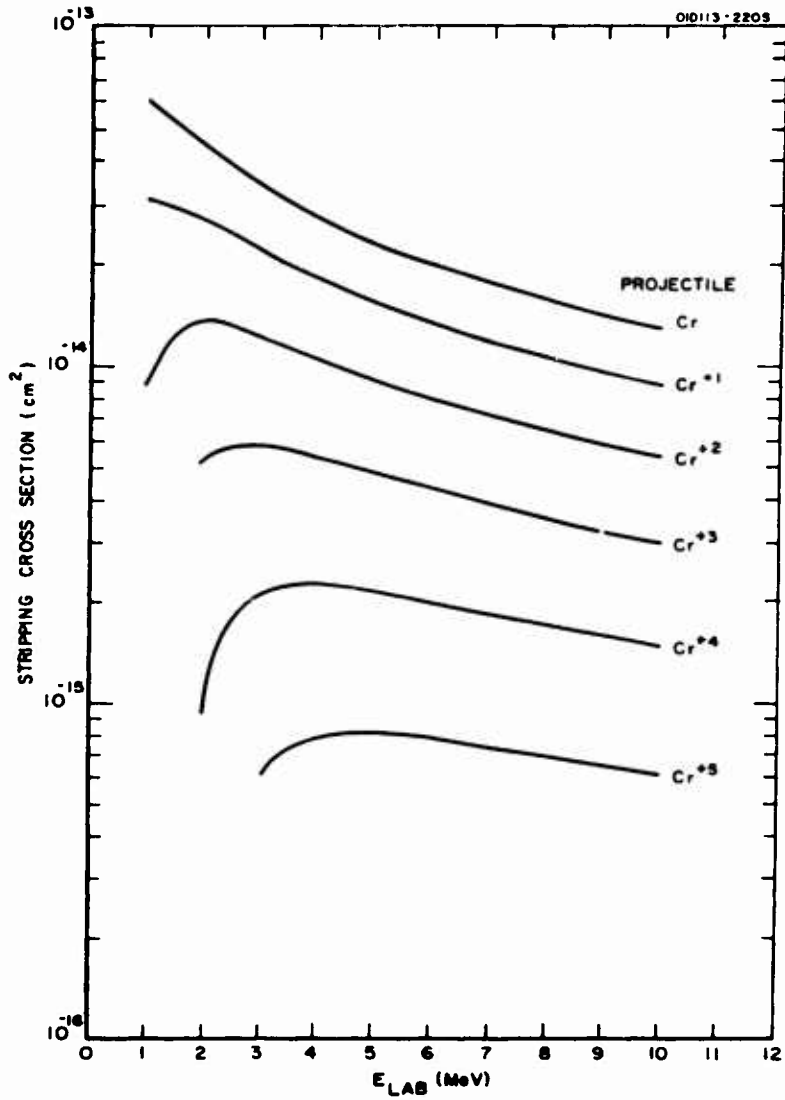


Figure 54. Valence Shell Contribution to the Electron Stripping Cross Section for More Highly Stripped Chromium Ions Incident on Argon.

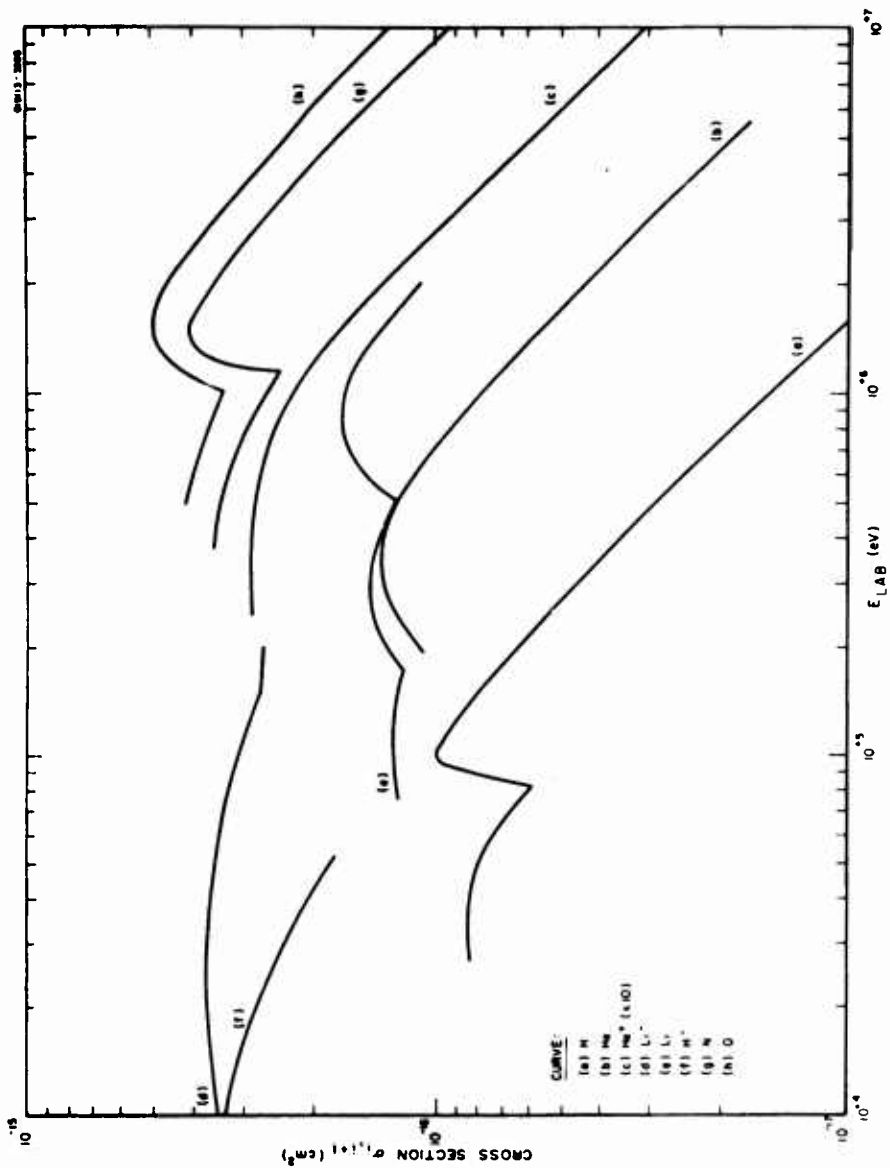


Figure 55. Electron Stripping Cross Sections for Various Projectile Systems in Helium Gas.

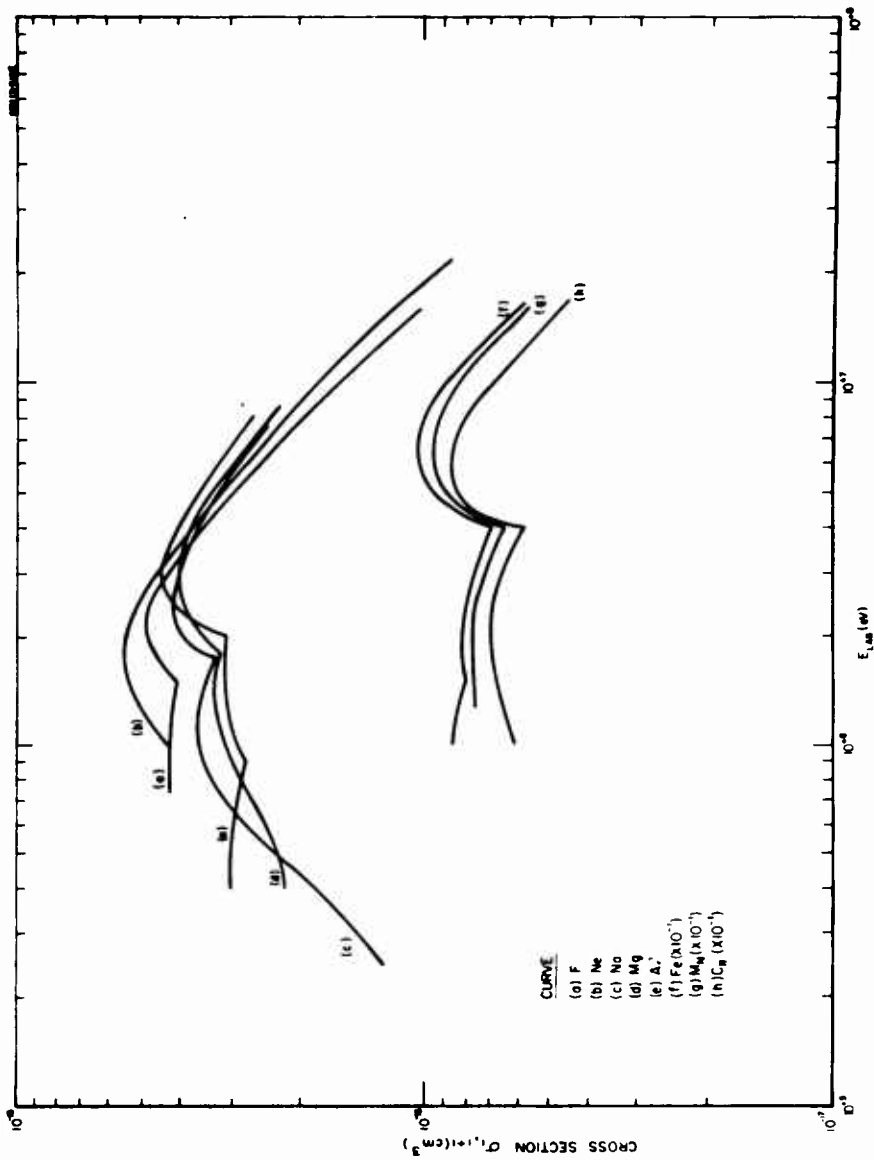


Figure 56. Electron Stripping Cross Sections for Various Projectile Systems in Helium Gas.

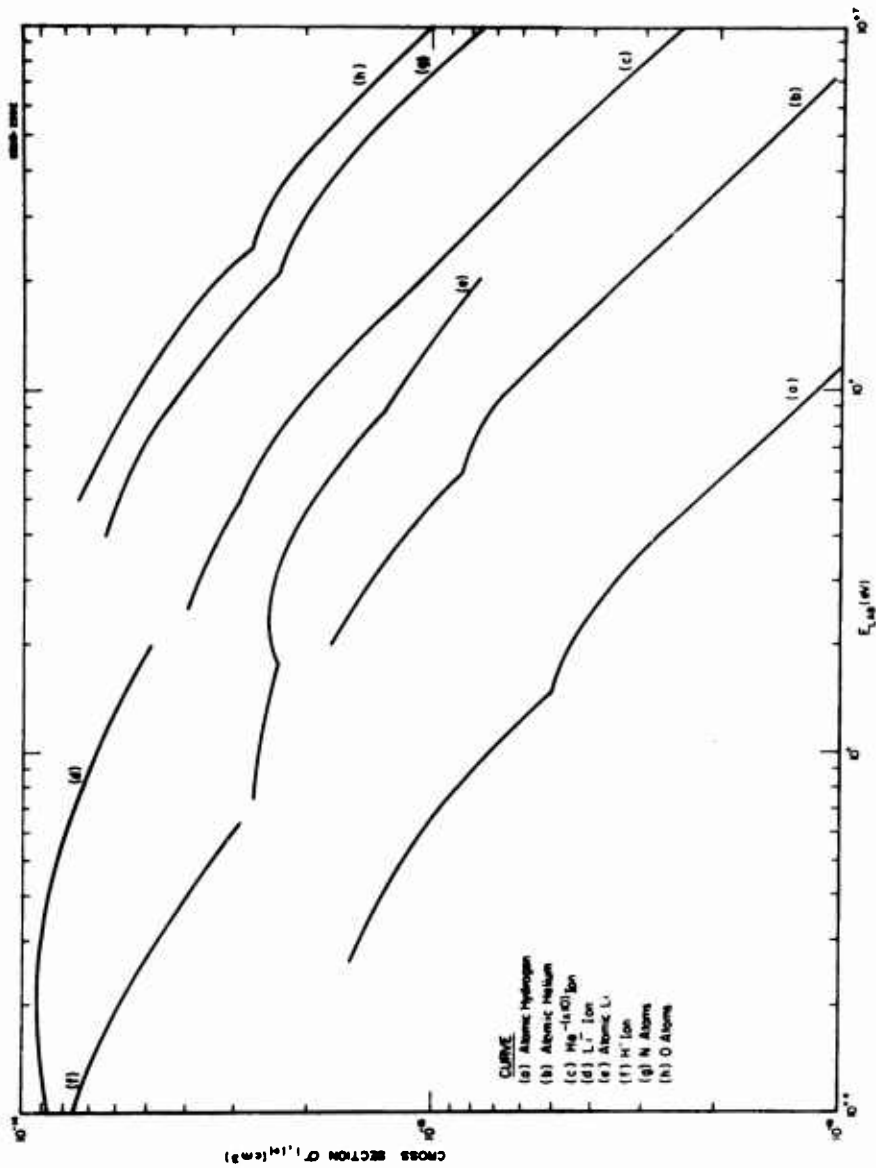


Figure 57. Electron Stripping Cross Sections for Various Projectile Systems in Atomic Nitrogen Gas.

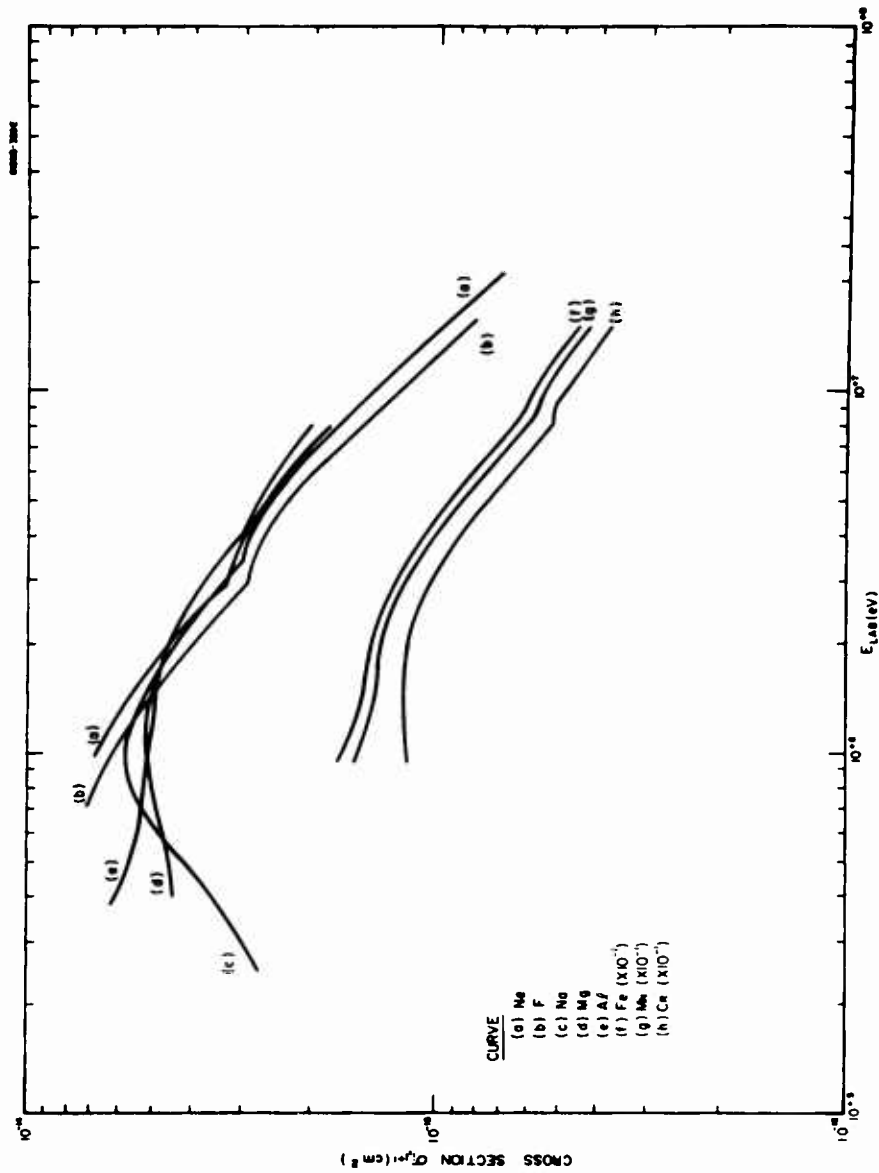


Figure 58. Electron Stripping Cross Sections for Various Projectile Systems in Atomic Nitrogen Gas.

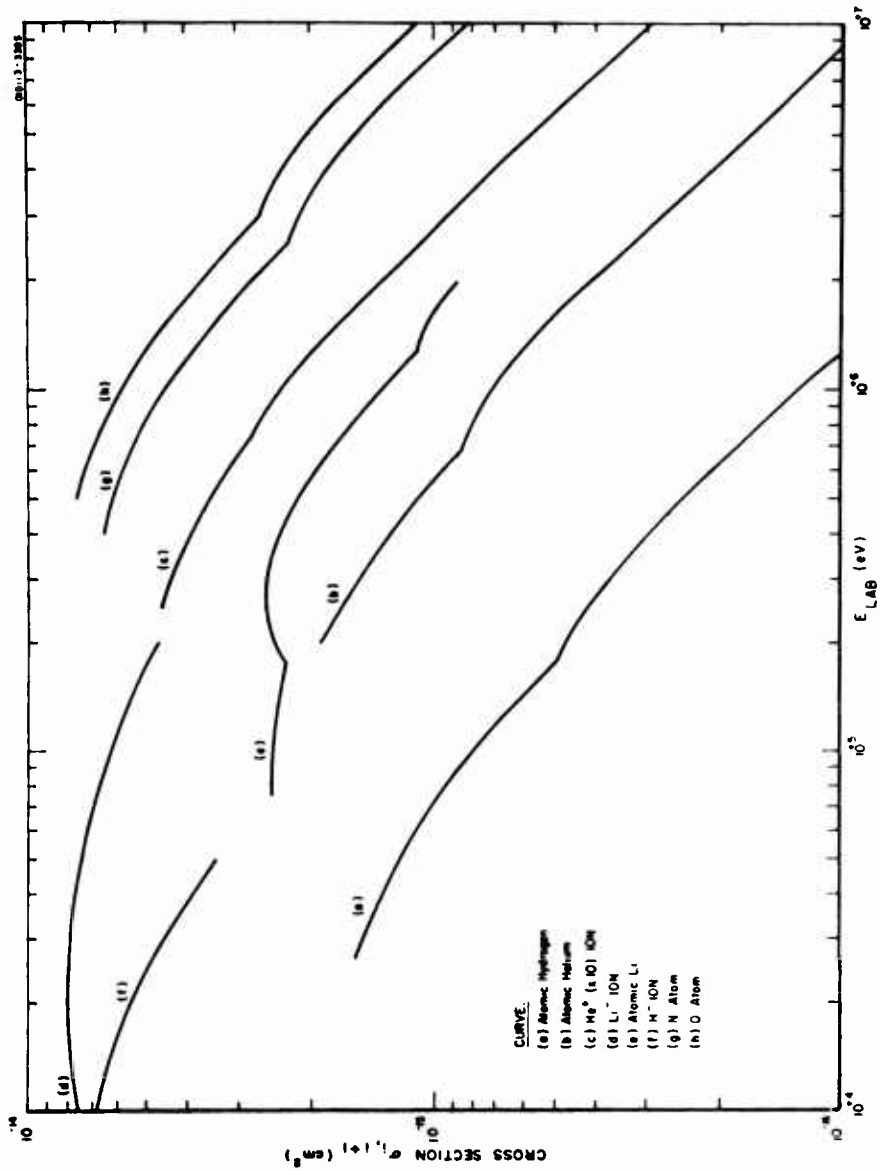


Figure 59. Electron Stripping Cross Sections for Various Projectile Systems in Atomic Oxygen Gas.

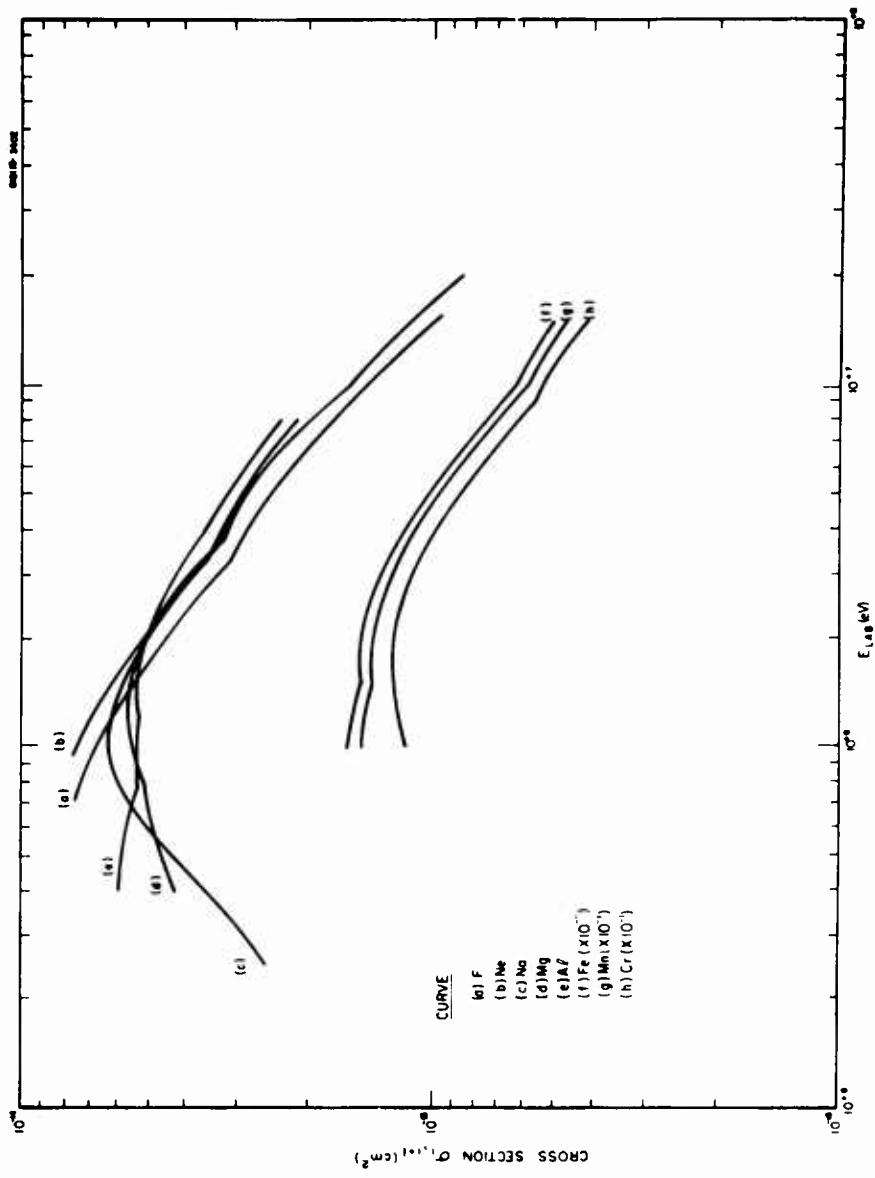


Figure 60. Electron Stripping Cross Sections for Various Projectile Systems in Atomic Oxygen Gas.

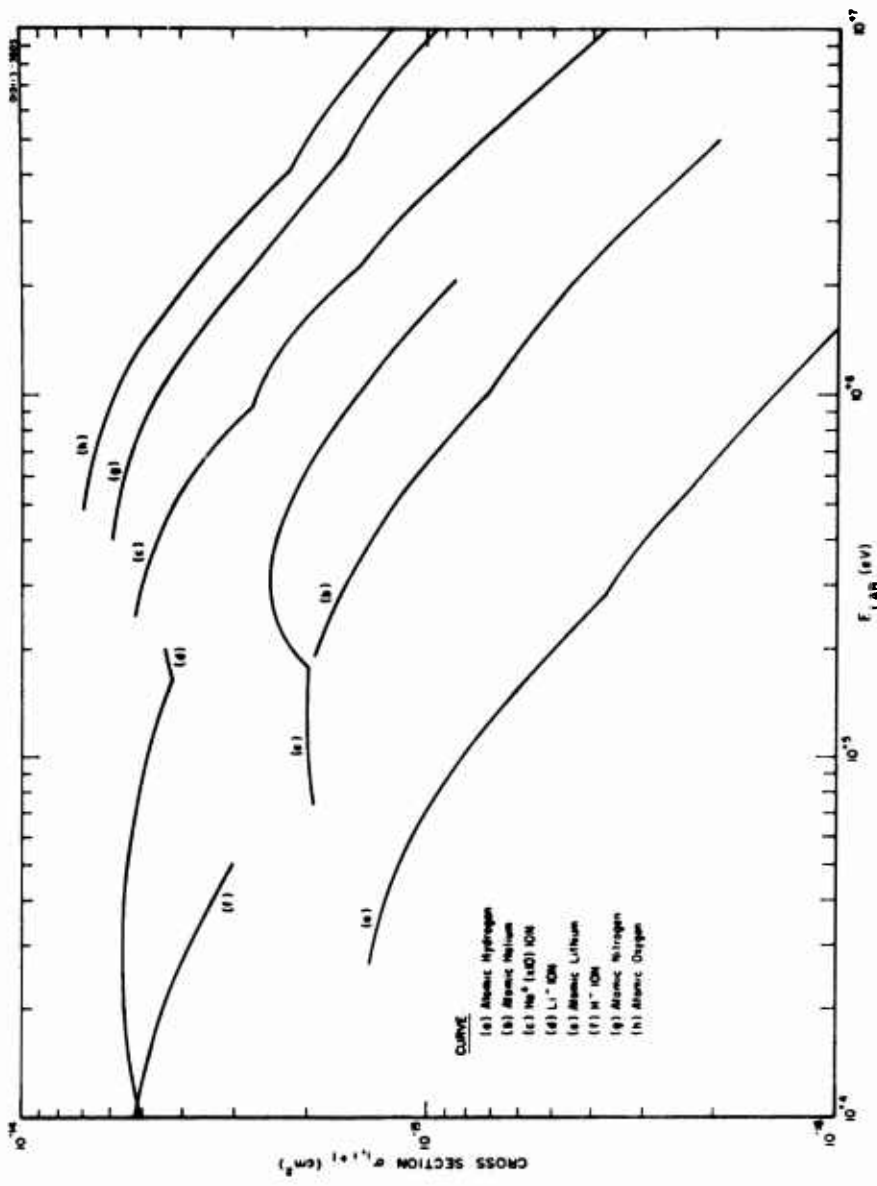


Figure 61. Electron Stripping Cross Sections for Various Projectile Systems in Neon.

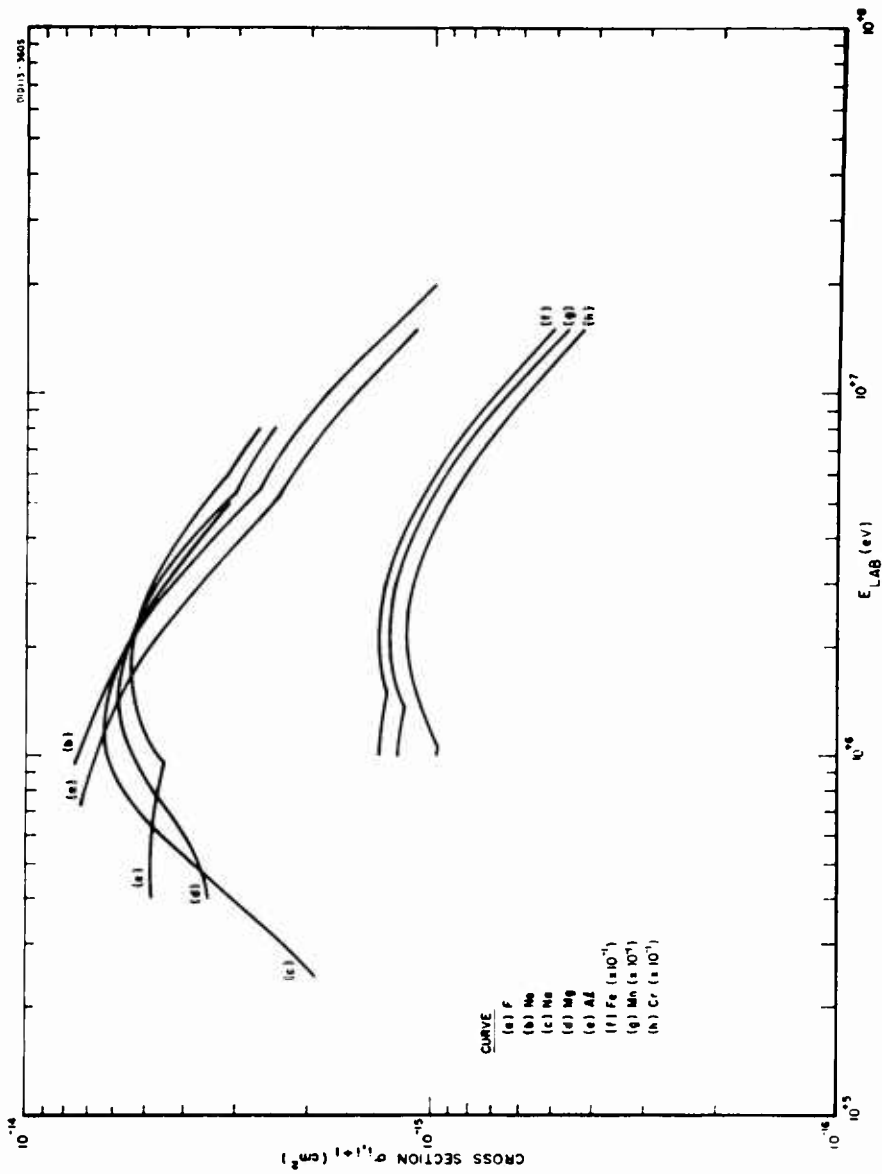


Figure 62. Electron Stripping Cross Sections for Various Projectile Systems in Neon.

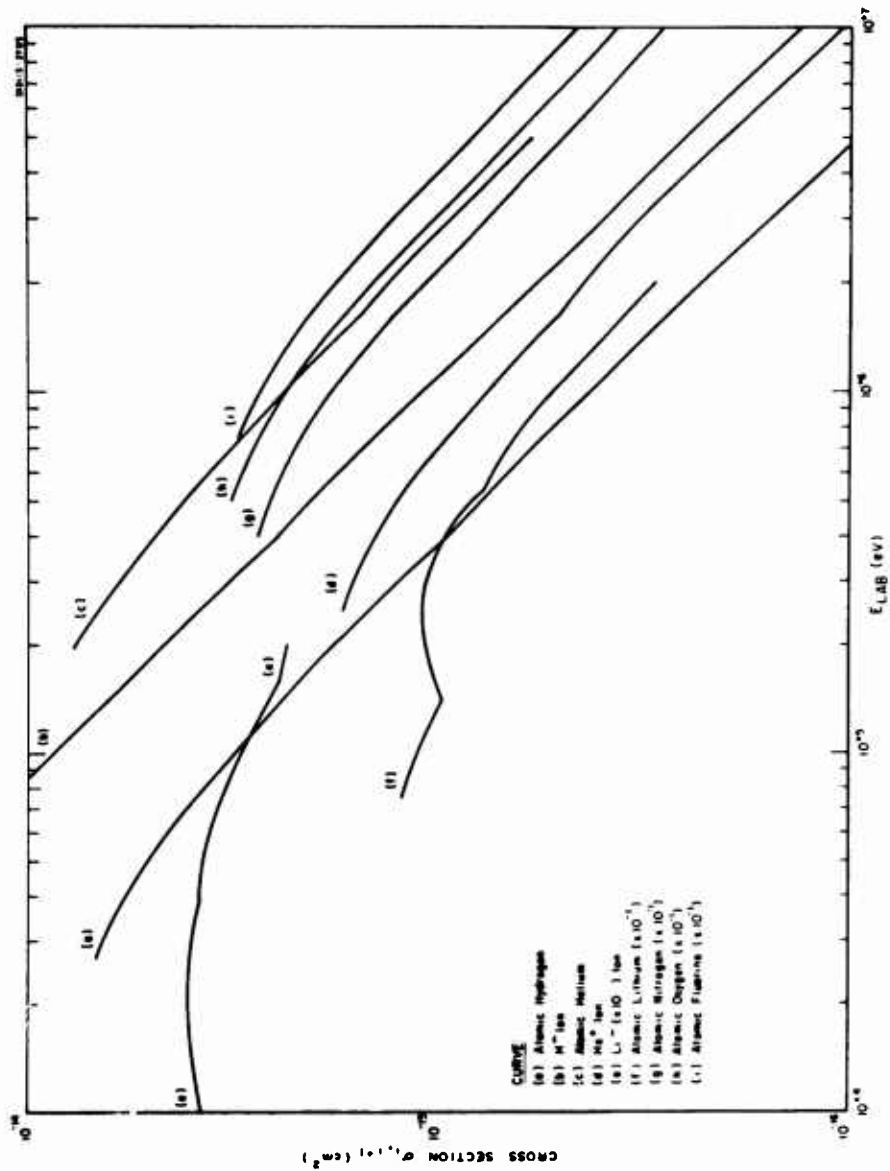


Figure 63. Electron Stripping Cross Sections for Various Projectile Systems in Argon.

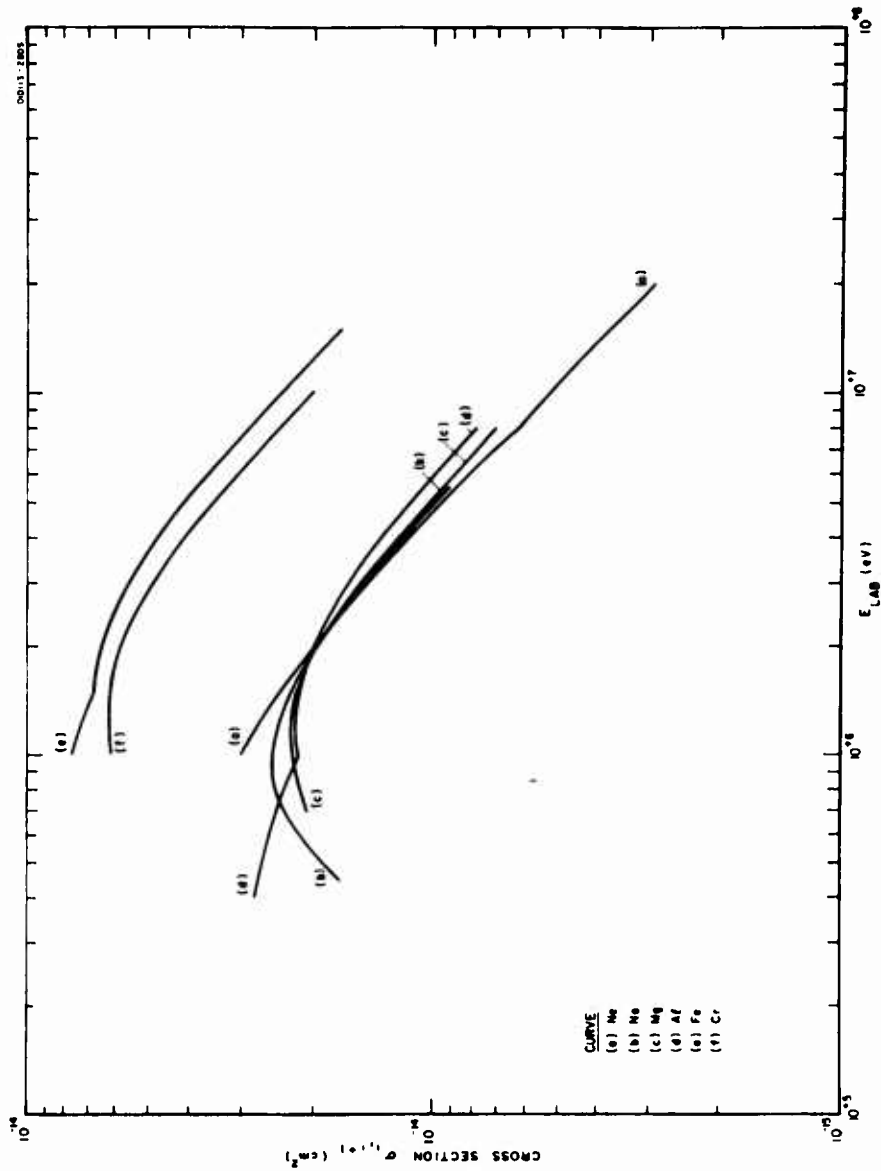


Figure 64. Electron Stripping Cross Sections for Various Projectile Systems in Argon.

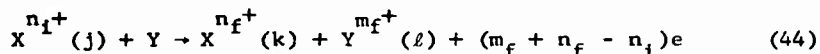
SECTION V

ENERGY LOSS OF FAST HEAVY IONS IN GASES

The Bethe (Ref. 23) theory of the stopping of fast charged heavy particles in neutral gases has been successful in the interpretation of the high impact energy data. The Bethe theory is based on the Born approximation with certain additional assumptions and ignores the possibility of excitation, electron capture, and electron loss by the projectile system. The neglect of inelastic processes for the projectile and the use of the Born approximation cause the Bethe theory to fail at low energies.

Dalgarno and Griffing (Ref. 35) have performed a detailed study of the rate of energy loss of protons in atomic hydrogen. They list the possible inelastic processes and obtain expressions for the contribution to the total stopping power for each process. The total stopping power is expressed in terms of the equilibrium fractional charge content of the beam and the energy loss cross sections for the various processes. Explicit results using the Born approximation cross sections for the relevant processes are given.

The formulation of the energy loss theory of Dalgarno and Griffing can be extended straightforwardly to beam and target systems with more electrons. If it is assumed that the stopping gas consists entirely of an atomic gas Y in its ground state, the inelastic processes that must be considered in detailed energy loss calculations are



where n_i , n_f , and m_f are positive or negative integers (if the negative ions exist) or zero, and j , k , and l represent the quantum numbers necessary to specify the possible states of the systems. If a proton beam incident on atomic hydrogen is considered, the range of values that n_i , n_f , and m_f can assume is small because

$$\begin{aligned} -1 &\leq n_i \leq +1 \\ -1 &\leq n_f \leq +1 \\ -1 &\leq m_f \leq +1 \end{aligned} \quad (45)$$

and only one state exists for the positive and negative ion. For many-electron target and projectile systems at high energies, more highly stripped projectile ions can become an important fraction of the equilibrium beam, and the number of reactions that must be considered becomes large. At sufficiently high energies, multiple ionization processes may become significant.

The electron stripping cross sections decrease much less rapidly with increasing projectile energy than the charge transfer cross sections. Because of the rapid decrease of the charge exchange cross sections with increasing energy, at high energies where the stripping cross sections calculated by using the free-scattering approximation are valid, the electron loss cross section for a typical neutral or once ionized projectile system is much larger than the corresponding electron capture cross section, as indicated by the results given in Section IV. To calculate the equilibrium charge fractions of the beam, it would be necessary to calculate charge exchange cross sections for highly stripped projectile ions incident on the neutral target gas. Because such cross sections are not presently available, meaningful calculations for the rate of energy loss at very high energies cannot be performed. Similarly, meaningful calculation for the rate of energy loss at lower energies must await the accurate determination of ionization and stripping cross sections in the desired energy range. Excitation of the target system does not enter into the equations that determine the equilibrium charge fractions of the beam, and excitation of the projectile systems influences the beam equilibrium only if the stopping gas is sufficiently dense or important metastable species formed. However, excitation processes make significant contributions to the energy loss cross section at most impact energies, and must be known in order to perform meaningful energy loss calculations.

The contribution to the energy loss cross section because of the charge transfer process



(where X and Y are not identical) is

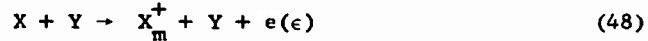
$$\sum_{\ell} \sum_{m} E_{\ell m} Q_{\ell m}$$

where $Q_{\ell m}$ is the cross section, and the energy $E_{\ell m}$ is given by

$$E_{\ell m} = T + E[X(\ell)] + E[Y^+(m)] - E(X^+) - E(Y) \quad (47)$$

where $E(Z)$ is the energy of the isolated system Z and T is the kinetic energy acquired by the captured electron. At moderate and high energies, the kinetic energy term T constitutes a significant part of $E_{\ell m}$.

The contribution to the energy loss cross section from the stripping reaction



where the ejected electron has a kinetic energy ϵ with respect to the parent nucleus, and the final state of the target system is the ground state, is given by

$$\sum_m \int_0^{\epsilon_{\max}^{(m)}} Q_m(\epsilon) (I_m' + \epsilon) d\epsilon \quad (49)$$

where $Q_m(\epsilon)$ is the cross section for the ejection of an electron with energy between ϵ and $\epsilon+d\epsilon$ and $\epsilon_{\max}^{(m)}$ is determined by the conservation of energy and momentum. Here I_m' is the sum of the ionization potential of the projectile and the excitation potential of the final projectile state m .

In the free-scattering approximation, only those excited states of the projectile that can be represented by the removal of a single valence or inner shell electron in a central field approximation are considered. The energy loss cross section for reaction (48) is approximated by

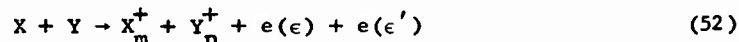
$$\frac{1}{2} \sum_{i=1}^n \int_{k_{1i}}^{k_{2i}} k^2 d\sigma_{e1} \quad (50)$$

where the variables are defined in Section III. Expression (50) can be considered a good approximation to expression (49) only if the major contribution to the integral in expression (49) comes from the part of energy space where $\epsilon > I_m'$, so that reliable results are expected only at high energies for systems where the stripped electron is loosely bound (I_m' small).

The contribution to the energy loss cross section from the reactions



and



cannot be obtained with similar accuracy from the free-scattering approximation because of the use of the closure properties. The contribution to the energy loss cross section from reaction (51) is

$$\sum_m \sum_n \int_0^{\epsilon_{\max}^{(m,n)}} Q_{m,n}(\epsilon) (I'_m + E_n + \epsilon) d\epsilon \quad (53)$$

where $Q_{m,n}(\epsilon)$ is the cross section and E_n is the excitation energy of the final target state. The contribution to the energy loss cross section from reactions (52) is

$$\sum_m \sum_n \int_0^{\epsilon_{\max}^{(m,n)}} d\epsilon \int_0^{\epsilon'_{\max}^{(m,n)}} d\epsilon' Q_{m,n}(\epsilon, \epsilon') (I'_m + E_n + \epsilon + \epsilon') \quad (54)$$

where $Q_{m,n}(\epsilon, \epsilon')$ is the corresponding cross section. By using the closure properties, the sum of expressions (53) and (54) is approximated by

$$\frac{1}{2} \sum_{i=1}^n \int_{k_{3i}}^{k_{4i}} K^2 d\sigma_{in} \quad (55)$$

The use of expression (55) is valid only if the major part of the contribution to the integrals in expression (53) comes from the part of the energy space where $\epsilon > I'_m + E_n$, and similarly for expression (54) where the condition is $\epsilon > I'_m + E_n + \epsilon'$.

The sum of expressions (50) and (55) have been calculated in units of eV cm^2 , for various projectile ions in argon gas. The results are shown in Figures 65 and 66. The approximate energy loss cross section maxima occur at higher impact energies than the corresponding electron stripping cross section maxima, and at large energies they show more gradual decrease with increasing impact energy.

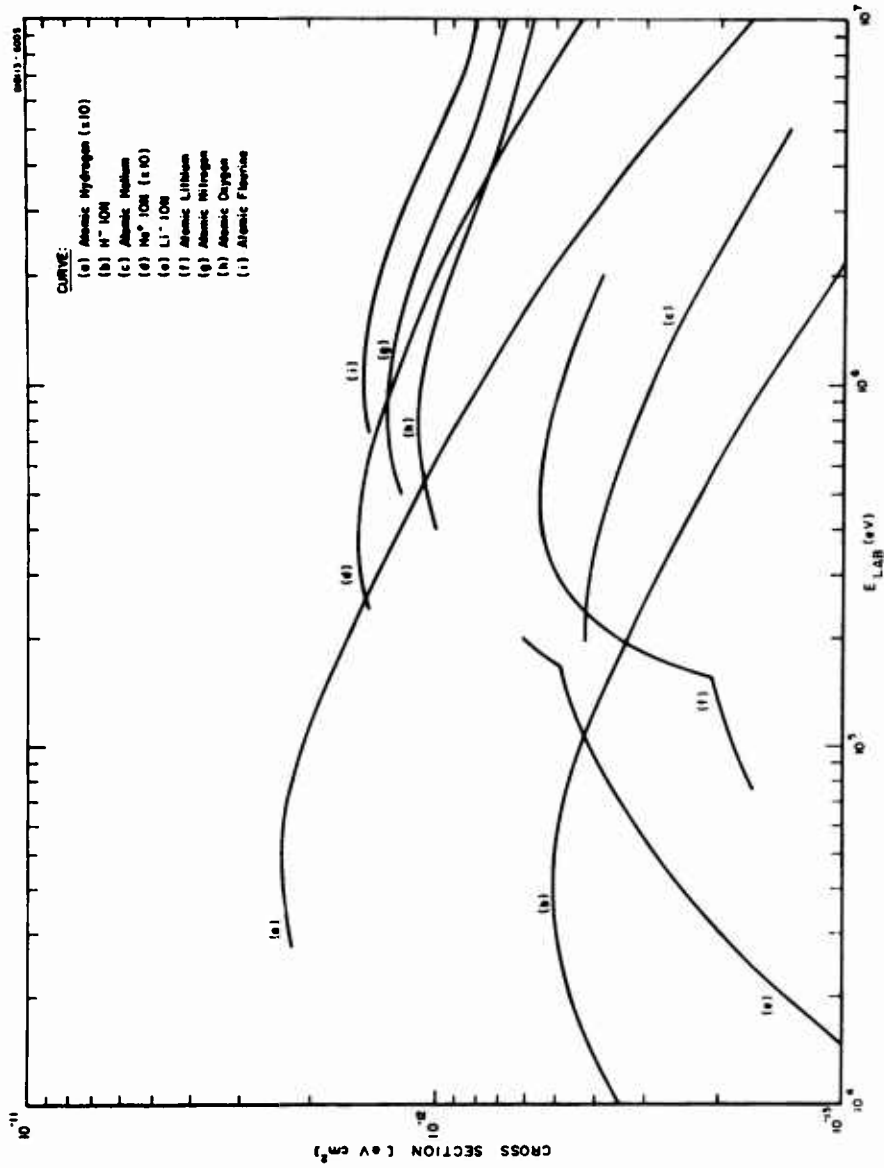


Figure 65. Cross Section for Energy Loss in Electron Stripping Processes for Various Ions in Argon Gas.

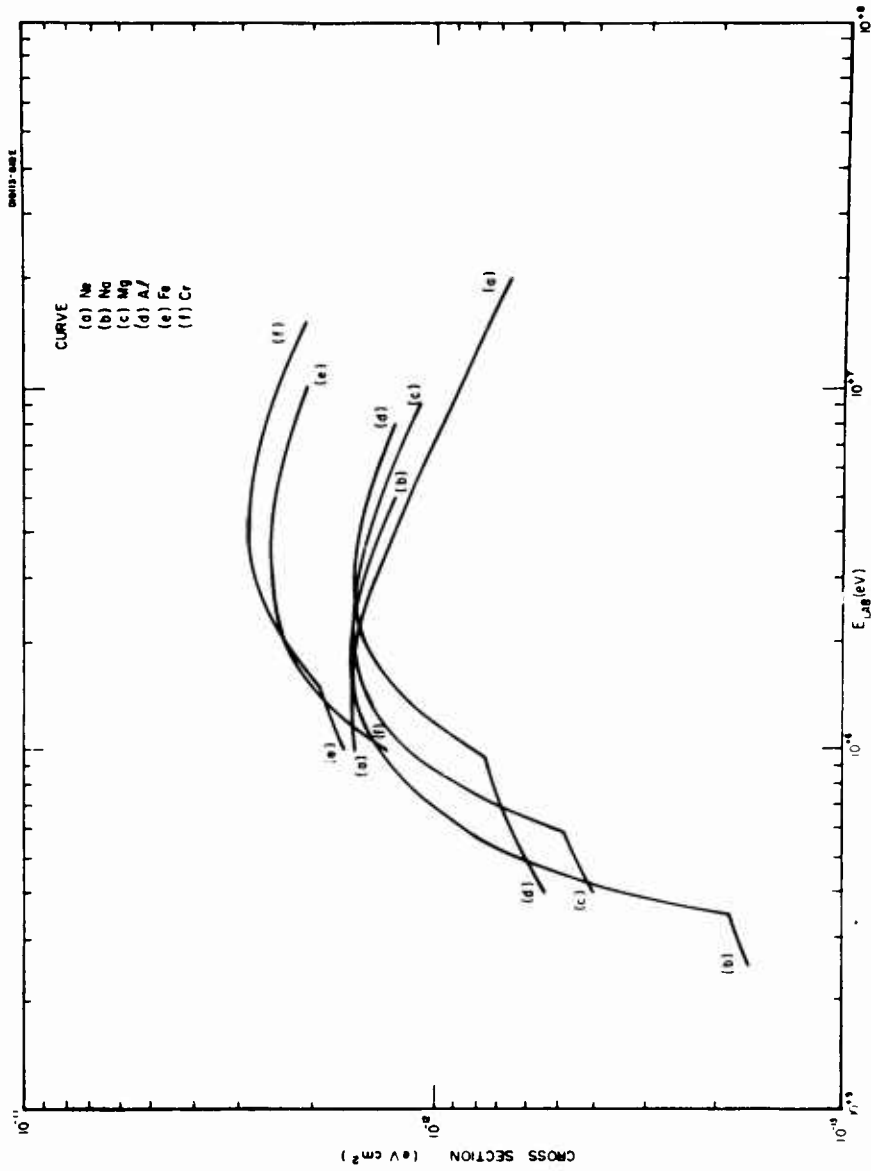


Figure 66. Cross Section for Energy Loss in Electron Stripping Processes for Various Ions in Argon Gas.

Page 96 omitted, no information deleted.

This page intentionally left blank.

APPENDIX I

PROGRAM XSCTN2 AND ASSOCIATED SECTIONS

Several modifications have been made to the program discussed in reference 1. A description of the present version of the program is included herein. The basic operation of the program remains unchanged. The modifications affect mainly the input and output and the option of a correction for the long-range behavior of the h_{ij} and h_{jj} matrix elements. Arrangements for timing the program's execution have also been made. An uncompleted modification to incorporate the "exchange" correction is included, marked by some parameters noted as "unused." These parameters should be provided.

XSCTN2 computes the charge exchange cross section by organizing integrations (MLTI04) of the two-state equations along a series of trajectories on the assumption that the capture probabilities behave as $\exp(-\gamma\rho)$. γ (GMM) is found by specifying two large impact parameters ρ_a (RHOA) and ρ_b (RHOB) at which the numerically derived capture probabilities $C_n(\rho_a)$ (CA) and $C_n(\rho_b)$ (CB) are computed so that

$$\gamma = \frac{\ln [C_n(\rho_b)/C_n(\rho_a)]}{(\rho_a - \rho_b)}$$

or else if ρ_a is set zero, γ is taken as ρ_b . γ is assumed to be the same for the capture probabilities obtained numerically (C_n), by the Rapp-Francis expression (C_r) and by application of the model (C_m). A series of pivotal impact parameters ρ_i is then generated with which to compute the cross section quadratures of Gauss-Laguerre type:

$$\begin{aligned} Q &= 2\pi \int_0^\infty d\rho \rho \exp(-\gamma\rho) [C \exp(\gamma\rho)] \\ &= 2\pi \sum_1 W_1 C(\rho_1) \exp(\gamma\rho_1) \end{aligned}$$

The first 10 terms of a 16-term quadrature are employed to compute Q_n , Q_r , and Q_m corresponding to C_n , C_r , and C_m .

MLTI04 performs the integrations along the trajectory, numerically (calls INTGRT) and analytically, by evaluating the Rapp-Francis expression and if MODE = 2, the analytic form of the solution. MLTI04 uses the assumed maximum distance (EFFRAD) of interaction to determine trajectory

length and also establishes a "logarithmically" spaced set of reporting "stations" along the trajectory (clustered more closely about the point of closest approach) at which significant quantities in the calculation are stored and from which are subsequently written. If MODE = 3 these intermediate quantities are not printed.

INTGRT performs the numerical integration along the trajectory by using Hamming's method. When entered, INTGRT performs a step in the solution of the equation by calling HAMMING,

$$\frac{d\vec{y}}{dx} = [C] \vec{y}$$

where $[C] \vec{y}$ is provided by calling RHS, which in turn calls QCM to generate the matrix $[C]$ at the required point. INTGRT is used not only to integrate the two-state Equations of Motion, but also to integrate two additional quantities with respect to distance along the trajectory, it adjusts the interval of integration. QCM organizes the subroutines W (through NTRNS) and QGLQ to perform respectively the nontranslational and translational integrals in the evaluation of the matrix elements. In the construction of the basic matrix elements each cross product arising from the expressions for wavefunctions and potential is treated separately.

XYZ sets up the coordinate dependent C11 and C22 arrays for the non-translational integral evaluation performed by W, X, Y, and Z.

QGLG performs the quadrature required in the translational integrals for S_{ij} , h_{ij} , and h_{ji} in which the auxiliary function is computed by QXF by using the array AXFN. This array is coded as follows: the auxiliary function f_{n_1, n_2} is identified by:

$$J = n_2 + 8n_1 + 1$$

The N-th term of the integrand in the quadrature with respect to λ is

$$i^{\ell} C \lambda^n j_{\ell}(\zeta) P_{\ell}^0(\cos \psi)$$

and is given by:

$$C = \text{AXFN}(N, 1, J) / \text{AXFN}(N, 2, J)$$

$$n = \text{AXFN}(N, 3, J)$$

$$\ell = \text{AXFN}(N, 4, J)$$

The functions QZETA, QCSPSI, QSBF, QALF, which generate, respectively, ζ , $\cos \psi$, $j_\ell(\zeta)$ and $P_\ell^0(\cos \psi)$, are also called. The data deck for XSCTN2 contains first various constants AXFN for the translational integrals. These are followed by a block of quantities that are either fixed or have proven relatively standard:

NGLQ: Number of Gauss-Laguerre pivots (GLQPVT) and weight (GLQWT) to be subsequently read in.
 EMCRT: Criteria applied to error measure in QGLQ.
 GLQPVT, GLQWT: Pivots and Weights for QGLQ.
 ZSBF: Value of argument modules for QSBF below which Taylor series is used.
 SBFCV: Criteria applied to convergence estimate for series in QSBF.
 CNCLT: Criteria applied to cancellation estimate for explicit evaluation in QSBF.
 E: Criteria applied to truncation error estimate in INTGRT.
 NGLM: Number of modified Gauss-Laguerre pivots (BLMPVT) and weights (GLMEWT) to be subsequently read in.
 NSTAT: The (odd) number of reporting stations desired on the trajectory.
 MODE: (=1) no Rosen-Zener model computed, (=2) Rosen-Zener model computed, (=3) as 2 but intermediate output (associated with NSTAT) omitted.
 NEXT: (=1) a new velocity/energy (V,KEV) read, (=2) a new "reaction block" read.
 NXCH: (=1) bypasses proposed "exchange" modification.
 NELCN: (=1) elastic matrix element correction not performed, (=2) correction performed.

Following these quantities are one or more reaction blocks and one or more velocities or energies depending on value given to NEXT.

APPN: (=0) causes immediate termination of execution, (=X, where X is any alphameric symbol except 0) causes output to be identified as Xs approximation.
 TAR: Alphameric identification of target species.
 ETAR: See C statement following read.
 DUM: Dummy variable.
 NTEL: Number of active target electrons (unused).
 ZTAR: Net charge in a.u. on target after collision.
 TO,VT: Target orbital and potential parameters (see reference 1)
 PRO: Alphameric identification of projectile.
 EPRO: See C statement following read.
 PRMSS: See C statement following read.
 NPTEL: Number of active projectile electrons (unused).
 ZPRO: New charge in a.u. on projectile before collision.
 PO,VT: Projectile orbital and potential parameters.
 RHOA, RHOB: ρ_a and ρ_b referred to above. If RHCA=0, RHOB is assumed to contain γ .
 EFFRAD: Assumed maximum distance at which systems interact.
 V,KEV: Velocity in a.u. and energy in KeV of collision, one should be zero.

The output of the program is labeled so as to be self-explanatory on cards and printer both.

FLOW CHART FOR XSCTN2 MAIN PROGRAM

Read quantities associated with nontranslational integrals.

Read quantities associated with translational integrals.

Read operational parameters: NSTAT, MODE, NEXT, NXCH, NELCN

Read first part of "reaction block" data: parameters of atomic systems.

Test APPN $\xrightarrow{\text{Zero}}$ exit.
 \downarrow Nonzero

Read second part of "reaction block" data: collision parameters.

Compute V or KEV given one.

Write reaction specification.

Test RHOA $\xrightarrow{\text{Zero}}$ Interpret RHOB as GMM.
 Nonzero \downarrow
 Call MLTIO4 twice generating CA, CB for RHOA, RHOB. Compute GMM.

Set up pivoted impact parameter VRHO appropriate to GMM.

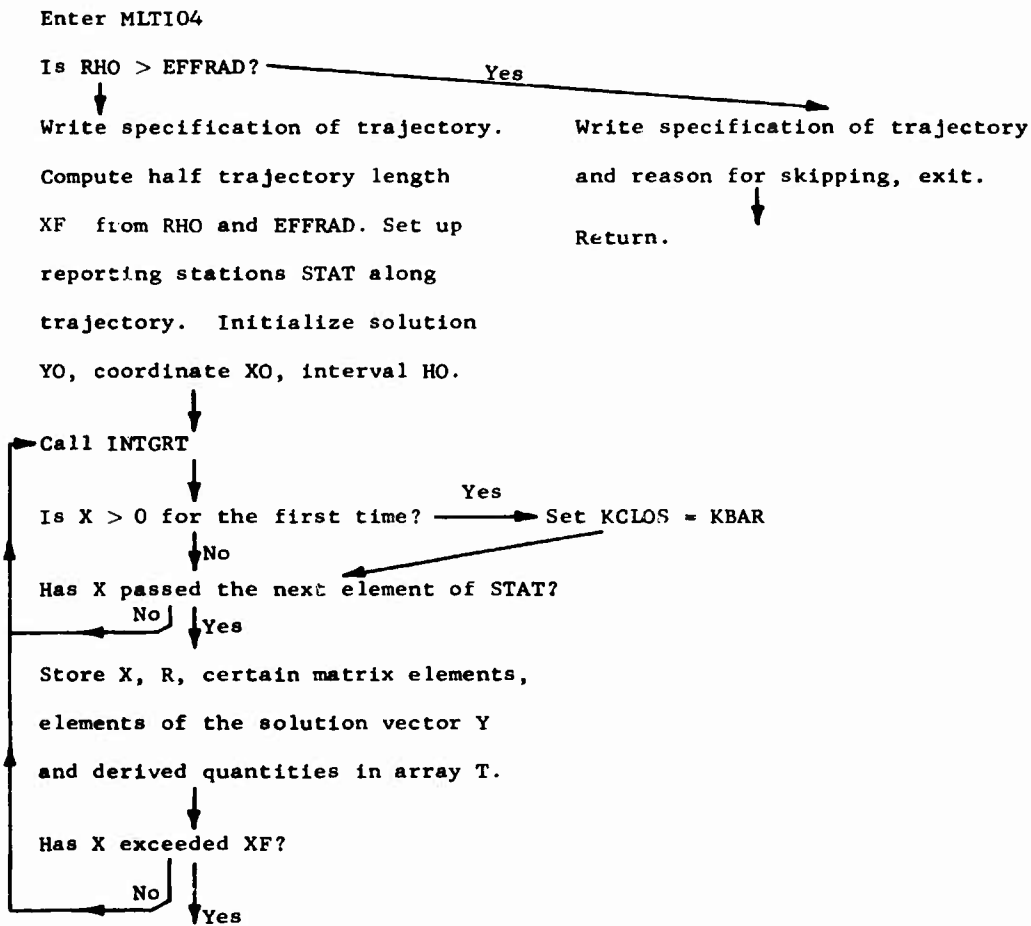
Call MLTIO4 repeatedly, computing numerical (CPR), Rapp-Francis (RAPP) and model (ANA) capture probabilities for approximately first 5/8 of VRHO.

Write final output for reaction consisting of: reaction specification; RHOA, RHOB, CA, CB and GMM; a table of impact parameters, 3 capture probabilities and their contributions to the total cross sections; final statement of 3 approximations to the cross section.

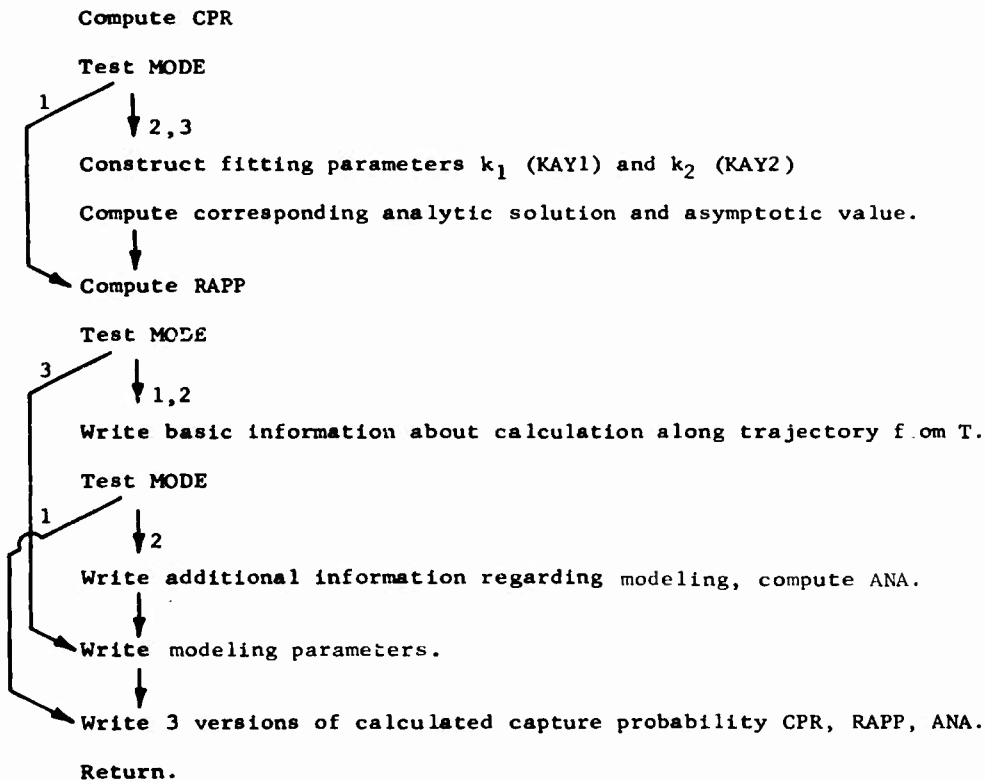
Test NEXT.



FLOW CHART FOR MLTIO4



FLOW CHART FOR MLT104 (cont.)



APPENDIX II

STRIPPING CROSS SECTION PROGRAM

The program that calculates the electron stripping cross section consists of a very short driver and six subprograms. The program is written for the CDC6000 series computers in FORTRAN. Actual testing and production were performed on a CDC6400 machine. The calculations required little computer time, only about 30 seconds being used to calculate the stripping and energy loss cross section for about 10 different projectile systems in one target gas system for a wide range of impact energies. The program is simple and straightforward, and contains numerous comment cards, so that exceptionally detailed program documentation is not required. A schematic flow diagram of the program is shown in Figure 67.

The main program STIP calls the important working subroutines and reads the parameter N, which is on the final data card for each calculation. The value to which N is set controls the reading of the next data set. All new data, new target data only, or new projectile data only is called for, with N = 1, 2, or 3, respectively. If N is zero or negative the program stops. Subroutine REDD reads the input data under the control of the parameter N. Subroutine WORK calculates the limits of integration and computes the electron stripping and energy loss cross sections by calculating the values of the integrals using Gauss quadratures. Subroutine WORK also controls the printing of the results.

Subroutine TERP prepares the interpolation arrays EFF and SEFF for the elastic and incoherent scattering factors from the input arrays. Subroutine FIT actually calculates the array elements for the interpolation arrays. A cubic fit is used for the interpolation. Function S calculates the incoherent scattering factor for a given momentum transfer by using the interpolation array SEFF for the cubic interpolation. Function F calculates the elastic form factor using the array EFF.

The major variables in the various segments of the program are identified as follows:

- N is the parameter that controls repeated executions for different target and projectile systems as described previously.
- NINT is the number of points used in the Gauss integrations.
- WT(I) is the I-th weight.
- PIV(I) is the I-th Gauss pivot.
- NPE is the number of input data points for the elastic form factor.
- ITYP1 and ITYP2 are parameters which allow the input data to be in the different units commonly used for the scattering factor data. Details are on the comment cards in the subroutine REDD.
- XKE is the one-dimensional array containing the tabulated values of K for which the elastic form factor is given.

XFKE is the array of elastic form factor values.
NPI is the number of input data points for the incoherent scattering factor.
XKI is the array of K values for which incoherent scattering factor data are given.
XFKI is the array of incoherent scattering factor data.
IZ is the number of electrons in the target system.
TMASS is the mass of the target system in atomic mass units.
EXCT is the target excitation energy as discussed in Section III-2.
NSP is the number of shells in the projectile system.
NES is the array containing the numbers of electrons in each projectile shell.
POT is the array of ionization potentials for the various projectile shells.
PMASS is the projectile mass in atomic mass units.
EMIN is the lowest laboratory collision energy in electron volts.
EMAX is the highest laboratory collision energy in electron volts.
DELTA E is the energy increment for the energy range.
RM is the reduced mass of the target-projectile system.
ECM is the center of mass system energy in electron volts.
EAU is the laboratory energy in atomic units.
V is the nuclei relative velocity in atomic units.
ULE is the upper limit of integration for the elastic scattering contribution.
ULI is the upper limit of integration for the inelastic scattering contribution.
WLE is the lower limit of integration for the elastic scattering contribution.
WLI is the lower limit of integration for the inelastic scattering contribution.
CROSS is the array that holds the contributions to the stripping cross section for each shell.
CROSI is the array that holds the contributions to the energy loss cross section for each shell.
TXS is the total stripping cross section.
TSY is the total energy loss in stripping cross section.
EFF is the array of parameters used in the interpolation for the elastic form factor.
SEFF is the array of parameters used in the interpolation for the incoherent scattering factor.

Following the listing of the program and subprograms, a listing of data for the calculation of the stripping and energy loss in stripping cross sections for hydrogen projectiles in argon gas is given. A detailed description is not presented because the comment cards in the subroutine REDD give sufficient information.

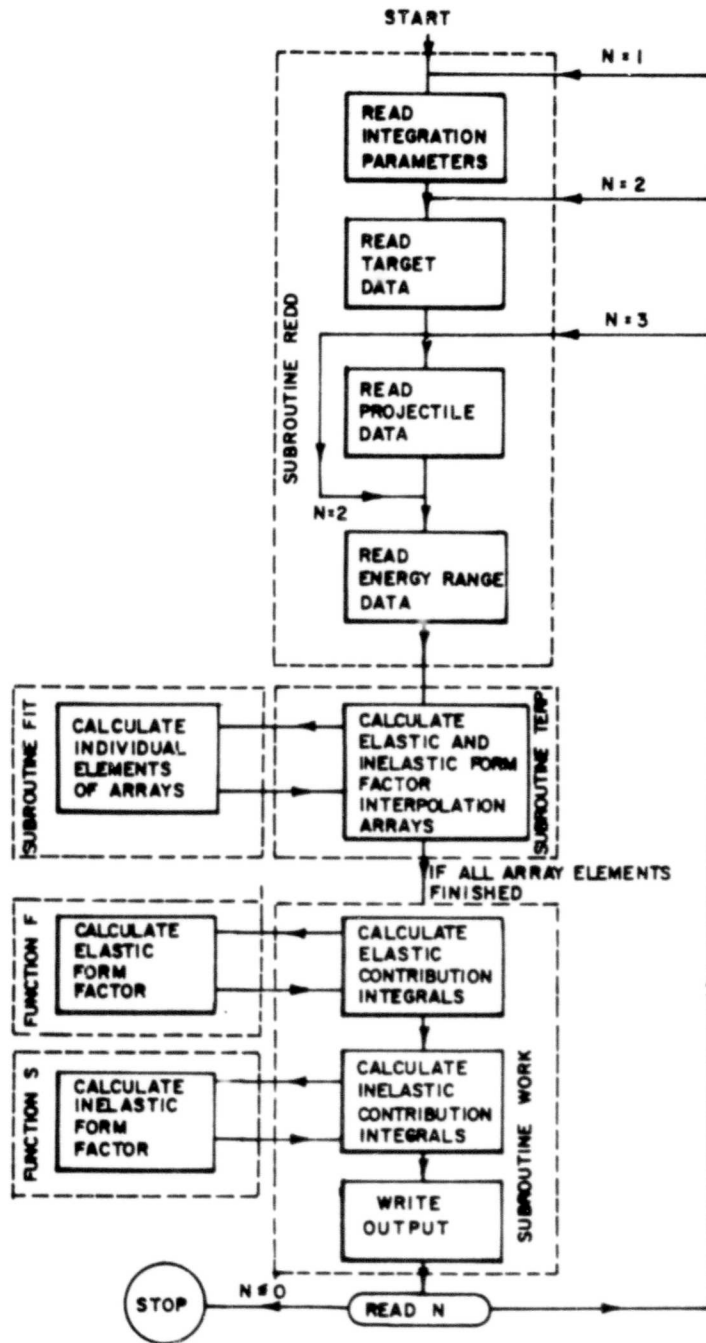


Figure 67. The Electron Stripping Program.

```
PROGRAM STIP(INPUT,OUTPUT,TAPE1 = INPUT,TAPE2 = OUTPUT)
C THIS PROGRAM CALCULATES THE STRIPPING CROSS SECTION USING A MODIFICATION
C OF THE DMITRIEV-NIKOLAEV FORMULATION,JETP 17,447(1963)
N=1
3 CALL REDD(N)
C N=1 TO READ ALL NEW DATA
C N=2 TO READ NEW TARGET DATA
C N=3 TO READ NEW PROJECTILE DATA
C WE ALWAYS READ A NEW ENERGY RANGE
CALL TERP
CALL WORK
READ (1,1) N
1 FORMAT(I4)
TF(N) 2,2,3
2 STOP
C SET N NEGATIVE TO STOP
END
```

```

SUBROUTINE REDD(N)
COMMON/INT/ WT(100),PIV(100),NINT
COMMON/TAR/WORDST(20),NPE,XKE(100),XFKE(100),NPI,XKI(100),XFKI(100)
1),IZ,TMASS,EXCT
COMMON/PROJ/WORDSP(20),NSP,NES(20),POT(20),PMASS
COMMON/ENGY/EMIN,EMAX,DELTA E
C THIS SUBROUTINE READS THE INPUT DATA
GO TO (1,2,3) N
C DATA FOR NUMERICAL INTEGRATION
1 READ(1,4) NINT
4 FORMAT(14)
C NINT IS THE NUMBER OF WEIGHTS AND PIVOTS USED
DO 5 I=1,NINT,1
READ(1,6) WT(I),PIV(I)
5 CONTINUE
6 FORMAT(2(E15.8,1X))
C WT AND PIV ARE THE WEIGHTS AND PIVOTS RESPECTIVELY
C READ THE TARGET DATA
2 READ(1,7) WORDST
7 FORMAT(10A8)
C WORDST ARE TWO ALPHANUMERIC CARDS GIVING DETAILS OF THE TARGET SYSTEM
READ(1,8) NPE,ITYP1,ITYP2
8 FORMAT(3(14,1X))
C NPE IS THE NUMBER OF DATA POINTS FOR THE ELASTIC FORM FACTOR
C ITP1=1 FOR K IN ATOMIC UNITS,NOT 1 FOR K IN TERMS OF SIN(THETA)/LAMBDA
C ITP2=1 FOR F(0)=1 , NOT 1 FOR F(0)=Z
READ(1,4) IZ
C IZ IS THE NUMBER OF ELECTRONS IN THE TARGET
DO 9 I=1,NPE,1
READ(1,6) XKE(I),XFKE(I)
9 CONTINUE
IF(ITYP1-1)10,11,10
10 DO 12 I=1,NPE,1
XKE(I)=6.64971*XKE(I)
12 CONTINUE
11 IF(ITYP2-1)13,14,13
13 DO 15 I=1,NPE,1
XFKE(I)=XFKE(I)/FLOAT(IZ)
15 CONTINUE
14 CONTINUE
READ(1,8) NPI,ITYP1,ITYP2
C NPI IS THE NUMBER OF DATA POINTS FOR THE INELASTIC FORM FACTOR
C ITP1=1 FOR K IN ATOMIC UNITS,NOT 1 FOR K IN TERMS OF SIN(THETA)/LAMBDA
C ITP2=1 FOR SINC(INF)=1, NOT 1 FOR SINC(INF)=Z
DO 16 I=1,NPI,1
READ(1,6) XKI(I),XFKI(I)
16 CONTINUE
IF(ITYP1-1)17,18,17
17 DO 19 I=1,NPI,1
XKI(I)=6.64971*XKI(I)
19 CONTINUE
18 IF(ITYP2-1)20,21,20
20 DO 22 I=1,NPI,1
XFKI(I)=XFKI(I)/FLOAT(IZ)

```

```

22 CONTINUE
21 READ(1,6) TMASS
C TMASS IS THE TARGET MASS IN AMU
C DATA READING STATEMENTS FOR TARGET COMPLETED
  READ(1,6) EXCT
C EXCT IS A LOWEST EXCITATION ENERGY FOR THE TARGET SYSTEM
  3 GO TO (23,24,23) N
23 READ(1,7) WORDSP
C WORDSP ARE TWO ALPHANUMERIC CARDS GIVING DETAILS OF THE PROJECTILE SYSTEM
  READ(1,4) NSP
C NSP IS THE NUMBER OF SHELLS CONSIDERED IN THE PROJECTILE
  DO 25 I=1,NSP,1
  READ(1,26) NES(I),POT(I)
25 CONTINUE
26 FORMAT(14,1X,E15.8)
C NES IS THE NUMBER OF ELECTRONS IN THE SHELL
C POT IS THE THRESHOLD ENERGY TO REMOVE THE ELECTRON, IN AU
  READ(1,6) PMASS
C PMASS IS THE PROJECTILE MASS, IN AMU
24 CONTINUE
  READ(1,27) EMIN,EMAX,DELTA E
27 FORMAT(3(E15.8,1X))
C EMIN IS THE LOWEST COLLISION ENERGY CONSIDERED
C EMAX IS THE HIGHEST COLLISION ENERGY CONSIDERED
C DELTA E IS THE INCREMENT IN COLLISION ENERGY
  RETURN
  END

```

```

SUBROUTINE WORK
COMMON/INT/ WT(100),PIV(100),NINT
COMMON/PROJ/WORDSP(20),NSP,NES(20),POT(20),PMASS
COMMON/ENGY/EMIN,EMAX,DELTA E
COMMON/TAR/WORDST(20),NPE,XKE(100),XFKE(100),NPI,XKI(100),XFKE(100
1),IZ,TMASS,EXCT
DIMENSION CROSS(20),CROSSI(20)
C THIS ROUTINE CALCULATES THE CROSS SECTION
WRITE(2,1)
1 FORMAT(1H1)
WRITE(2,2)
2 FORMAT(22H TARGET IDENTIFICATION)
WRITE(2,3) WORDST
3 FORMAT(1X,10A8)
WRITE(2,4)
4 FORMAT(26H PROJECTILE IDENTIFICATION)
WRITE(2,3) WORDSP
RM=PMASS*TMASS/(PMASS+TMASS)
C EMIN,EMAX,DELTA E ARE IN EV IN THE LABORATORY SYSTEM
E=EMIN
5 ECM=E*TMASS/(PMASS+TMASS)
EAU=F727.21
C ECM IS THE CM ENERGY IN EV, EAU IS THE LAB ENERGY IN AU
V=SQRT(2.0*EAU/(PMASS*1822.3))
C V IS THE RELATIVE VELOCITY ,IN AU
ULE=2.0*V
ULI=V
WRITE(2,6) E,ECM,V
6 FORMAT(11H E(LAB,EV)=,E15.8,10H E(CM,EV)=,E15.8,23H RELATIVE VELOC
1ITY(AU)=,E15.8)
DO 7 I=1,NSP,1
WLE=SQRT(2.0*POT(I))
IF(1.0-2.0*EXCT/(V*V)) 100,101,101
100 WLI=2.0*ULI
GO TO 10
12 101 AA=V*(1.0-SQRT(1.0-2.0*EXCT/(V*V)))
11 IF(AA-WLE) 8,8,9
8 WLI=WLE
GO TO 10
10 9 WLI=AA
10 CONTINUE
C PERFORM THE ELASTIC INTEGRATION
IF(ULE-WLE)11,11,12
11 CROSS(I)=0.0
CROSSI(I)=0.0
GO TO 7
12 SUM1=0.0
SUM3=0.0
DO 13 J=1,NINT,1
X=0.5*(ULE+WLE)+0.5*(ULE-WLE)*PIV(J)
ZZ=F(X)
ZZ=WT(J)*((1.0-ZZ)**2)/(X*X*X)
ZZ1=0.5*ZZ*X*X
SUM1=SUM1+ZZ

```

```

SUM3=SUM3+ZZ1
13 CONTINUE
SUM1=SUM1*0.5*(ULE-WLE)*FLOAT(IZ*IZ)
SUM3=0.5*SUM3*(ULE-WLE)*FLOAT(IZ*IZ)
C DO THE INELASTIC INTEGRATION
IF(ULI-WLI) 14,14,15
14 SUM2=0.0
SUM4=0.0
GO TO 16
15 SUM2=0.0
SUM4=0.0
DO 17 J=1,NINT,I
X=0.5*(ULI+WLI)+0.5*(ULI-WLI)*PIV(J)
ZZZ=S(X)
ZZ=WT(J)*ZZZ/(X*X*X)
ZZZ=0.5*ZZZ*X*X
SUM2=SUM2+ZZZ
SUM4=SUM4+ZZZ
17 CONTINUE
SUM2=SUM2*0.5*(ULI-WLI)*FLOAT(IZ)
SUM4=0.5*SUM4*(ULI-WLI)*FLOAT(IZ)
16 SUM=SUM1+SUM2
SUMP=SUM3+SUM4
CROSS(I)=SUMP*7.03773E-16*FLOAT(NEST(I))/V*V)
CROSS(I)=SUM*7.03773E-16*FLOAT(NES(I))/V*V)
7 CONTINUE
TXS=0.0
TSY=0.0
DO 18 I=1,NSP,1
TSY=TSY+CROSS(I)
TXS=TXS+CROSS(I)
18 CONTINUE
WRITE(2,19) TXS
19 FORMAT(24H TOTAL CROSS SECTION IS ,E15.8)
WRITE(2,24) TSY
24 FORMAT(30H ENERGY LOSS CROSS SECTION IS ,E15.8)
WRITE(2,21)
WRITE(2,20) T CROSS(I),I=1,NSP)
WRITE(2,21)
WRITE(2,20) (CROSS(I),I=1,NSP)
20 FORMAT(6(1X,E15.8))
21 FORMAT(28H CONTRIBUTIONS OF THE SHELLS)
WRITE(2,22)
22 FORMAT(1F 7
E=E+DELTA E
IFTE-EMAX) 5,5,23
23 RETURN
END

```

```

SUBROUTINE TERP
COMMON/TAR/WORDST(20),NPE,XKE(100),XFKE(100),NPI,XKI(100),XFKI(100)
1),I2,TMASS,EXCT
COMMON/TPT/EFF(4,100),SEFF(4,100)
COMMON/EZP/CEXTP
C THIS ROUTINE CALCULATES THE INTERPOLATION ARRAYS
C FOR THE ELASTIC FORM FACTOR
MAX=NPE-3
DO 1 I=1,MAX,1
X11=XKE(I)
X21=XKE(I+1)
X31=XKE(I+2)
X41=XKE(I+3)
F1=XFKE(I)
F2=XFKE(I+1)
F3=XFKE(I+2)
F4=XFKE(I+3)
CALL FIT(X11,X21,X31,X41,F1,F2,F3,F4,D1,D2,D3,D4)
EFF(1,I)=D1
EFF(2,I)=D2
EFF(3,I)=D3
EFF(4,I)=D4
1 CONTINUE
C CALCULATE THE EXTRAPOLATION CONSTANT CEXTP
CEXTP=(-XFKE(NPE)+SQRT(XFKE(NPE)))/(XFKE(NPE)*XKE(NPE)*XKE(NPE))
C FOR THE INELASTIC FORM FACTOR
MAX=NPI-3
DO 2 I=1,MAX,1
X11=XKI(I)
X21=XKI(I+1)
X31=XKI(I+2)
X41=XKI(I+3)
F1=XFKI(I)
F2=XFKI(I+1)
F3=XFKI(I+2)
F4=XFKI(I+3)
CALL FIT(X11,X21,X31,X41,F1,F2,F3,F4,D1,D2,D3,D4)
SEFF(1,I)=D1
SEFF(2,I)=D2
SEFF(3,I)=D3
SEFF(4,I)=D4
2 CONTINUE
RETURN
END

```

SUBROUTINE FIT(X11,X21,X31,X41,F1,F2,F3,F4,D1,D2,D3,D4)

X12=X11*X11

X13=X11*X12

X22=X21*X21

X23=X21*X22

X32=X31*X31

X33=X32*X31

X42=X41*X41

X43=X41*X42

Q2=(X12-X22)*(X11-X31)-(X12-X32)*(X11-X21)

Q3=(X13-X23)*(X11-X31)-(X13-X33)*(X11-X21)

Q4=(F1-F2)*(X11-X31)-(F1-F3)*(X11-X21)

S2=(X12-X32)*(X11-X41)-(X12-X42)*(X11-X31)

S3=(X13-X33)*(X11-X41)-(X13-X43)*(X11-X31)

S4=(F1-F3)*(X11-X41)-(F1-F4)*(X11-X31)

D4=(Q4*S2-S4*Q2)/(Q3*S2-S3*Q2)

D3=(Q4-D4*Q3)/Q2

D2=(F1-F2-D4*(X13-X23)-D3*(X12-X22))/X11

D1=F1-D4*X13-D3*X12-D2*X11

RETURN

END

```

FUNCTION S(X)
COMMON/TAR/WORDST(20),NPE,XKE(100),XFKE(100),NPI,XKI(100),XFKI(100)
1),I2,TMASS,EXCT
COMMON/TPT/EFF(4,100),SEFF(4,100)
COMMON/EZP/CEXP
C THIS FUNCTION CALCULATES THE INELASTIC FORM FACTOR FROM THE ARRAY SEFF
IF(X) 1,2,3
1 WRITE(2,4)
STOP
4 FORMAT(33H NEGATIVE MOMENTUM TRANSFER ERROR)
2 IF(XKI(1)) 5,5,6
5 S=XFKI(1)
RETURN
6 S=SEFF(1,1)+SEFF(2,1)*X+SEFF(3,1)*X*X+SEFF(4,1)*X*X*X
RETURN
3 IF(X-XKI(1)) 6,5,7
7 IF(X-XKI(2)) 6,8,9
8 S=XFKI(2)
RETURN
9 IF(X-XKI(3)) 6,10,11
10 S=XFKI(3)
RETURN
11 IF(X-XKI(NPI)) 12,13,14
14 FEZP=1.0/((1.0+CEXP*X*X)**2)
S=1.0-(FEZP*FEZP)
RETURN
13 S=XFKI(NPI)
RETURN
12 MAX=NPI-3
IF(X-XKI(NPI-1)) 15,16,17
17 S=SEFF(1,MAX)+SEFF(2,MAX)*X+SEFF(3,MAX)*X*X+SEFF(4,MAX)*X*X*X
RETURN
16 S=XFKI(NPI-1)
RETURN
15 IF(X-XKI(NPI-2)) 18,19,17
19 S=XFKI(NPI-2)
RETURN
18 I=2
II=4
26 IF(X-XKI(II)) 20,21,22
20 S=SEFF(1,II)+SEFF(2,II)*X+SEFF(3,II)*X*X+SEFF(4,II)*X*X*X
RETURN
21 S=XFKI(II)
RETURN
22 IF(I-MAX) 23,24,24
24 WRITE(2,25)
STOP
25 FORMAT(17H LOGIC ERROR IN S)
23 I=I+1
II=II+1
GO TO 26
END

```

```

FUNCTION F(X)
COMMON/TPY/EFF(4,100),SEFF(4,100)
COMMON/TAR/WORDST(20),NPE,XKE(100),XFKE(100),NPI,XKI(100),XFKI(100)
1) IZ, YMASS, EXCT
COMMON/EZP/CEZTP
C THIS FUNCTION CALCULATES THE ELASTIC FORM FACTOR FROM THE ARRAY EFF
IF(X) 1,2,3
1 WRITE(2,4)
STOP
4 FORMAT(33H NEGATIVE MOMENTUM TRANSFER ERROR)
2 IF(XKE(1)) 5,5,6
5 F=XFKE(1)
RETURN
6 F=EFF(1,1)+EFF(2,1)*X+EFF(3,1)*X*X+EFF(4,1)*X*X*X
RETURN
3 IF(X-XKE(1)) 6,5,7
7 IF(X-XKE(2)) 6,8,9
8 F=XFKE(2)
RETURN
9 IF(X-XKE(3)) 6,10,11
10 F=XFKE(3)
RETURN
11 IF(X-XKE(NPE)) 12,13,14
14 F=1.0/((1.0+CEZTP*X*X)**2)
RETURN
13 F=XFKE(NPE)
RETURN
12 MAX=NPE-3
IF(X-XKE(NPE-1)) 15,16,17
17 F=EFF(1,MAX)+EFF(2,MAX)*X+EFF(3,MAX)*X*X+EFF(4,MAX)*X*X*X
RETURN
16 F=XFKE(NPE-1)
RETURN
15 IF(X-XKE(NPE-2)) 18,19,17
19 F=XFKE(NPE-2)
RETURN
18 I=2
II=4
26 IF(X-XKE(II)) 20,21,22
20 F=EFF(1,II)+EFF(2,II)*X+EFF(3,II)*X*X+EFF(4,II)*X*X*X
RETURN
21 F=XFKE(II)
RETURN
22 IF(1-MAX) 23,24,24
24 WRITE(2,25)
STOP
25 FORMAT(17H LOGIC ERROR IN F)
23 I=I+1
II=II+1
GO TO 26
END

```

37

9.65400885E-02 +4.83076657E-02
9.65400885E-02 -4.83076657E-02
9.56387200E-02 +1.44471962E-01
9.56387200E-02 -1.44471962E-01
9.38443990E-02 +2.39287362E-01
9.38443990E-02 -2.39287362E-01
9.11738786E-02 +3.31868602E-01
9.11738786E-02 -3.31868602E-01
8.76520930E-02 +4.21351276E-01
8.76520930E-02 -4.21351276E-01
8.33119242E-02 +5.06899909E-01
8.33119242E-02 -5.06899909E-01
7.81938958E-02 +5.87715757E-01
7.81938958E-02 -5.87715757E-01
7.23457941E-02 +6.63044267E-01
7.23457941E-02 -6.63044267E-01
6.58222228E-02 +7.32182119E-01
6.58222228E-02 -7.32182119E-01
5.86840935E-02 +7.94483796E-01
5.86840935E-02 -7.94483796E-01
5.09980593E-02 +8.49367614E-01
5.09980593E-02 -8.49367614E-01
4.28358980E-02 +8.96321156E-01
4.28358980E-02 -8.96321156E-01
3.42738629E-02 +9.34906076E-01
3.42738629E-02 -9.34906076E-01
2.53920653E-02 +9.64762256E-01
2.53920653E-02 -9.64762256E-01
1.62743947E-02 +9.85611512E-01
1.62743947E-02 -9.85611512E-01
7.01861001E-03 +9.97263862E-01
7.01861001E-03 -9.97263862E-01

ARGON ELASTIC FORM FACTORS FROM HANDBOOK OF X-RAY CRYSTALLOGRAPHY
INELASTIC FROM JCP 47, 1892 (1967)

18 +000 +000

18

.00000000E+00 +1.80000000E+01
5.00000000E-02 +1.75400000E+01
1.00000000E-01 +1.63000000E+01
1.50000000E-01 +1.46500000E+01
2.00000000E-01 +1.29300000E+01
2.50000000E-01 +1.14200000E+01
3.00000000E-01 +1.02000000E+01
3.50000000E-01 +9.25000000E+00
4.00000000E-01 +8.54000000E+00
5.00000000E-01 +7.56000000E+00
6.00000000E-01 +6.86000000E+00
7.00000000E-01 +6.23000000E+00
8.00000000E-01 +5.61000000E+00
9.00000000E-01 +5.01000000E+00
1.00000000E+00 +4.43000000E+00
1.10000000E+00 +3.90000000E+00
1.20000000E+00 +3.43000000E+00

1.30000000E+00 +3.03000000E+00
21 +000 +000
.00000000E+00 +0.00000000E+00

5. E-03 +6.00000000E-03
1.00000000E-02 +2.40000000E-02
5.00000000E-02 +5.71000000E-01
1.00000000E-01 +1.95600000E+00
1.50000000E-01 +3.55800000E+00
2.00000000E-01 +5.03300000E+00

3.00000000E-01 +7.37700000E+00
4.00000000E-01 +8.99800000E+00
5.00000000E-01 +1.01060000E+01
6.00000000E-01 +1.09670000E+01
7.00000000E-01 +1.17260000E+01
8.00000000E-01 +1.24240000E+01

9.00000000E-01 +1.30610000E+01
1.00000000E+00 +1.36290000E+01
1.50000000E+00 +1.54890000E+01
2.00000000E+00 +1.63240000E+01
3.00000000E+00 +1.71320000E+01
4.00000000E+00 +1.75730000E+01

5.00000000E+00 +1.78000000E+01
8.00000000E+00 +1.79780000E+01
3.99440000E+01
8.08530000E+00

ATOMIC HYDROGEN

1
1 +5.00000000E-01
1.00000000E+00
2.75000000E+04 +1.00000000E+06 +2.50000000E+04

3
ATOMIC HYDROGEN

1
1 +5.00000000E-01
1.00000000E+00
1.00000000E+06 +1.00000000E+08 +1.00000000E+06

1

REFERENCES

1. Dalgarno, A.; Florance, E. T.; Macomber, H. K.; Webb, T. G.; Theoretical Studies of Heavy Ion Exchange in Air, AFWL-TR-67-1, May 1967, Air Force Weapons Laboratory, Kirtland AFB, NM.
2. Dmitriev, I. S.; Nikolaev, V. S.; "Calculations of the Cross Sections for Electron Loss by Fast Ions in Light Media," Sov. Phys.-JETP 17, p. 447, 1963.
3. Bates, D. R.; McCarroll, R.; "Charge Transfer," Advances in Physics, 11, p. 39, 1962.
4. Dalgarno, A.; Florance, E. T.; Macomber, H. K.; Webb, T. G.; Theoretical Studies of Heavy Ion Exchange in Air, AFWL-TR-65-203, March 1966, Air Force Weapons Laboratory, Kirtland AFB, NM.
5. Green, T. A.; "Impact-Parameter Calculation of Electron Capture in Close H^+ -He Collisions," Phys. Rev., 152, p. 18, 1966.
6. Macomber, H. K.; Webb, T. G., "Influence of Back-Coupling and Distortion in a Charge-Exchange Reaction," Proc. Phys. Soc., 92, p. 839, 1967.
7. Oppenheimer, J. R.; "On the Quantum Theory of the Capture of Electrons," Phys. Rev., 31, 349, 1928.
8. Brinkman, H. C.; Kramer, H. A.; "Capture of Electrons by α -Particles," Proc. Acad. Sci. Amst., 33, p. 973, 1930.
9. Bates, D. R.; Dalgarno, A.; "Electron Capture, III. Capture into Excited States in Encounters Between Hydrogen Atoms and Fast Protons," Proc. Phys. Soc. (London), A66, p. 972, 1953.
10. Mapleton, R. A.; (a) "Electron Capture from $He(1s^2)$ by Protons," Phys. Rev., 122, p. 528, 1961; (b) "Electron Capture from Atomic Hydrogen by Protons," Phys. Rev., 126, p. 1477, 1962.
11. Hughes, R. H.; Dawson, H. R.; Doughty, B. M.; Kay, D. B.; Stigers, C. A.; "Electron Capture into the 3s State of Hydrogen by Fast-Proton Impact on Gases," Phys. Rev., 146, p. 53, 1966.
12. Jaecks, D.; Van Zeyl, B.; Geballe, R.; "Production of Metastable Hydrogen Atoms in Proton-Rare-Gas Collisions," Phys. Rev., 137, A340, 1965.
13. Abstract of Papers, V International Conference on Physics and Electronic and Atomic Collisions, NAVKA, Leningrad, 1967, See especially the papers in Sessions I-3, 1-(4), and 4-4.

REFERENCES (continued)

14. Russek, A.; "Ionization Produced by High-Energy Atomic Collisions," Phys. Rev., 132, p. 246, 1963.
15. Fano, V.; Lichten, W.; "Interpretation of Ar⁺-Ar Collisions at 50 keV," Phys. Rev. Lett., 14, p. 627, 1965.
16. Kessel, Q.C.; Everhart; (a) "Coincidence Measurements of Large-Angle Ar⁺-on-Ar Collisions," Phys. Rev., 146, p. 16, 1966; (b) "Statistical Model for the Ar⁺-on-Ar Collision," Phys. Rev., 146, p. 27, 1966.
17. Demkov, Yu. N.; Komarov, I.V.; "Ionization in Slow Two-Atom Collisions," Sov. Phys.-JETP, 23, p. 189, 1966.
18. Smirnov, B. M.; Firsov, O. B.; "Interaction Between Negative Ions and Atoms," Sov. Phys.-JETP, 20, p. 156, 1965.
19. Bates, D. R.; Griffing, G. W.; "Inelastic Collisions Between Heavy Particles," (a) "I: Excitation and Ionization of Hydrogen," Proc. Phys. Soc. (London), A66, p. 961, 1953; (b) "II: Contributions of Double-Transitions to the Cross Sections," A67, p. 663, 1954; (c) "IV: Contribution of Double Transitions to Certain Cross Sections Including that Associated with the Ionization of Hydrogen Atoms in Fast Encounters with other Hydrogen Atoms," A68, p. 90, 1955.
20. Boyd, J.; Moiseiwitsch, B. L.; Stewart, A. L.; "Inelastic Collisions Between Heavy Particles. V: Electron Loss for Fast He⁺ Ions Passing Through Atomic Hydrogen, and Ionization of Hydrogen Atoms by Fast He⁺ Ions," Proc. Phys. Soc. (London), A70, p. 110, 1967.
21. Bates, D. R.; Williams, A.; "Inelastic Collisions Between Heavy Particles. VII: Electron Loss From Fast Hydrogen Atoms Passing Through Helium," Proc. Phys. Soc. (London), A70, p. 306, 1957.
22. Mott, N. F.; Massey, H. S. W.; The Theory of Atomic Collisions, Third Edition, Oxford, 1965.
23. (a) Bethe, H.; "Zur Theorie des Durchgangs Schneller Korpuskularstrahlen Durch Materie," Ann. Physik, 5, p. 325, 1930; (b) Fano, U.; "Penetration of Protons, Alpha Particles, and Mesons," Ann. Rev. Nucl. Sci., 13, p. 1, 1963; (c) Dalgarno, A.; "Range and Energy Loss," In Atomic and Molecular Processes, Bates, D. R., ed.; Academic Press, p. 623, 1962.
24. Kim, Y. K.; Inokuti, M., "Atomic Form Factor and Incoherent-Scattering Function of the Helium Atom," Phys. Rev., 165, p. 39, 1968.
25. Hart, J. F.; Herzberg, F.; "Twenty-Parameter Eigenfunctions and Energy Values of the Ground States of He and He-Like Ions," Phys. Rev., 106, p. 79, 1957.

REFERENCES (continued)

26. International Tables of X-Ray Crystallography, The Kynoch Press, Birmingham, 1962, Vol. III.
27. Freeman, A.J.; (a) "Atomic Scattering Factors for Spherical and Aspherical Charge Distributions," Acta Cryst., 12, p. 261, 1959; (b) "X-Ray Incoherent Scattering Functions for Non-spherical Charge Distributions: O, O⁺, O⁺², O⁺³, F, F⁻, Si⁺⁴, Si⁺³, Si, and Ge," 12, p. 929, 1959.
28. Cromer, D. T.; Mann, J. B.; "Compton Scattering Factors for Spherically Symmetric Free Atoms," J. Chem. Phys., 47, p. 1892, 1967.
29. Moore, C. E.; Atomic Energy Levels, Vol. I, II, and III, National Bureau of Standards Circular, 467, 1949; 1952; and 1958.
30. Slater, J. C., "One-Electron Energies of Atoms, Molecules, and Solids," Phys. Rev., 98, p. 1039, 1955.
31. Layton, J. K.; Fite, W. L.; Experimental Studies of Heavy Ion Exchange in Air, AFWL-TR-67-2, Air Force Weapons Laboratory, Kirtland AFB, NM.
32. Allison, S. K.; "Experimental Results on Charge-Changing Collisions of Hydrogen and Helium Atoms and Ions at Kinetic Energies Above 0.2 keV," Rev. Mod. Phys., 30, p. 1137, 1958.
33. Berkner, K. H.; Kaplan, S. N.; Paulikas, G. A.; Pyle, R. V.; "Electron Capture by High-Energy Deuterons in Gases," Phys. Rev., 140, p. A729, 1965.
34. Smythe, R.; Toevs, J. W.; "Collisional Electron Detachment from Hydrogen Atoms and Negative Hydrogen Ions Between 4 and 18 MeV," Phys. Rev., 139, p. A15, 1965.
35. Dalgarno, A.; Griffing, G. W.; "Energy Loss of Protons Passing Through Hydrogen," Proc. Roy. Soc., A232, p. 423, 1955.

UNCLASSIFIED

Security Classification

DOCUMENT CONTROL DATA - R & D

(Security classification of title, body of abstract and indexing annotation must be entered when the overall report is classified)

1. ORIGINATING ACTIVITY (Corporate author) GCA Corporation, GCA Technology Division Bedford, Massachusetts 01730		2a. REPORT SECURITY CLASSIFICATION UNCLASSIFIED	
		2b. GROUP	
3. REPORT TITLE THEORETICAL STUDY OF CHARGE EXCHANGE CROSS SECTIONS			
4. DESCRIPTIVE NOTES (Type of report and inclusive dates) 16 June 1967-20 August 1968			
5. AUTHOR(S) (First name, middle initial, last name) A. Dalgarn; T. G. Webb; G. A. Victor			
6. REPORT DATE January 1969		7a. TOTAL NO. OF PAGES 138	7b. NO. OF REFS 35
8a. CONTRACT OR GRANT NO F29601-67-C-0088	b. PROJECT NO. 5710	9a. ORIGINATOR'S REPORT NUMBER(S) AFWL-TR-68-114	
c. Subtask No. 07.003 (RHA3061)	d.	9b. OTHER REPORT NO(S) (Any other numbers that may be assigned this report) Contractor's report number: GCA-TR-68-3-A	
10. DISTRIBUTION STATEMENT This document is subject to special export controls and each transmittal to foreign governments or foreign nationals may be made only with prior approval of AFWL (WLRT), Kirtland AFB, NM, 87117. Distribution is limited because of the technology discussed in the report.			
11. SUPPLEMENTARY NOTES		12. SPONSORING MILITARY ACTIVITY AFWL (WLRT) Kirtland AFB, NM 87117	
13. ABSTRACT (Distribution Limitation Statement No. 2) Charge exchange cross sections for fast heavy ions representative of several groups in the periodic table with atmospheric and other atoms have been calculated by using a quantal two-state one-electron method. The principal ions considered have been singly charged K, I, and Cr while target atoms and/or molecules have been N, O, Ar, Ne, H and He. Singly charged lithium, sodium, rubidium, and cesium have also been considered as projectiles in the target gases. Stripping cross sections for fast heavy ions incident on atmospheric and other atoms have been calculated by using an independent scattering model based on the Born approximation. The relationship between the quantal predictions and available experimental results is illustrated and certain improvements to the simple theory are discussed. A comparison is also made between the electron loss theory and available experimental results. Capture into excited states is discussed, and estimates are made of the appropriate cross sections. The rate of energy loss by heavy ions in air is discussed.			

DD FORM 1 NOV 65 1473

UNCLASSIFIED

Security Classification

14	KEY WORDS	LINK A		LINK B		LINK C	
		ROLE	WT	ROLE	WT	ROLE	WT
	Charge exchange Heavy ions Stripping Electron capture Atomic collisions						